Machinability, Modeling and Optimization In Face Milling Inconel 718 with Coated Carbide Inserts

Submitted in partial fulfillment of the requirements

for the award of the degree of

Doctor of Philosophy

by

Talasila Sadasiva Rao

(Roll No. 700810)

Supervisor

Prof. A. Venu Gopal

Mechanical Engineering Department

National Institute of Technology, Warangal

DEPARTMENT OF MECHANICAL ENGINEERING

NATIONAL INSTITUTE OF TECHNOLOGY

WARANGAL

2015

Dedicated

To

My Wife & Children

DEPARTMENT OF MECHANICAL ENGINEERING

NATIONAL INSTITUTE OF TECHNOLOGY

WARANGAL - 506004 (TELANGANA), INDIA.

CERTIFICATE

This is to certify that the work presented in the thesis entitled **"Machinability, Modelling and Optimization In Face Milling 718 with Coated Carbide Inserts"** which is being submitted by **Mr. Talasila Sadasiva Rao (Roll No. 700810),** is a bonafide work submitted to National Institute of Technology, Warangal in partial fulfillment of the requirement for the award of the degree of **Doctor of Philosophy** in **Mechanical Engineering**. To the best of our knowledge, the work incorporated in the thesis has not been submitted to any other university or institute for the award of any other degree or diploma.

Prof. A.Venu Gopal
Mechanical Engineering Department
National Institute of Technology
Warangal – 506004.

ACKNOWLEDGEMENTS

My Guide, Prof. A.Venugopal is my mentor. But this expression is a cliché to express my true feelings. The support I received from my guide from day one proved to be catalystic to me. From selecting the topic to the very end, all his suggestions were very creative and constructive to my thesis. Throughout the gruelling experimental work as well as the writing part, my guide's support was incalculable for which I will be grateful all my life. I could complete my thesis just because of my guide's encouragement.

With profound respect, I wish to express my sincere thanks to the Doctoral Scrutiny Committee (DSC) members comprising of Prof. C.S.P. Rao, Head Mechanical Engineering as Chairman and members Prof. B.V. Appa Rao, Department of Chemistry, Dr.A. Kumar, Associate Professor, Mechanical Engineering Department and Prof. B.Kotiveerachary, former DSC Member for their constructive advice and support. I am greatly indebted to Prof. K. Madhu Murthy and Prof. L. Krishnanand (former Chairmen, DSC) for their constant support and timely suggestions to improve my research perception.

I would like to seize this opportunity to express my gratitude to the Director, Prof. T. Srinivasa Rao for extending financial, academic and technical support for carrying out my research work.

I wish to express my sincere thanks to Dr. N. Narasaiah, Head- Metallurgical and Materials Engineering Department for helping me to work on SEM/EDS.

I express my deep sense of gratitude to the Research Scholars Mr. V.S. ROHIT and Dr. K. Satyanarayana for their immeasurable help while conducting my research experiments.

I also express my sincere thanks to Sri K.Yella Swamy, W/s Foreman and the other Mechanics for their help in conducting machining experiments.

My special thanks to all my friends and my family members who stood by me throughout my research work.

Last but not the least, I convey my thanks to one and all who have contributed to the realization of this thesis.

Talasila Sadasiva Rao.

DECLARATION

This is to certify that the work presented in the thesis entitled **Machinability, Modeling and Optimization in Face Milling Inconel 718 with coated carbide inserts** is a bonafide work done by me under the supervision of **Prof. A. Venu Gopal** and was not submitted elsewhere for the award of any degree.

I declare that this written submission represents my ideas in my own words and where others' ideas or words have been included, I have adequately cited and referenced the original sources. I also declare that I have adhered to all principles of academic honesty and integrity and have not misrepresented or fabricated or falsified any idea/data/fact/source in my submission. I understand that any violation of the above will be a cause for disciplinary action by the institute and can also evoke penal action from the sources which have thus not been properly cited or from whom proper permission has not been taken when needed.

Talasila Sadasiva Rao

Roll. No. 700810

Date: 14-12-2015.

ABSTRACT

Heat resistant superalloys (HRSA) are extensively used in Aerospace industries. High strength at elevated temperatures and low chemical reactivity, make them ideal for applications in the gas turbine engines. Inconel 718 is a Nickel based HRSA that can be welded easily. The ease of fabrication has resulted in increased adoption of Inconel 718. However, it is difficult to machine because of its high strength and low thermal conductivity. The scope of the present study is to analyze the effect of process parameters in face milling of Inconel 718 with coated carbide inserts under different machining conditions and understand the tool wear mechanisms.

Understanding the effect of process parameters (i.e. speed, feed and depth of cut) and tool parameters on cutting Force (the load acting on the tool), tool flank wear and surface roughness (quality of the machined product) is essential for establishing a machining process. The process needs to be optimized to achieve the best surface finish while minimizing tool wear. Establishing optimum parameters and understanding effects of process parameters requires extensive experimentation. A model developed from the experimental data can be used for analyzing the process and can also be used to establish similar processes at a later date. Also, understanding the amount of tool wear and the underlying mechanism helps us in selecting process parameters and provides valuable insight for developing future tools. The high strength of Inconel 718 results in very high temperatures in the machining zone. To prevent thermal distortion of workpiece and excessive tool wear, flood coolant is commonly used for machining superalloys. But with increased environmental restrictions and cost of coolant application, sustainable methods of cooling the machining zone are essential.

The experiments were conducted on a Vertical milling machine (Bharat Fritz Werner Ltd, 3kW) with a face milling cutter having coated carbide inserts (Widia SPMW 120408 – TN 7535). Cutting forces were measured using a 4 component Piezo-electric dynamometer (Kistler 9272). Surface roughness was measured using portable surface roughness tester (Handysurf E-35A). A Scanning electron microscope (VEGA3 SB) with a dispersive X-ray microanalyzer was used for measuring tool wear and conducting energy dispersive spectroscopy (EDS) for understanding the mechanism of tool wear.

Experiments were conducted based on L9 orthogonal array to understand the effect of speed, feed, depth of cut and approach angle on cutting force, surface roughness and tool wear. Depth of cut had maximum influence on cutting force, while feed had maximum effect on surface roughness and cutting speed had maximum effect on tool wear. Gray relational analysis was used for multi-objective optimization of cutting force, surface roughness and tool wear giving

equal weightage to each of them. The Optimized parameters were found to be cutting speed 60 m/min, feed 0.16mm/rev, depth of cut 0.1 mm and approach angle 45^{o}.

Full factorial experiments were conducted to develop a reliable model and understand the interaction effects between process parameters. ANOVA analysis was performed to check for the significance of interaction effects. Interaction between feed and approach angle was observed. This can be mainly due to their combined effect on chip thickness and length of tool contact. Another interaction between feed and depth of cut was also observed. This is due to their combined effect on slenderness ratio that causes vibrations. A process model was developed using Artificial Neural Networks using a two layer feed forward network with 10 neurons in the hidden layer. The fit of the model was found to be satisfactory.

SEM studies revealed the presence of Built-Up-Edge at lower speeds. EDS was used to find elemental compositions on the surface of the tool before and after machining. This helped in establishing diffusion wear as the dominant tool wear mechanism.

Minimum quantity lubrication (MQL) was used as a sustainable alternative to flood coolant to improve machinability of Inconel 718. Vegetable oil and vegetable oil nano-fluid with Al_2O_3 nano particles were used to form emulsions with pressurized air. It was found that cutting force reduced by 34.29% for vegetable oil and 43.66% for nano-fluid. The effectiveness of nano-fluid based and vegetable oil based MQL for Inconel 718 face milling has been established.

Keywords: Inconel 718, Gray Relational Analysis, Orthogonal Arrays, Artificial Neural Networks, Minimum Quantity Lubrication, Nano-fluids

Contents

List of Figures

List of Tables

Abbreviation and Notation

HRSA	Heat Resistant Super-Alloy
FCC	Face centered Cubic structure
BUE	Built-Up-Edge
CVD	Chemical Vapor Deposition
CBN	Cubic Boron Nitride
SEM	Scanning Electron Microscope
PVD	Physical Vapour Deposition
DA	Direct Aged
BUL	Built-Up-Layer
TEM	Transmission Electron Microscopy
S/N	Signal-to-Noise Ratio
ANOVA	Analysis of Variance
ANN	Artificial Neural Networks
EDS	Energy dispersive spectroscopy
A.R	Axial rake
R.R	Radial Rake
A.A	Approach angle
T.R	True rake angle
F_y	Cutting Force (in N)
R_a	Surface roughness (in µm)
L	Tool life (in min)
V	Cutting speed (m/min)
D	Diameter of the milling cutter
f_t	Feed per minute
f_r	Feed per revolution
f_z	Feed per tooth
T	Number of teeth
N	Revolutions per minute
r	Nose radius
OA	Orthogonal arrays
MSD	Mean square deviation
SS	Sum of Squares
SS_d	Sum of Squared deviations

SS_e	Sum of squared error
SS_T	Total sum of square deviations
Seq SS	Sequential sum of squares
Adj SS	Adjusted sum of squares
DF	Degrees of freedom
MS	Mean squares
NDM	Near dry machining
CNT	Carbon nano tubes

1 INTRODUCTION

1.1 Background

With the advent of twentieth century, the need for highly corrosion resistant materials for high temperature applications was felt acutely. Stainless steel was initially used in early decades but was found to be limited in strength. The need for materials with high strength at high temperatures drastically increased with the introduction of gas turbine engines for aerospace applications. The emergence of superalloy industry, took place by adapting a cobalt alloy, Vitallium, which is used in dentistry and aerospace applications [1].

1.1.1 Superalloys

A super-alloy, also known as heat resistant super-alloy (HRSA), has high mechanical strength and creep resistance. They show resistance to mechanical and chemical degradation at temperatures close to their melting points. It also has good surface stability apart from corrosion and oxidation resistance. They can also withstand mechanical and thermal shocks. The initial development of super alloys has been mainly for aerospace and power industries. They are mostly used in hottest sections of the turbine where the temperatures and loads are very high. A modern jet engine cannot be produced without using super-alloys because of the high temperatures employed in it for improving thermal efficiency. Their unique strength and creep properties are being used in many new areas like electronics, defence, paper and pulp, dental, orthopedic and seawater services. Some of the commonly used super-alloys are Haste alloy, Inconel, Waspaloy, Rene alloys, Haynes alloy, Incoloy, MP98T, TMS alloys and CMSX single crystal alloys.

A typical super alloy has an Austenitic FCC structure. The austenitic structure enhances work-hardening. The main base material of the alloy is Nickel, Cobalt or Iron. The high temperature strength of the alloys is due to solid solution strengthening. It is an alloying process where atoms of one element are added to the lattice of the base element. When the concentration is above a certain value, it causes precipitation of second phase which increases the strength. Oxidation and corrosion resistance is due to the presence of elements like Aluminium and Chromium. These elements form protective oxides which act as a thermal barrier [1].

1.1.2 Inconel 718

Inconel is a family of austenitic nickel-chromium based super-alloy. It is a trademark of Special Metals Corporation. Inconel 718 is gamma double prime strengthened with good weldability. It contains age hardened Niobium. This gives high strength to it without sacrificing ductility.

Inconel 718 is non-magnetic, oxidation and corrosion resistant. It can be used in the range of -423°F to 1300°F [2]. The typical composition of alloy is given in the following table:

Table 1.1 Inconel 718 Limiting composition [2]

Element	Percentage	Element	Percentage
Nickel & Cobalt	50-55	Carbon	0.08 max
Chromium	17-21	Manganese	0.35 max
Iron	Balance	Silicon	0.35 max
Niobium & Tantalum	4.75-5.5	Phosphorous	0.015 max
Molybdenum	2.8-3.3	Sulfur	0.015 max
Titanium	0.65-1.15	Boron	0.006 max
Aluminium	0.2-0.8	Copper	0.30 max
Cobalt	1.00 max		

The alloy consists of $Ni_3(Al,X)$ where X can be Niobium, Titanium, Tantalum. This phase is known as γ'. γ phase contains Chromium, Molybdenum or Cobalt. The reason for high creep strength is the difficulty of movement of dislocations through γ'/γ microstructure [3].

Inconel 718 has numerous applications due to its unique properties like the ease and economy with which it can be fabricated. Good tensile, fatigue, creep and rupture strength have resulted in wide range of applications. Examples of these are components for liquid fuelled rockets, rings, casings and different sheet metal parts for aircraft and land-based gas turbine engines, and cryogenic tanks. It is ideal for making hot extrusion tooling. It is also used for fasteners and instrumentation parts [2].

1.1.3 Machining and Machinability

Machining is the process of removal of unwanted material from a workpiece in the form of chips. If the workpiece is a metal, then it is called metal cutting [4]. It is one of the most important manufacturing processes. Parts manufactured by other manufacturing processes, including near-net and net-shape methods have to be further processed by machining to satisfy the present day requirements of the designs. The parts must be interchangeable, reliable which require the part to be manufactured with precise dimensional tolerances. Machining is required

at various stages of production, ranging from rough cuts for cleanup of castings and forgings to high precision work with tolerances in microns [5].

Importance of machining activities can be understood from the following statement of M.E. Merchant, "Today in industrialized countries, the cost of machining amounts to more than 15% of the value of all manufactured products in those countries"[6]. In US alone, over $100 billion is spent on metal removal operations. Machining industry converts 10% of all the metal produced into wastage. By correct choice of tooling and selection of process parameters, savings to the tune of 20% are possible [7]. Such savings can provide a competitive edge in terms of improved quality and lower costs.

Machinability can be defined as the ease with which the material can be machined. The word ease of machining is vague and the criteria to be considered depend mainly on the design requirements. The criteria commonly used are:

1. Tool life
2. Cutting forces on tool and power consumption
3. Surface finish

1.2 Motivation for the present work

Beginning with the work of F.W. Taylor in 1880, a great amount of research has been done on machining which helped in understanding the process and the surfaces produced by the processes. This has helped in improving the productivity of the process. The complexities involved in analyzing the machining process are:

1. Work hardening of the previous processes plays an important role
2. Different materials have different mechanisms of material removal
3. The process is asymmetrical and unconstrained except for one side i.e. bounded by the cutting tool
4. Strain and strain rates are very high
5. The process is sensitive to variations in tool geometry, tool material, temperature, environment (cutting fluids) and process dynamics (chatter and vibration).

These complexities make mathematical modeling of the process difficult. Though simple models for understanding basic mechanics have been developed, they cannot be used directly for parameter selection and tooling analysis. The analysis of the process is hence done by the use of statistical methods to develop empirical models, other experimental studies.

Inconel 718 has excellent properties suitable for aerospace applications. But machining Inconel 718 is challenging because of the following reasons [8]:

1. High strength results in higher cutting forces resulting in higher temperature at the tool tip.
2. Low thermal conductivity (around 11W/m^{o}C) of Inconel 718, results in lower removal of heat through chip, thus further increasing temperature at the tip.
3. The presence of hard, abrasive inter-metallic compounds and carbides causes severe abrasive wear.
4. High work hardening causes notching of the tool. This can cause burrs on the workpiece.
5. Metallurgical route by which component is produced has an important effect. It is easier to machine Inconel 718 in solution annealed condition than in heat-treated condition.
6. As the components are used in critical applications, care has to be taken to ensure surface integrity of the component's surface.
7. Due to high toughness and high forces involved, the material tends to form pressure welds, thus resulting in built-up-edge (BUE).

A common strategy used for all high strength materials is the use of flood coolant for the purpose of chip breakage and reducing the temperatures around the cutting zone. With increasing environmental regulations and high cost of coolant application which is 8-10% of the total cost (when the tooling costs are around 5-7%), this solution is not sustainable [6].

From the above discussion, the motivation for the present work can be summarized as:

1. Developing an experimental strategy for analysis of machining process in face milling of Inconel 718.
2. Establishing process parameters and optimizing the machining of Inconel 718
3. Using an alternative metal working fluid application to make the process sustainable.

2 REVIEW OF LITERATURE

2.1 Introduction

Inconel 718 is a gamma prime strengthened alloy that can be used up to 1300^0F temperature [8]. It is extensively used in gas turbines and cryogenic storage tanks. With the advantages of ability to age and work hardening; it has become an important part of the aerospace industry. However, it is a difficult to machine because of the following reasons:

1. Rapid work hardening
2. High heat generated during cutting
3. High cutting forces due to their strength

Due to the above reasons, use of flood coolant has been a very important strategy for machining. With increased coolant costs and tighter environmental regulations, use of alternative coolant strategies needs to be explored. The present chapter discusses the previous studies that have been carried out in machining of Inconel 718 and various strategies used to improve productivity.

2.2 Literature Review

The Literature review has been divided into the following areas:

1. Machining studies
2. Metallographic studies
3. Modeling and optimization
4. Metal working fluid application strategies

2.2.1 Machining studies

Machining involves very high strain rates coupled with sliding along the rake and flank surfaces. This makes machining highly complex to analyze and develop simple models from the physics of the problem. This has resulted in conducting extensive machining studies to understand the effect of various parameters on the cutting forces and the quality of surface produced during machining. The present discussion focuses on machining studies conducted on Inconel 718.

Hashmi et al, [3] studied the influence of the machining conditions on the average cutting forces for half-immersion end milling in the up and down-milling modes. Because Inconel 718 is a nickel-based alloy that is difficult to machine, a high cutting force being generated in the machining of this advanced material. The cutting tests were carried out under dry conditions

using carbide inserts. The cutting forces decrease as the cutting speed increases for up-and down-end milling. The cutting forces increase as the feed rate increases for up-and down-end milling. The cutting forces increase as the axial depth of cut increases for up-and down-end milling.

Sharif et al, [9] studied the cutting performance and failure characteristics of two PVD TiN coated and uncoated tungsten carbide grades with identical geometry. Face milling tests of Inconel 718 super alloy were performed to investigate the effect of cutting speed and feed on tool performance under wet conditions. It was noted that coating resulted in marginal improvement, as it was delaminated by adhering work piece material at the beginning of the cut, impeding the performance of the tool for the rest of the experiment. The coated tools were tested at the cutting speeds of 25, 50, 75 and 100 m/min. The purpose of testing the coated tools at cutting speeds of 75 and 100 m/min was to investigate the behavior of coating at high cutting conditions. Testing of uncoated carbide tool was done at 25 and 50 m/min in order to compare with the coated tools under identical conditions of cutting. Depth of cut was 1 mm and feed rates were 0.08 and 0.14 mm per tooth, and were kept constant during the machining trials. A combination of progressive chipping and flank wear was the general mode of failure, former being dominant at high speeds and latter at the low speed region. Results showed that uncoated tool performed better than coated tools at low speed while coated tools gave slightly better performance as the speed was raised.

Li et al, [10] have carried their research work on the tool wear propagation and cutting force variations in the end milling of Inconel 718 with coated carbide inserts. The experimental results showed that significant flank wear was the predominant failure mode affecting the tool life. The tool flank wear propagation in the up milling operations was more rapid than that in the down milling operations. The cutting force variation along with the tool wear propagation was also analyzed. While the thermal effects could be a significant cause for the peak force variation within a single cutting pass, the tool wear propagation was believed to be responsible for the gradual increase of the mean peak force in successive cutting passes. The variation of the peak cutting force components was analyzed. It was found that for each cutting pass, the peak values of the cutting force components showed a steady increase within a certain range. The force variation ranges overlapped between successive cutting passes. Along with the tool wear propagation in successive cutting passes, the overall trend of the mean peak values in the X, Y, and Z directions for both the down and up milling operations was in a gradual increase. Variation of the peak cutting force components could be attributed to a number of possible

factors. The relationship between tool wear propagation and cutting force variation can be used for machining process planning and for the development of effective tool condition monitoring strategies.

Muammer Nalbant et al, [11] studied the effects of cutting tool coating material and cutting speed on cutting forces and surface roughness. For this purpose, nickel based super alloy Inconel 718 is machined at dry cutting conditions with three different cemented carbide tools in CNC lathe. Metal removing process is carried out at five different cutting speeds (15, 30, 45, 60, 75m/min) while 2mm depth of cut and 0.20mm/rev feed rate are to be constant. Main cutting force is considered as a criterion. In the experiments, depending on the tool coating material, lowest main cutting force is found to be 506 N at 75 m/min with multicoated cemented carbide insert whose top layer is coated by Al_2O_3. Lowest average surface roughness (0.806 μm) is obtained at the cutting speed of 15 m/min with single coated (TiN) cemented carbide inserts.

Rahman et al, [12] studied the effect of cutting conditions on the machinability of Incone1 718. Flank wear of the inserts, workpiece surface roughness and cutting forces will act as the performance indicators for tool life while machining is carried out using a CNC lathe. Two types of coated cemented carbide inserts, grades EH20Z-UP (TiN coated by physical vapour deposition) and AC25 (TiN coated by chemical vapour deposition), were used. Various combinations of side cutting edge angles (SCEA), cutting speeds and feed rates were tested at a constant depth of cut. Cutting results indicate that SCEA, together with cutting speed and feed rate, do play a significant role in determining the tool life of an insert when machining Inconel 718.

Arunachalam et al, [13] have carried their research to study the residual stresses and surface finish components of surface integrity when machining (facing) age hardened Inconel 718 using two grades of coated carbide cutting tools specifically developed for machining heat resistant super alloys. The cutting conditions were obtained from investigations based on optimum tool performance. The effect of insert shape, cutting edge preparation and nose radius on both residual stresses and surface finish was studied at this optimum cutting condition. This investigation suggested, that coated carbide cutting tool inserts of round shape, chamfered cutting edge preparation, negative type and small nose radius (0.8mm) and coolant will generate primarily compressive residual stresses.

Li et al, [14] studied the importance of cutting speed on tool wear and tool life when cutting nickel based alloys with carbides and ceramics. For optimizing the cutting speed in the turning of Inconel 718, a series of tool life experiments has been carried out using various coated

carbides and ceramics by means of rapid face-turning without coolant. At lower speeds (120 m/min), the tools are prone to depth-of-cut (DOC) notching, with minimal damage to the tool nose. A transition is observed at about 240 m/min, increasing the speed to 300 m/min leading to a reduction in DOC notching and an increase in nose and flank wear. The experiment results show that PVD-coated carbides KC7310 are more suitable for cutting Inconel 718 than CVD-coated carbides KC935, and ceramic inserts of KY2000 with negative rake angle and KY2100 of round type are the best choice for the high speed turning of Inconel 718. Based on the Taylor equation and the minimum production time, the optimum cutting speed was optimized in the cylindrical turning of Inconel 718 for each tested insert.

Costes et al, [15] carried the research work by using new tool materials such as cubic boron nitride (CBN) or ceramics for increasing productivity when machining heat resistant alloys. However, CBN tools are mostly used by the automotive industry in hard turning, and the wear of those tools is not sufficiently known in aerospace materials. In addition, the grade of these tools is not optimized for super alloys because they belong to a small part of the market (although expanding at a reasonable rate). So, this investigation has been conducted to show which grade is optimal and what the wear mechanisms are during finishing operations of Inconel 718. It is shown that a low CBN content with a ceramic binder and small grains gives the best results. The wear mechanisms on the rake and flank faces were investigated. Through SEM observations and chemical analysis of the tested inserts, it is shown that the dominant wear mechanisms are adhesion and diffusion due to chemical affinity between elements from workpiece and insert.

Fang and Wu [16] investigated high speed turning on Ti–6Al–4V and Inconel 718 for a comparative study to find out whether research finds of one material can be applied to another. All the 3 components of forces were analyzed. It has been found that cutting forces are significantly dependent on interactions between work material, geometry of the tool and cutting conditions.

Cantero et al, [17] observed wear patterns in finish turning of Inconel 718. Turning tests were carried out on Pinacho smart turn 6/165 two insert based on CP500 and TS2000 substrate equipped with Kistler dynamometer 9257B for cutting force measurement in coolant and dry condition. For insert with substrate CP500 Kr 0, dominant wear modes were notching in all tested conditions and reduced tool life was observed. This material is not proper in machining Inconel 718 in the conditions involved in tests. For insert with substrate TS2000 Kr 0, BUE, chipping and notch wear were observed. In dry turning, flank wear caused tool life termination

at 50 m/min in 9 minutes. For 70 m/min, chipping caused tool breakage in 2 minutes and did not allow the flank wear to evolve. Use of coolant increased tool life but could not avoid chipping. When insert with substrate TS2000 Kr 45 was used, chipping wear was diminished and BUE and notching was avoided for lower speed and for higher speed chipping occurred at early stages only.

Liao et al, [18] investigated behaviour of end milling Inconel 718 super alloy by cemented carbide tools. End milling of Inconel 718 under various cutting speeds by cemented carbide tools was conducted. Tool failure, at lower speeds, is mainly in the form of chipping and breakage of the cutting edge. At medium cutting speeds, reduction of cutting force is seen and tool life is improved with the increase of speed. But when cutting speed is further increased, most of the chips are welded to tool. The cutting temperature would rise drastically and plastic deformation of cutting tool takes place eventually. Based on this study, it is found that high cutting temperature and difficult chip disposal are two main problems encountered in high speed end milling of Inconel 718. Cutting speed is related closely to cutting force and tool wear/failure in end milling of Inconel 718 alloys. The effect of feed is relatively insignificant.

Dudzinski et al, [19] found that cemented carbide tools are largely used for machining nickel-based alloys. At very low cutting speeds of 20–30 m/min, the K20 grade appears to be the best for cutting Inconel 718. Higher cutting speeds, certainly up to 100 m/min, under dry conditions may be achieved with coated carbide tools. The PVD (Ti,Al) N coating seems to be the most suitable. It displays high oxidation resistance, high-temperature chemical stability, high hot hardness and low thermal conduction.

Chun et al, [20] conducted tests using uncoated, TiN coated, and TiCN coated cemented tungsten carbide equal to ISO K10 (WC-Co type). These inserts have round cutting edges of radius 5 mm. Milling parameter fixed throughout these trials was a depth of cut 0.3 mm, cutting speed was 50~250 m/min, feed rate 0.02, 0.05, 0.1 and 0.12 mm/tooth. The dominant wear model, flank wear, affects tool life at lower cutting speeds; crater or notch wear affects tool life at higher cutting speeds. The rapid wear of uncoated carbide tools suggests that these tools are not suitable for machining nickel based alloy. A coating is absolutely necessary to obtain sufficient tool life and an acceptable surface integrity. The TiCN coating seems to be the better coating to limit welding and unstable built-up-edge. Abrasive wear is also reduced by its higher hardness. Surface roughness increased during tool life due to wear on the cutting edge. Results show that the TiCN coated tool produces lower values of surface roughness at higher cutting

speeds. The workpiece surface was damaged due to chip adhesion at high cutting speed when worn out tools were used.

The important conclusions can be summarized as follows:

1. Studies were conducted mainly in turning and end milling. Very few studies were conducted on face milling.
2. Input parameters mainly studied are cutting parameters i.e. speed, feed and depth of cut. Some studied SCEA (Side cutting edge angle) as an input parameter.
3. Cutting inserts used were mainly coated carbides. They have been compared with Ceramics and uncoated carbides. Coated carbides have been found to perform better than uncoated ones. Ceramics have been used in some high speed machining operations.
4. Effect of speed and feed on cutting force and surface roughness has been studied. Some papers have focused on interactions between input parameters.
5. Comparative studies on various coating materials have been conducted

2.2.2 Metallographic studies

Metallography is the study of physical structure and components of metals and alloys using microscope. In metal cutting, it allows us to understand type of wear by analyzing chemical composition and surface of tool insert, workpiece and chip. Surface analysis helps us in ascertaining adhesion and abrasive wear, while chemical composition analysis is useful for finding out diffusion wear. The following studies give an overview of metallographic studies used in machining studies.

Dosbaeva et al [21] studied the origin of defects during machining of direct aged (DA) Inconel 718 super alloy by understanding tool wear. Optical metallography and SEM/EDS have been used to make metallographic observations. Morphology of machined parts and cross sections of machined surface have been investigated to understand the origin of defects. The cracks on the machined surface are due to shearing of primary complex TiC/NbC carbides present in Inconel 718 DA alloy. It has also been observed that Nb-rich regions interact with the environment during machining forming a low strength oxide layer that results in tears on the surface.

Fox et al [22] investigated the effect of nano-multilayered AlTiN/Cu PVD coating on tool life. Studies of the structure, properties, tribological and wear performance of the nano-multilayered AlTiN/Cu PVD coating have been performed. The structure of the coating has been investigated using High Resolution Transmission Electron Microscopy. Various properties of the coating

including microhardness, thermal conductivity and coefficient of friction vs. temperature were measured and tool life, wear behaviour and chip formation was observed. Because of the self-lubricating property of the coating and low thermal conductivity, tool life has increased.

Sonawane et al [23] carried out deformation studies by the use of quick stop device and photomicrographs of high-speed machining [2.24]. It has been found that shear angle is reduced and shear plane is converted into shear body when serrated chips formed were analyzed. Cracks appeared and adiabatic shear that occurred was also analyzed. Shear strain, shear strain rate and shear stress model in the adiabatic shear band were established. The effects of cutting parameters on character of the serrated chip were studied through observing chip metallographic graph.

Cutting performance and wear characteristics of PVD coated and uncoated tools in Face milling Inconel 718 was studied using identical geometry [9]. Tools were observed under SEM after 5s and tool failure to understand the wear phenomena. It has been found that chipping was predominant at low speeds and thus uncoated carbides were preferred. At high speeds, flank wear was predominant suggesting the use of coated carbide tools to reduce the effect.

Basim and Bashir [24] presented the results of experimental work in dry turning of nickel based alloys (Haynes – 276) using Different tool geometry of cemented carbide tools. The turning tests were conducted at four different cutting speeds (112, 152, 201and 269 m/min) while feed rate and depth of cut were kept constant at 0.2 mm/rev and 1.5 mm, respectively. The tool holders used were SCLCR with insert CCMT-12 and CCLNR – M12-4 with insert CNGN-12. The influence of cutting speed, tool inserts type and workpiece material was investigated on the machined surface roughness. The worn parts of the cutting tools were also examined under scanning electron microscope (SEM). The results showed that cutting speed significantly affected the machined surface finish values in relation with the tool insert geometry. For the same cutting conditions, the maximum cutting speed possible was 112m/min for CNGN-12 while it was 269m/min for CCMT-12.

Devillez et al, [25] associated dry machining and high cutting speeds to study the behaviour of coated carbide tools during orthogonal cutting tests. Cutting and feed forces were measured and tool wear mechanisms analysed for various cutting conditions. For the 0.1 mm/rev feed rate and the uncoated tool, the forces decrease with the cutting speed and their values are in the range 200–1000 N. For the same feed rate, the forces measured with all the coated tools are in a lower interval 200–600 N. At this higher feed rate and independent of the tested tool, the cutting forces values are in the same range 300–1000 N. Greater cutting speeds increase drastically the tool

wear rate and are inadequate for dry machining Inconel 718 with cemented carbide coated tools. Rapid cutting edge chipping and breakage are observed at cutting speeds equal to and higher than 100 m/min, which modify greatly the chip formation and the chip flow on the rake face and may explain the increasing of cutting force ratio beyond this critical value of 100 m/min. The dominant wear modes observed at the early stage of cutting are welding and adhesion of workpiece material onto the cutting tool faces. Work material adheres to the cutting edge to form a built-up-edge (BUE), and a built-up-layer (BUL) on tool faces. The use of energy dispersive X-ray analysis and white light interferometer to observe the wear mechanisms is very convenient. Energy dispersive X-ray allows the composition analysis of the tool wear patterns, particularly the characterisation of the built-up-layers observed after dry machining Inconel 718. It can be noted that the built-up-layer, if it is stable, has protective effect on the tool, more precisely on the cutting edge. A good correlation was observed between the evolution of the cutting forces and the tool wear.

Thakur et al, [26] studied the effect of machining parameters on the surface characteristics/quality of the machined part with respect to the specific cutting pressure, micro-structural alteration and micro-hardness while high speed dry turning of super alloy Inconel 718. The specific cutting pressure was chosen as a process indicator to determine the machinability of Inconel 718. It is usually influenced by the cutting speed and material. The specific cutting pressure is a function of cutting force and also specific cutting pressure decreases with increasing speed for a given feed and depth of cut. At low values of the feed rate, the material is subjected to lower strain rate. Also, the results indicate a reduction of specific cutting pressure as cutting speed is increased at constant feed rate and depth of cut, probably due to the reduction of the shear strength of the material caused by the increase of temperature in the cutting zone. Microstructure is observed to find some alterations caused by the chip removal process. It is seen clearly from the microstructure of raw material before machining that it consists of equiaxed grains of gamma (γ) austenitic phase. But, after machining there was grain refinement and grain deformation. From figures it is clearly observed that in the case of the machined surfaces that there are deformed grains with deformed twin bands and also some slip lines get formed during cutting process. From the microstructure it was observed that in case of machining of Inconel 718 the plastic deformation rate is high compared to other steels having equivalent hardness. It means that the amount of plastic deformation in cutting low thermal conductivity material, Inconel 718 is high. The degree of work hardening and its extent can be reduced by using properly optimized cutting parameters during high speed machining.

The important applications of metallographic studies in machining can be summarized as follows:

1. Use of SEM/EDS for metallographic observations to understand wear phenomena, formation of BUE (Built Up Edge) and BUL (Built Up Layer)
2. Morphology studies on cross sections of machined surface to understand origin of surface defects
3. TEM (Transmission Electron Microscopy) to study structure of coating.
4. Use of quick stop device and photomicrograph to study high speed machining for analyzing shear zone
5. EDX analysis for characterization of Built-up layers after dry machining, residual stresses
6. Observing micro-structural changes in the material before and after machining.

2.2.3 Modeling and optimization

Modeling can be defined as the process of developing a mathematical expression that can be used to estimate output parameters of a system from the given set of input parameters. As conducting machining experiments is time consuming and expensive, developing models from the experimental data can reduce the amount of experimentation for future applications of the tool and workpiece combination. It also helps us in understanding the effect of different parameters on the machining process. Optimization is the selection of best possible input parameters for a given criteria on the outputs. In case of machining, the criteria can be minimum tool wear, minimum cutting time, best surface quality, least cutting force or a combination of these criteria. The following study discusses the important methods used in metal cutting studies.

Anderson et al, [27] presented a cutting force model for multi-toothed cutting processes, including a complete set of parameters influencing the cutting force variation that has been shown to occur in face milling, and to analyze the extent these parameters influence the total cutting force variation for selected tool geometry. The scope is to model and analyze the cutting forces for each individual tooth on the tool, to be able to draw conclusions about how the cutting action for an individual tooth is affected by its neighbours. The experimental results from the case studied in this paper show that there are mainly three factors influencing the cutting force variation for a tool with new inserts. Radial and axial cutting edge position causes approximately 50% of the force variation for the case studied. Approximately 40% arises from

eccentricity and the remaining 10% is the result of spindle deflection during machining. The experimental results presented in the work show a new type of cutting force diagrams where the force variation for each individual tooth when two cutting edges are engaged in the workpiece at the same time. The wear studies performed shows are distribution of the individual main cutting forces dependent on the wear propagation for each tooth.

Choudhury et al, [28] presented the Taguchi optimization methodology, which is applied to optimize cutting parameters in end milling when machining hardened steel AISIH 13 with TiN coated P10 carbide insert tool under semi-finishing and finishing conditions of high speed cutting. The milling parameters evaluated are cutting speed, feed rate and depth of cut. An orthogonal array, signal-to-noise (S/N) ratio and Pareto analysis of variance (ANOVA) are employed to analyze the effect of these milling parameters. The analysis of the result shows that the optimal combination for low resultant cutting force and good surface finish are high cutting speed, low feed rate and low depth of cut. Using Taguchi method for design of experiment (DOE), other significant effects such as the interaction among milling parameters are also investigated. The study shows that the Taguchi method is suitable to solve the stated problem with minimum number of trials as compared with a full factorial design.

Vosniakos et al, [29] presented a neural network modeling approach for the prediction of surface roughness (Ra) in CNC face milling. The data used for the training and checking of the network's performance were derived from experiments conducted on a CNC milling machine according to the principles of Taguchi design of experiments method. The factors considered in the experiment were the depth of cut, the feed rate per tooth, the cutting speed, the use of cutting fluid. The responses measured were the engagement and wear of the cutting tool and the three components of the cutting force. The feed forward artificial neural networks (ANNs) trained with the Levenberg–Marquardt algorithm. The most influential of the factors were determined using DoE principles. The ANN model was able to predict the surface roughness with a mean squared error equal to 1.86% and to be consistent throughout the entire range of values.

Yung-Kuang et al, [30] have carried the research work in optimization of CNC turning operation parameters for SKD11 (JIS) using the Gray relational analysis method. Nine experimental runs based on an orthogonal array of Taguchi method were performed. The surface properties of roughness average and roughness maximum as well as the roundness were selected as the quality targets. An optimal parameter combination of the turning operation was obtained via Gray relational analysis. By analyzing the Gray relational grade matrix, the degree

of influence on each controllable process factor on to individual quality targets can be found. The depth of cut was identified to be the most influential on the roughness average and the cutting speed is the most influential factor on the maximum roughness and roundness. Additionally, the analysis of variance (ANOVA) is also applied to identify the most significant factor; the depth of cut is the most significant controlled factors for the turning operations according to the weighed sum grade of the roughness average, roughness maximum and roundness.

Thakur et al [31] studied the relationship of degree of work hardening and tool life as a function of cutting parameters like cutting speed, feed, depth of cut, untreated tungsten carbide and cryogenic-treated tool. It has been found that proper selection of cutting parameters minimized work hardening characteristics and improved tool life.

Manoj et al, [32] studied on the boro-carburizing and boronizing of AISI 1015 steel on tensile strength and it was carried out by Taguchi -gray relational method. The orthogonal array $L_9(3^4)$ was used to conduct the experiment. The thickness of boride layer increased with increase in process temperature and time. The thickness of boride layers for boronized AISI 1015 steel was more than the pre-carburized and boronized AISI 1015 steel. The micro hardness decreased with increase in distance from the surface to the core. However, the hardness gradient reduced gradually from the surface to the core in case of boro-carburized treatments compared to boronized treatments. The optimal process parameters and their levels for pre-carburized AISI 1015 steel are carbon content 0.45% at 950 ºC temperature and 4h process duration. The results revealed that process time, case carbon content and process temperature influenced the yield strength and percentage elongation. The ultimate strength is influenced by the process temperature, process time and carbon content. The process temperature was the most influential control factor that affects the tensile strength properties.

Kurt [33] carried out Experimental and theoretical analysis of forces in turning. Stresses have been calculated by using FEM. Mathematical models for forces and stresses have been developed using ANN. From FEM analysis it has been found that insert may be worn at distance equal to the depth of cut on the base cutting edge of the cutting tool. The wear mode can be predicted as mainly notch wear.

Senthilkumar et al [34] carried out optimization of parameters for machining of Inconel 718. Genetic algorithms coupled with artificial neural networks were used to develop models. The results of the model were plotted as Pareto optimal front and are used to obtain optimal

machining parameters. Predicting surface roughness was not possible as both main effects and interactions were not significant. In facing operation, feed was found to be statistically significant factor on surface roughness.

Uhlmann et al [35] developed a 3D Finite Element model to analyse the entire physical phenomena in large elastic-plastic deformations during machining. A comparative study between ABAQUS and DEFORM 3D was carried out. Temperature, strain and stress distributions for different speeds were computed using the model and compared with the experimental results. It is found that material model with flow softening predicted forces and chip formation closely compared to traditional Johnson-cook model.

Pawade et al [36] along with cutting parameters, varied approach angle to evaluate the effect on surface roughness and forces in face milling. L9 orthogonal array was used for DOE. Gray relation analysis was carried out for multi-objective optimization. The optimized parameters were found to be Cutting speed 475m/min, feed rate 0.1mm/rev, depth of cut 0.5mm and CW2 edge geometry.

Chandra Nath et al [37] have conducted machinability studies on face milling with Indexable copy face mill inserts on materials like SS 403cb+, Inconel 718 and Inconel 625. The input parameters are cutting speed and feed rate. The response parameters were tool life and wear, material removal rate and force coefficients. It has been found that Inconel 625 has poorest machinability. The cost of machining was found to be 5 to 6 times more for Inconel 718 and 625 when compared with SS 403cb+.

The methods used for modeling and optimization can be summarized as follows:

1. Analysis of milling forces for the effect of multiple tooth and development of new cutting force diagrams.
2. Analysis of effect of parameters at various cutting parameter ranges.
3. Conducting experiments based on Design of Experiments (DOE) methodology.
4. Taguchi method for optimization involving orthogonal array, S/N ratio and Pareto analysis of ANOVA (Analysis of Variance). It is also useful for finding the effect of interaction of various parameters.
5. Use of ANN (Artificial Neural Networks) for model development.
6. Genetic algorithm coupled with ANN was used for model development.
7. FEM used for estimating stresses, temperature, and stress- strain distributions.
8. Gray relational analysis was used for multi-objective optimization

2.2.4 Metal working fluid applications strategies

Environmental hazards and rising metal working fluid costs have led to the development of dry machining. But high heat generated during dry machining can cause considerable thermal expansion that can cause dimensional and geometric errors. This has led to the development of Minimum Quantity Lubrication (MQL) or also known as Near Dry Machining (NDM). The following papers give a brief overview of various strategies used in MQL.

Kamata et al, [38] studied the effect of Minimal quantity lubrication (MQL) in finish-turning of a nickel-base super alloy, Inconel 718, with three different types of coated carbide tools. Three selected coatings were TiCN/Al2O3/TiN (CVD), TiN/AlN super lattice (PVD) and TiAlN (PVD). Cutting speeds were set at relatively higher values i.e.1 and 1.5m/s. At a cutting speed of 1.0m/s, TiCN/Al2O3/TiN coating in MQL cutting exhibited the best performance while TiN/AlN super lattice coating in MQL cutting exhibited the second best performance. The longest tool life was attained by TiCN/Al2O3/TiN coating in wet cutting, but the surface finish was not good. It was found that there is an optimum value for air pressure in finish-turning of Inconel 718 with MQL. It was also found in an experiment using argon as a carrier gas of oil mist that the carrier gas of MQL plays an important role for cooling the cutting point. As the cutting speed was increased to1.5m/s, the tool lives were drastically shortened. In addition, the surface finish in MQL cutting increased because the worn tool flank surface became rough.

Sridhara et al [39] summarized recent developments in research on the stability of nanofluids, enhancement of thermal conductivities, viscosity, and heat transfer characteristics of alumina (Al_2O_3) based nanofluids. Al_2O_3 particles in the range of 13-302 nm have been used to prepare nanofluids. Enhancement in thermal conductivity is 2-36%. The paper discusses the effect of volume fraction, particle size, base fluids, preparation method, and temperature on thermal conductivity of nanofluids.

Obikawa et al[40] have studied the effect of reinforced ceramic tool in air-jet assisted high speed machining of Inconel 718. It has been found that in air jet assisted machining, the width of flank wear lays an important role compared to size of notch wear. The mechanism of tool wear was notch and flank wear of SiC whisker reinforced alumina tool.

With a view to eliminate cutting fluids in machining Inconel 718 by using dry cutting at high speeds, Devellez et al [41] carried out experiments in dry and wet conditions. Micro-hardness and residual stresses were evaluated in both the cases. With proper parameter selection, the

surface quality has been found acceptable. No significant differences in residual stresses and micro-hardness have been observed in both cases.

Kurt [33] studied the effect of high pressure jet assistance (HPJA) in rough turning Inconel 718. An FE model has been developed to extract additional data and understand the influence of HPJA in comparison with dry machining. It has been observed that the jet is able to decrease the cutting forces, chip radius and tool–chip contact length. Contact pressure and temperature fields on the cutting tool are also reduced as well as the sticking part of the contact zone. Authors confirmed that the effects of convection are able to change and even amplify the influence of the pure mechanical load induced by the jet.

Zhang et al [42] investigated tool life and cutting forces in end milling under Minimum quantity cooling lubrication (MQCL). In order to reduce the impact of environmental effects of cutting fluids, bio-degradable oil like vegetable oil was used to prepare aerosol for MQCL. Tool wear and cutting forces were studied. Vegetable oil has been found to be effective in reducing forces and improving tool life.

Dhokia et al [43] carried out Cryogenic CNC end milling on Inconel 718 to study the effect of the coolant on surface roughness. The authors conclude Cryogenic cooling has significant potential in improving surface roughness.

The use of high pressure coolant enhances notch wear in ceramic inserts. To prevent this, Vagnorius [44] tried a SiAlON coating. It has been observed that though notch wear was present, it was not critical to affect tool life. Chip breaking was also found to have improved.

Vasu et al [45] prepared Nano-fluid using TRIM E709 emulsifier with Al_2O_3 nano-particles. This was used as a coolant to reduce heat in grinding. It was found that surface roughness and heat penetration decreased with the use of nano-cutting fluid.

Khandekar et al [46] analyzed wettability characteristics of nano-cutting fluid (Al_2O_3 based) on a carbide tool tip using the macroscopic contact angle method. Comparative study of tool wear, cutting force, workpiece surface roughness, and chip thickness among dry machining, machining with conventional cutting fluid as well as Nano-cutting fluids were cnducted. Nano-cutting fluids were found superior to both dry and wet machining.

Kaynak [47] studied the influence of Cryogenic machining for turning Inconel 718 and compared it with dry and MQL machining. The response parameters were, flank wear, crater wear, notch wear, cutting temperature, chip morphology and surface roughness of machined

samples. It was found tht effectiveness of cryogenic machining increased with use of great number of nozzles.

Le Coz and Dudzinski [48] have used thermocouples inserted in the workpiece surface and subsurface layers to measure machined surface temperature. The measurements were used to determine temperature gradients and used to reconstruct thermal heating of the cutting edge at every tool revolution and different cutting speed values. It has been observed that for low-conductivity materials like Inconel 718, the temperature rise was not observed at 0.5mm below the surface but was observed on the surface.

Cheng-Dong et al [49] have studied the application of environmentally friendly minimum quantity lubrication technology to Inconel 812 overlays. Inconel 182 overlays are used as anti-corrosion material in nuclear steam turbines. The effects of MQl have been analyzed using force signals in horizontal milling operations. MQL was found effective in up-milling where generally tool wear is dominant. MQL was found to be ineffective in down-milling as the self-excited vibrations due to large impact were intensified by the high speed droplets.

The methods used for lubrication from the literature can be summarized as follows:

1. Use of oil mist and Argon for cooling the cutting point
2. Enhancement of thermal conductivity by adding Al_2O_3 Nano-particles
3. Optimal parameter selection for dry machining can give similar surface quality as in case of wet machining
4. Use of High pressure jet assistance decreases chip radius and chip contact length. Along with the impact of jet, effects of convection reduce the temperature around the cutting zone.
5. Cryogenically treated tool provides improved tool life.
6. Use of bio-degradable vegetable oil to reduce the impact on environment
7. Improvement of surface roughness through cryogenic cooling
8. SiAlON coating to improve tool life when high pressure jet is used.

2.3 Objectives

The machinability studies conducted on Inconel 718 have been in turning and end milling operations. Very few studies have been devoted to face milling. Face milling is an important operation as it is mainly used for machining all the mating surfaces. Surface quality of the mating surfaces is an important criterion for leakage at the interface. With its application in aerospace industry, in depth analysis of face milling of Inconel 718 is essential.

Effect of tool holder parameters on the machining process is an important aspect especially in the case of high strength alloys where the tool life is in minutes. One of the important tool holder parameter in the case of face milling cutter is approach angle. It can affect the stability of the process as it directly affects the resultant force direction.

Use of coated cutting inserts for high strength alloy machining is now an industry standard due to their versatility and high tool life. Machining Inconel 718 using such established inserts provides a great cost advantage.

Use of fractional factorial experiments strategy from Design of Experiments (DOE) allows us to reduce the number of experiments to be conducted. This is essential especially for tool wear experiments which are time consuming where a large amount of material can be saved. The significance of cutting parameters and their optimization can be done through use of fractional factorial experiments.

Cutting parameters in some cases can produce interaction effects that are important to understand the productive region of the machining zone. Conducting full factorial experiments gives us an idea of all the interactions present and further the results are used in developing an ANN model. ANN requires high number of data sets for developing a satisfactory model.

Understanding mechanism of tool wear is essential for understanding the effectiveness of coating and for developing new coating materials. Mechanism of tool wear can change with changing cutting parameters. Thus, analyzing tool wear in the selected machining zone gives a comprehensive understanding of machining process. The mechanism of tool wear is analyzed by SEM and EDS analysis.

MQL and Nano-fluids have to be tested on Inconel 718. Effectiveness of MQL and Nano-MQL in relation to dry machining in case of face milling is yet to be analyzed. Analysis has to be done on a wide range of parameters to establish MQL conditions for machining Inconel 718.

From the above discussion, the objectives of the present work can be summarized as follows:

- To study the effect of approach angle and process parameters (speed, feed and doc) on tool life, cutting force and surface finish in face milling of Inconel 718.
- To optimize the process parameters in order to improve surface finish by using DOE and Gray Relation Analysis.
- To analyse the diffusion wear of insert using Energy dispersive Spectroscopy (EDS).
- To conduct full factorial experiments for developing an ANN model.
- To study the effect of vegetable oil, Al_2O_3 based vegetable oil Nano-fluid as an MQL coolant by comparing it with dry machining.

3 EXPERIMENTAL SETUP

Milling is an important operation for generating flat mating surfaces, where surface quality is an important aspect of their performance. For many components, milling can be the final operation. It is an intermittent process and is prone to vibration. Due to the action of multiple cutting edges, analysis of the process is very difficult. As the tool is in continuous rotation, no direct method of measuring tool wear can be applied. Thus, to understand the process, an elaborate set-up of various sensors is used. Indirect parameters such as cutting force, surface quality and acoustic emission are used to understand tool wear and to get the details of machining. These measured parameters are then correlated to tool wear measured at the end of each pass.

The chapter gives a detailed idea about milling with focus on face milling. It describes the equipment and the experimental set-up used to perform the study. A brief idea of the cutting insert and tool holder used for the experiment is given.

3.1 Introduction to Face Milling

Milling is a machining process that uses rotary multi-tooth cutters to remove material from the workpiece. The cutting tool is given rotary motion and the workpiece is given linear feed. It is the most common method to produce flat and prismatic surfaces. It is estimated that milling constitutes 28% of the total number of operations and 30% of the total machining time [50]. Milling is an intermittent process with non-uniform chip thickness. The cutter is subjected to high impact loads at the entry and the exit. This makes the process prone to vibration and chatter.

Face milling is the most widely used milling process. It involves high material removal and with the advent of CNC machines, understanding the process in great detail has become very important. Face milling can be considered analogous to face turning except that the cutter in milling is given rotary motion and the workpiece is only given feed. To analyze the process, understanding the geometry of the cutter is important.

3.1.1 Geometry of Face milling cutter

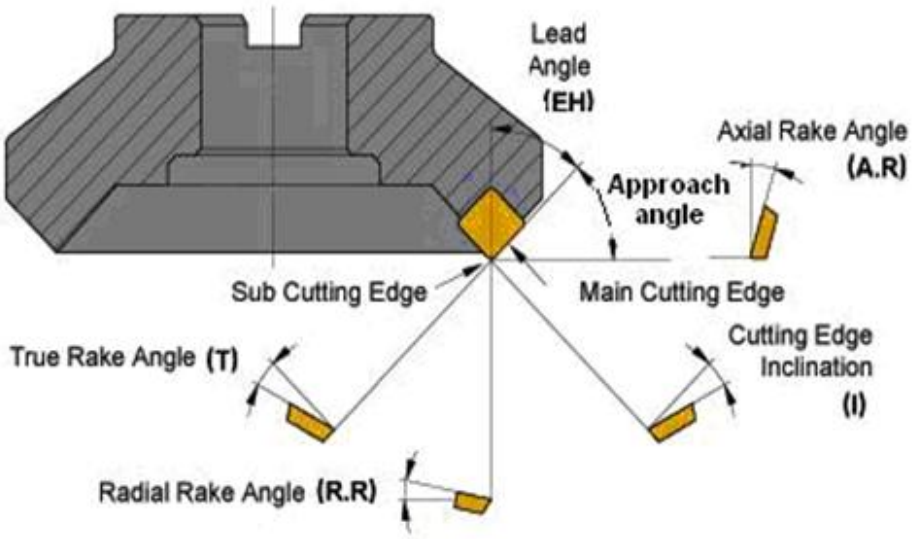

Figure 3.1 Face milling cutter nomenclature [51]

Figure 3.1 Face milling cutter nomenclature shows the nomenclature of the angles of a face milling cutter. The function and effect of each angle is summarized in the Table 2 below:

Table 3.1 Effect and function of angles of face milling cutter

Type of angle	Symbol	Function	Effect
Axial rake angle	A.R	Determines chip disposal direction	Positive value enhances Machinability
Radial rake angle	R.R	Determines sharpness of the edge	Negative angle helps in chip disposal
Approach angle	A.A	Determines chip thickness	Small values produce small chips but causes back force.
True rake angle	T	Determines actual sharpness	Large positive values enhance Machinability and causes minimum welding. Large negative angles are used when strong cutting edge is required
Inclination angle	I	Determines chip disposal direction	Large positive angles provide chip disposal but lowers cutting edge strength

3.1.2 Importance of Approach angle

Several factors must be considered to determine which approach angle is the best for a specific operation. The approach angle must be small enough to cover the depth of cut. The part being machined may require a large approach angle in order to clear a portion or form a certain shape on the part. As the approach angle decreases, the forces act in the direction of the work piece. This could cause deflections while machining thin sections of the part. The approach angle also determines the thickness of the chip. The lesser the approach angle for the same feed rate or chip load per tooth, the thinner the chip becomes. As in single point tooling, the depth of cut is distributed over a longer surface of contact. Therefore, approach angle cutters are recommended when maximum material removal is the objective. Thinning the chip allows the feed rate to be increased or maximized. Chip thickness is reduced by decreasing the approach angle for the same feed.

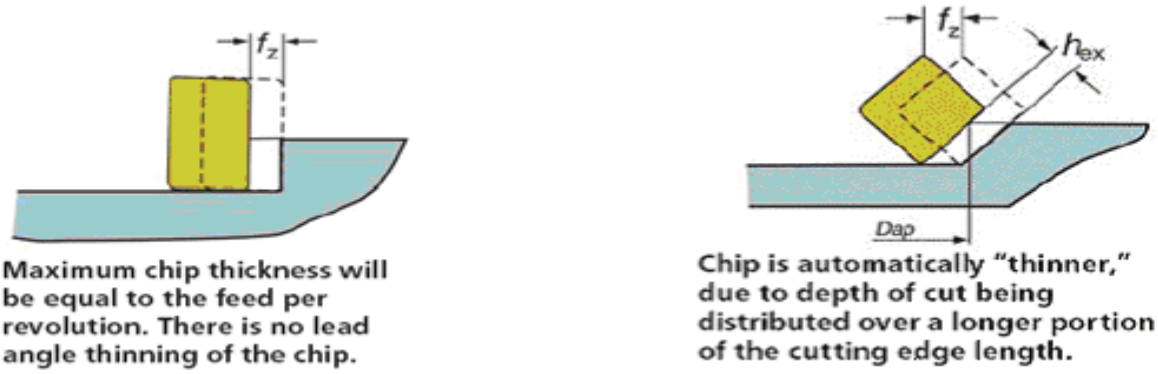

Figure 3.2 Variation of chip thickness with respect to approach angle [50]

Approach angles can range from zero to 45 degrees. The most common approach angles available on standard cutters are 0, 15, 30 and 45 degrees. Approach angles lesser than 45 degrees are usually considered special, and are used for very shallow cuts for fine finishing, or for cutting very hard work materials. Milling cutters with less approach angles also have greater heat dissipating capacity. Extremely high temperatures are generated at the insert cutting edge while the insert is in the cut. Carbide, as well as other tool materials, often softens when heated, and when a cutting edge is softened it will wear away more easily. However, if more of the tool can be employed in the cut, as in the case of lesser approach angles, the tool's heat dissipating capacity will be improved which, in turn, improves tool life.

An important factor in controlling chatter is that whenever the approach angle is decreased, axial force is increased and radial force is reduced. The use of less approach angle cutters is especially beneficial when machining materials with scaly or work hardened surfaces. With a less approach angle, the surface is spread over a larger area of the cutting edge. This reduces the detrimental effect on the inserts, extending tool life. Less approach angles will also reduce

burring and breakout at the work piece edge. The most obvious limitation on approach angle cutters is part configuration. If a square shoulder must be machined on a part, a 90 degree approach angle is required. It is impossible to produce a 90 degree approach angle milling cutter with square inserts because of the need to provide face clearance. Often a near square shoulder is permissible .In this case 89 degree approach angle cutter may be used.

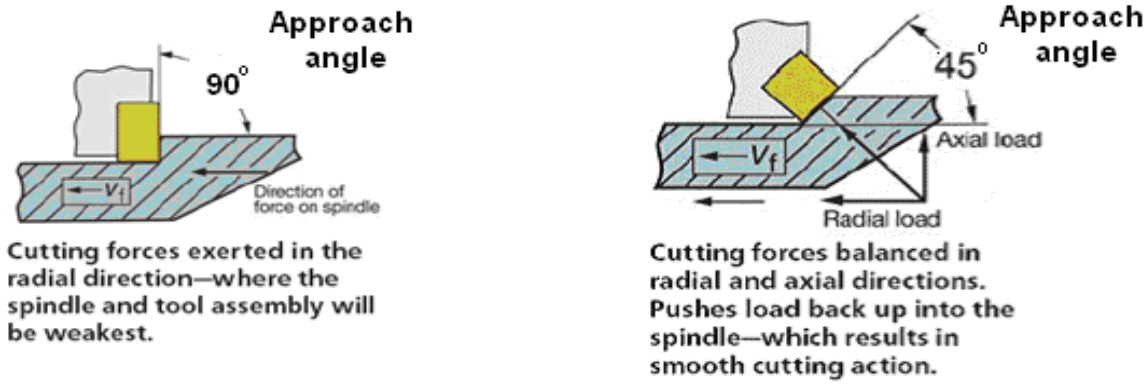

Figure 3.3 Variation of forces with respect to Approach angle [50]

3.1.3 Cutting Forces in Face milling

Cutting forces in milling are in 3 dimensions similar to turning operations as shown in Figure 3.4. They are as follows:

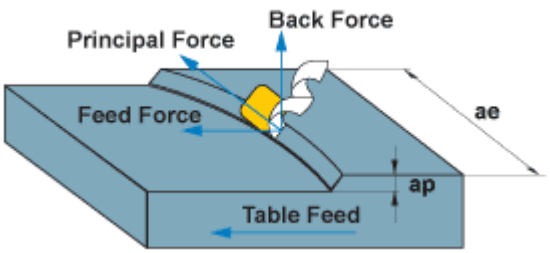

Feed Force - F_x

Principal Force/ Cutting Force – F_y

Back Force - F_z

Figure 3.4 Cutting forces in face milling

1. Principal force: It acts in the direction opposite to the milling cutter direction. This decides the motor power and torque required.
2. Feed force: It is in the direction of feed and is due to the table feed. This force affects the screw and nut mechanism and also acts as a radial force on the spindle. Higher values can cause spindle deflection and vibrations.
3. Back force: It acts in the axial direction pushing the cutter upwards. It is due to the depth of cut given during machining. The force acts on the thrust bearings of the spindle.

3.2 Experimental set-up

Experiments have been conducted in face milling on Inconel 718 using coated carbide tools. The present work is focused to study the effect of speed, feed, depth of cut and approach angle on cutting force (F_y), tool life (T) and surface roughness (R_a). Figure 3.5 shows the experimental set-up used for the study. The vertical milling machine was fitted with a face milling cutter. The work piece was held in a vice that was fixed on dynamometer as shown in the figure.

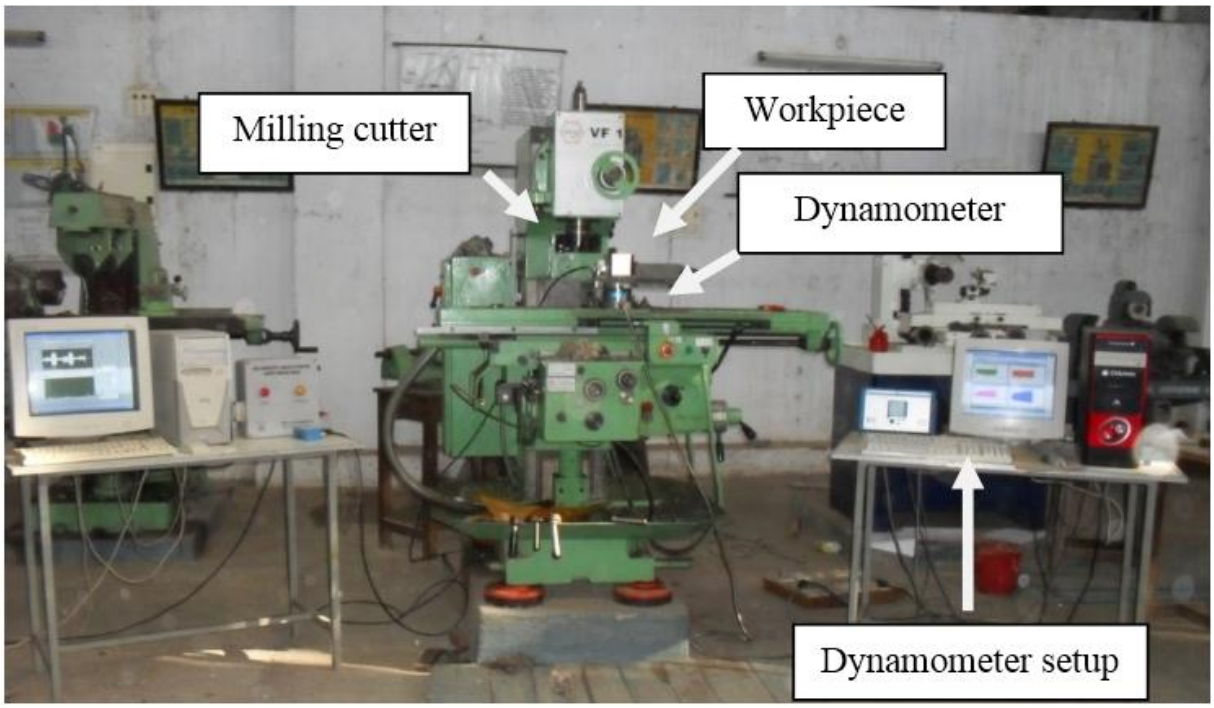

Figure 3.5 Experimental set-up

3.2.1 Work material

The workpiece material used in the machining test was Inconel 718. The dimension of the workpiece was 100 mm × 90 mm×75 mm. The hardness of the workpiece material was measured and found to be 38 HRC. The Inconel 718 alloy contains significant amount of iron, niobium and molybdenum along with lesser amount of Aluminium and Titanium. The chemical composition and mechanical properties of Inconel 718 are shown in Table 3.2 and Table 3.3 respectively.

Table 3.2 Composition of Inconel 718

Element	C	Si	Mn	Ti	Co	Cr	Fe	Mo	Nb	Al	Ni
Wt (%)	0.08	0.35	0.35	0.60	1.00	19.00	17.00	3.00	5.00	0.80	52.82

Table 3.3 Mechanical properties of Inconel 718

Property	Value
Tensile strength (MPa)	1310
Yield strength (MPa)	1110
Elastic modulus (GPa)	206
Poisson's ratio	0.28
Hardness (HRC)	38
Density (g/cm^3)	8.19
Melting point (°c)	1453
Thermal conductivity(W/m K)	11.4

3.2.2 Cutting tool and its accessories

The insert used in the machining test was Widia SPMW 120408 - TN 7535. The cutter used was a Widia M400 face milling cutter of diameter 150mm as shown in Figure 3.6. M400 cutter is a cartridge based milling system developed for flexibility. It can be used for face milling or square shoulder milling, roughing or finishing.

The following are the insert specifications:

- S – Insert shape (square)
- P – Normal clearance angle (11^0)
- M – Tolerance class
- W – Characteristic of insert fixing (With hole, without chip grooves, and one counter sink (40^0 -60^0)
- 12 – Length of insert (12 mm)
- 04 – Thickness (4.76 mm)
- 08 – Nose radius (0.8 mm)
- TN-7535- Grade of insert

The insert has three layers of CVD coatings TiN-TiCN-Al_2O_3 on a Cemented carbide substrate. The physical and chemical properties of Coated carbide tools are shown in Table 3.4. The top coating of TiN decreases a friction coefficient between the chip and the tool. Al_2O_3 coating in the middle layer is for adhesion resistance while TiCN coating is for abrasion resistance. It is used in medium and heavy machining for steel and nodular cast iron. It can be used for rugged

conditions. Thus, it can be used with Inconel 718, a super-alloy whose cutting can result in high forces and temperatures.

Table 3.4 Chemical and physical properties of carbide tools

Co (vol. %)	WC (vol. %)	TaC (vol. %)	NbC (vol. %)	Hardness (HV)	Grain size (mm)	Coating thickness(µm)		
						TiCN	Al_2O_3	TiN
17.1	81	1.2	0.6	2000	1.7	4	1	0.5

3.2.2.1 Milling cutter body

The cutter body has provision for replaceable cartridges which can accommodate various types of insert from WIDIA. Three cartridges have been designed for M400 milling cutter for different approach angles and single tip seat design.

Figure 3.6 Face milling cutter body

3.2.2.2 Cartridges

The design of all cartridges is based on past drawings and design standards of Kennametal. The axial rake angle -6º and radial rake angle -8º are used for design. These two angles are provided on the seat tip of the cartridge as shown in Figure 3.7. All the cartridges have the same axial and radial rake angle and only the approach angle is varied. These two rake angles should be the same for all cartridges because these angles will influence the cutting forces and the important dimensions such as overall length of cartridge after fixing in the insert (47 mm), thickness of cartridge (which is measured from base to the highest point of insert-15.88mm), counter bore dimension, thickness (15mm) and width (20mm) of cartridges are kept constant for all cartridges. 42CrMo4 material is used for manufacturing cartridges. Hardness of material is around 40 to 44 HRC. In the present context three cartridges of angles 35º, 45º and 55º have been used.

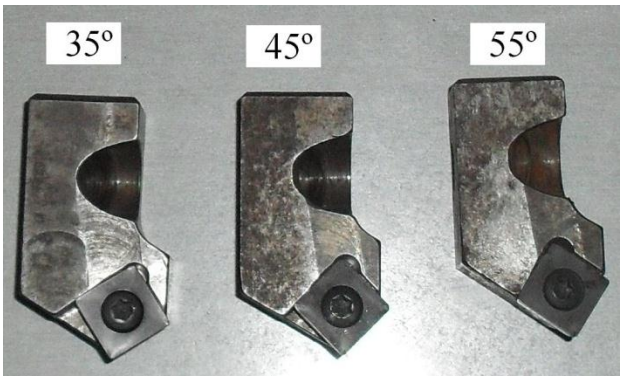

Figure 3.7 Cartridges for varying approach angle

3.2.3 Machine tool

The machine tool used in the cutting test was a three axis vertical milling machine tool of Bharat Fritz Werner Ltd. The machine table could be moved in Cartesian coordinates in X, Y and Z direction. A Kistler Type 9272 quartz three component dynamometer is mounted on the machine tool to measure the cutting forces. The workpiece is mounted on the dynamometer through a vice. Kistler Acoustic emission sensor of piezoelectric transducer type is mounted on the workpiece with the help of a magnetic clamp for sensing the acoustic signal generated during machining. Specifications of vertical milling machine are as follows:

Table 3.5 Specifications of vertical milling machine

Longitudinal movement	560 mm
Transverse movement	250 mm
Vertical movement	390 mm
Speed range	45-2000 rpm
Feed range	16-800 mm/min
Motor power	3 kW

3.2.4 Cutting force dynamometer

A Kistler Dynamometer is used to measure the cutting forces during milling operation. The multi component dynamometer provides dynamic and quasi-static measurement of the 3 orthogonal components of force (F_x, F_y and F_z) acting from any direction onto the top plate as well as the moment M_z. as shown in Figure 3.8. The dynamometer has the high rigidity and hence high natural frequency. The high resolution enables measuring very small dynamic changes.

3.2.4.1 Working Principle

The force and the moment M_z acting on the dynamometer are transmitted through the top plate to a 4 component load washer. This 4 component sensor consists of three pairs of quartz rings, where by one is sensitive to compression and the other two are sensitive to shear either X-resp, in Y-direction. An additional set of shear sensitive quartz plates is arranged on such a way to yield an electrical charge proportional to the moment M_z acting on the axis of the sensor. The acting force is directly resolved into its three components. The charges yielded by the quartz plates are collected with electrodes connected to the connector of the sensor.

Depending on the direction of the force and movements, positive or negative charges occur at the connections. Negative charges give positive voltages at the output of the charge amplifier, and vice versa.

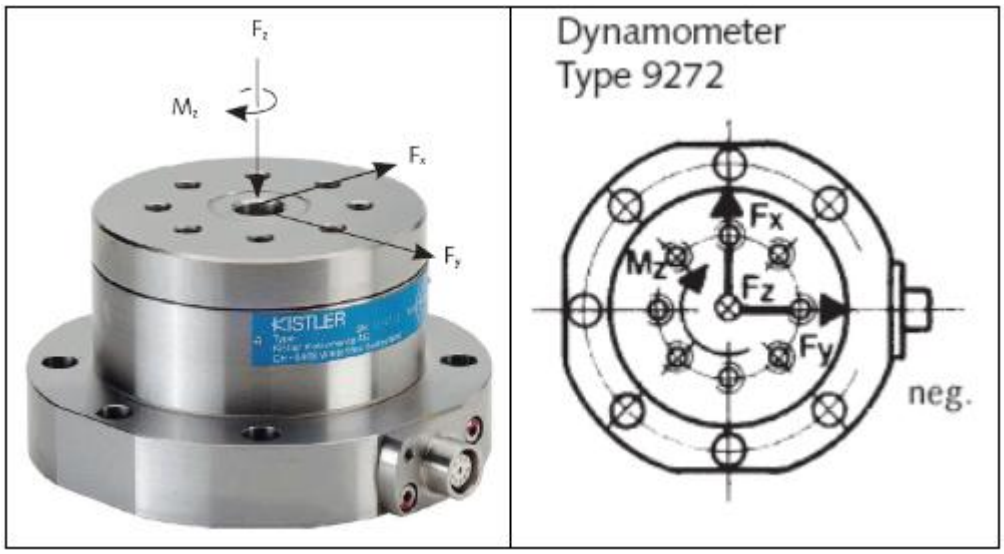

Figure 3.8 4-component Kistler Dynamometer

3.2.4.2 Measuring cutting force in Face milling

The machining force produced by the milling process is resolved directly into three significant components by the multi component dynamometer

- Feed force (F_x) is in the axial direction along the work piece
- Cutting force (F_y) is in the tangential direction
- Axial force, which is in the spindle direction

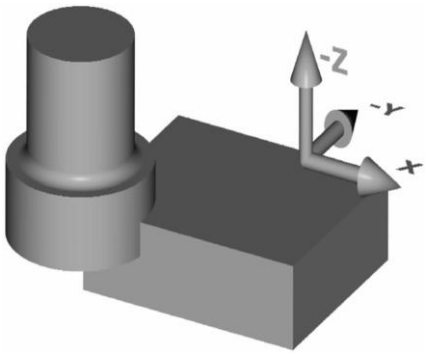

Figure 3.9 Components of Face milling forces

3.2.5 Surface roughness tester

Handy surf instrument is used to measure the surface roughness of components. It is based on a tactile measurement principle. The surface is measured by moving a stylus across the surface. As the stylus moves up and down along the surface, a transducer converts these movements into a signal which is then transformed into a roughness number and usually a visually displayed profile.

Figure 3.10 Measuring surface roughness using Handy surf

3.2.6 Tool Wear Measurement

The Mitutoyo Toolmaker's Microscope TM-500 is easy-to-use, compact-size Tool maker's Microscopes that feature a vertical supporting column. Designed with measurement of workpiece contours and inspection of surface features, the TM-500 supports a wide range of applications from shop-floor inspection, measurement of tools and machined parts, to precision

measurement of test tools in a measuring room. Figure 3.11 gives information about the parts of the Tool maker's microscope.

3.2.6.1 Specifications of Tool maker's microscope

a. Optical Tube

- Optical axis: 30° from vertical
- Cross-hair reticule
- Adjustable diopter
- Angle dial: Graduation 1°
    - Angle of rotation 360°
    - Angle reading 6' (Vernier)
    - Vernier zero position adjustable

b. Eyepiece

- Magnification 15x

c. Objective

- Magnification 2x
- Working distance: 67mm

d. XY stage

- Dimensions: 152 X 152mm
- Stage glass size: 96 X 96mm
- Maximum height: 115mm

e. Transmitted illuminator

- Light source: 24V, 2W
- Continuously adjustable light intensity
- Green filter

f. Surface illuminator

- Light source: 24V, 2W
- Continuously adjustable light intensity

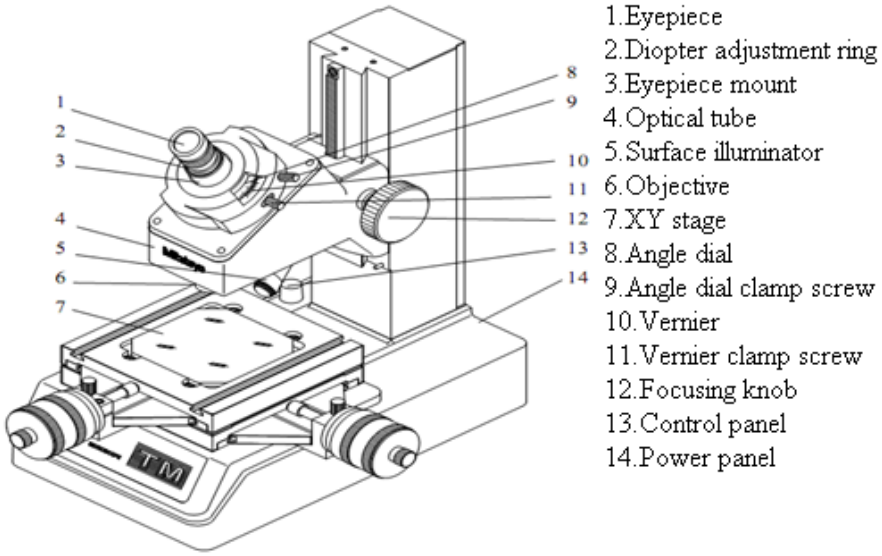

Figure 3.11 Tool Maker's Microscope

In the present work, Tool maker's microscope is used to measure the flank wear of the cutting tool. Readings from the digital heads is noted down and analysis is made thereafter.

3.3 Conclusion

With the set-up described above, the machining analysis of Inconel 718 was conducted. The set-up was used to carry out multi objective optimization, development of Artificial Neural networks model and conducting minimum quantity lubrication studies. Initial machining for SEM and EDS studies was also carried out using the same set-up. The details regarding the above mentioned studies is the subject of subsequent chapters.

4 ANALYSIS OF THE PROCESS AND MULTI-OBJECTIVE OPTIMIZATION

Productivity and quality improvement in Machining can provide significant gains in the final product quality, which can help generate additional revenues. Conducting machining experiments is always considered costly and time consuming, thus many machines in the actual manufacturing environment run at sub-optimal level, which is set by trial and error. The present chapter focuses on Taguchi Method of optimization which can provide optimum parameters even by conducting a small number of experiments. In machining, the objective of optimization has multiple criteria. For example, in the present study the objectives are lowering of cutting forces, surface roughness and tool wear. This makes multi-objective optimization suitable for machining studies. The present study uses Gray relational analysis, a method from Gray theory for multi-objective optimization.

The experiments have been carried out in dry conditions on the Bharat Fritz Werner Ltd vertical milling machine. The work material used was Inconel 718. The tool material used in the experimental work is coated carbide grade of specification SPMW 120408 TN-7535.The present work is focused to study the effect of process parameters such as cutting speed, feed, depth of cut and approach angle of the cutter on cutting force, tool life and surface roughness using DoE, Taguchi's method, ANOVA and Gray relational analysis.

4.1 Process parameter selection

The process parameters considered in the present study are cutting speed, depth of cut and feed and approach angle. These have profound influence on cutting force, surface finish and tool wear.

4.1.1 Cutting speed

Cutting speed of a cutting tool is that where the cutting edge passes over the surface of the work piece in unit time. It is normally expressed in terms of surface speed in "m/min". It is a very important aspect in machining since it considerably affects the tool life and efficiency of machining. Selection of a proper cutting speed has to be made very judiciously. If it is too high, the tool gets over-heated and its cutting edge may fail, needing regrinding. If it is too low, too much time is consumed in machining and full cutting capacities of the tool and machine are not utilized, and it results in lowering of productivity and increasing of the production cost. Cutting speed *V* is expressed as

$$V = \frac{\pi DN}{1000} \quad \text{4-1}$$

Where *V*= Cutting speed in m/min, *N*= Speed in rpm, *D*= Diameter of the milling cutter in mm

4.1.1.1 Effect of cutting speed on force and surface roughness

At lower cutting speeds, the contact between chip and tool is longer resulting in pressure welds on chip-tool interface. At higher speeds, the temperature increases and duration of contact decreases, reducing the pressure welds. This reduces the cutting force required and BUE formation. At very high speeds, the cutting force is almost constant with change in speeds.

At low speeds, due to formation of pressure welds, the chip gets welded to the rake face of the tool. After reaching a critical size, the welded chip on the rake face breaks off taking away some portion of the rake face of the tool. This is a cyclic process and the small protrusion formed is called Built-up-edge (BUE) and it makes the cutting edge blunt. In some cases, it forms on the clearance face, rubbing on the already machined surface. This results in poor surface finish. At higher speeds, there is no formation of BUE, thus resulting in a uniform cutting and better surface finish.

4.1.2 Feed

It represents the table travel in any direction, measured in millimeters; feed can be given to the table either by hand or through automatic means. Whatever may be the mode of feeding, it can be expressed in three ways:

1. Feed per minute (F_t) : The table travel in millimeters in one minute in any direction. It is expressed as mm/min
2. Feed per tooth (F_z): The table travel in millimeters during the period when the cutter revolves through an angle corresponding to the distance between the cutting edges of two adjacent teeth.
3. Feed per revolution (F_r): The table travel in millimeters during the period when the cutter makes one full revolution. It is expressed in mm/rev.

If $T = Number\ of\ teeth, N = revolutions\ per\ minute\ of\ the\ cutter, F_z = F_t TN$.

4.1.2.1 Effect of feed on Force and surface roughness

Feed increases the undeformed chip thickness, thus increasing the area of the chip. But, the specific cutting pressure per unit area will decrease. Thus, the feed increase results in increase in force but the increase is not directly proportional.

Feed ridges are the main reason for surface roughness. Height of the feed ridges is given by

$H = \frac{f_z^2}{8r}$, *where* f_z *is feed per tooth in milling and* r *is the nose radius*……4-2

As the feed ridge increases, the value of surface finish also increases. Feed is the most significant factor. To reduce the effect of feed ridges, either a nose radius tool, or a chamfered edge tool is commonly used. If the feed/tooth goes beyond the planishing edge width, then the ridges are formed according to the axial run-out of the cutter.

4.1.3 Depth of cut

It is the depth or distance parallel to axis of the cutter by which the tool penetrates into the work.

4.1.3.1 Effect of depth of cut on Force and surface roughness

Increase in depth of cut increases the cross sectional area. It does not change specific cutting pressure as it does not affect the chip thickness. This makes the specific cutting pressure constant. As the cross section area increases, the force too increases proportional to the depth of cut. When comparing feed and depth of cut, depth of cut has a greater influence on force. Depth of cut does not influence the feed ridges. But it can affect the vibrations of the machine tool in combination with feed. This combination is quantified by slenderness ratio.

$$\text{Slenderness ratio} = \frac{\text{depth of cut}}{\text{Feed/tooth}} \quad \ldots\ldots\ldots\ldots\ldots\ldots\ldots\ldots\ldots\ldots\ldots\ldots\ldots\ldots\ldots\ldots\ldots\ldots 4\text{-}3$$

If this ratio increases, the vibrations increase and result in increase of surface finish. Large nose radius and small depth of cut increases vibrations and surface roughness.

Using the above theoretical aspects, and considering the working range of the machine which is 30-120m/min, cutting speeds were taken at three levels as 40,60 and 80m/min. Based on the metal cutting guide provided by the insert manufacturer [8], the maximum speed was limited to 80m/min. Feed and depth of cuts have limits based on the insert chip breaker profile. Using the broad range mentioned, trial experiments were conducted and parameters were fixed as shown in Table 4.1 .

Table 4.1 Experimental factors and their levels

Symbol	Cutting parameters	Unit	Level 1	Level 2	Level 3
A	Cutting speed	m/min	40	60	80
B	Feed rate	mm/rev	0.16	0.22	0.28
C	Depth of cut	mm	0.10	0.15	0.20
D	Approach Angle	Degrees	35	45	55

4.2 Design of Experiments (DOE)

A Design of Experiment (DOE) is a structured, organized method for determining the relationship between factors affecting a process and the output of that process. It is used to

quantify the effect of factors and interactions between factors by analyzing data from the experiments. There are many different techniques that come under Design of Experiments. The current study uses Taguchi method, which is commonly used in industrial situations.

4.2.1 Taguchi Method

Taguchi techniques are statistical methods developed by Genichi Taguchi to improve the quality of manufacturing goods. Basically, classical experimental design involves varying one input parameter at a time. When the number of input parameters increases, classical method results in a huge number of experiments. To avoid this, the present research uses Taguchi method. Taguchi method uses an efficient method called orthogonal arrays for reducing the total number of experiments. From the preliminary experimental results, three levels of cutting parameters have been selected as shown in the table7. In this study, an L9 orthogonal array with four columns and nine rows are used.

The developer of Taguchi proposed that engineering optimization of a process or product should be carried out in a three step approach i.e. System design, parameter design and tolerance design. In system design the engineer applies scientific and engineering knowledge to produce a basic functional prototype design, this design includes the product design stage and process design stage.

In the product design stage, the selection of materials, and tentative design parameters are finalized from basic design principles. These parameters are not optimized and act as a starting point for the next stage.

The objective of parameter design is to optimize the settings of the process parameter values for improving quality characteristics and to identify the product parameter values under the optimal process parameter values. In addition, it is expected that the optimal process parameter values obtained from parameter design are insensitive to variation in the environmental conditions and other noise factors. Finally, tolerance design is used to determine and analyze tolerances around the optimal settings recommended by parameter design.

Tolerance design is required if the reduced variation obtained by the parameter design does not meet the required performance. However based on the above discussion, parameter design is the key step in the Taguchi method in achieving high quality without increasing cost. To obtain high cutting performance in turning, the parameter design proposed by Taguchi method is adopted in this project work.

Basically, experimental design methods were developed originally by Fisher. Taguchi method extends experimental design intro robust design, the goal is to increase / decrease the value of the output and simultaneously reduce variance. The experimental results are then transformed into a signal to noise (S/N) ratio. Taguchi recommends the s/n ratio to measure the quality characteristics deviating from the desired values. Usually, there are three categories of quality characteristic in the analysis of s/n ratio i.e. Lower-the Better, Higher-the Better and Nominal-the Better. S/N ratio for each level of process parameters is computed based on S/N ratio analysis. Regardless of the category of the quality characteristics, a greater S/N ratio corresponds to the better quality characteristics. Therefore, optimal level of process parameters is the level with the greater S/N ratio. Furthermore, a statistical analysis of variance (ANOVA) is performed to see which process parameters are statistically significant. With S/N ratio and ANOVA analyses, optimal combination of the process parameters can be predicted. Finally, a confirmation experiment is conducted to verify the optimal process parameters obtained from the parameter design [52].

To summarize, the parameter design of the Taguchi method includes the following steps:

1. Identification of the quality characteristics and selection of design parameters to be evaluated.
2. Determination of the number of levels for the design parameters and possible interactions between the design parameters.
3. Selection of the appropriate orthogonal array and assignment of design parameters to the orthogonal array.
4. Conducting of the experiments based on the arrangement of the orthogonal array.
5. Analysis of the experimental results using the S/N ratio and ANOVA analyses.
6. Selection of the optimal levels of design parameters.
7. Verification of the optimal design parameters through the confirmation experiment.

The objectives that can be achieved through parameter design of Taguchi Method are:

1. Determination of the optimal design parameters for a process or a product
2. Estimation of each design parameter to the contribution of the quality characteristics
3. Prediction of the quality characteristics based on the optimal design parameters

4.2.2 Orthogonal arrays

In order to reduce the total number of experiments “Sir Ronald Fisher” developed the solution “Orthogonal Arrays”. The orthogonal array can be thought of as a distillation mechanism

through which the engineers experiment passes. The array allows us to vary multiple input parameters at a time and obtain their effects in the terms of average and the dispersion.

Taguchi employs design of experiments that uses specially constructed tables, known as "Orthogonal Arrays (OA)" to conduct experiments.

Orthogonal Arrays (OA) are a special set of Latin squares, constructed by Taguchi to lay out the product design experiments. An orthogonal array is a type of experiment where the columns for the independent variables are "Orthogonal" to one another. Orthogonal arrays are employed to study the effect of several control factors. Orthogonal arrays are used to investigate quality.

In this array, the columns are mutually orthogonal. That is for any pair of columns all combination of factors occur; and they occur in equal number of times. Here, there are 4 parameters, A, B, C and D, each at three levels. This is called an 'L_9' design, with 9 experiments to be conducted. Specific test characteristics for each experimental evaluation are identified in the associated row of the table. Thus L_9 (3^4) means that nine experiments are to be carried out to study four variables with three levels. There are greater savings in testing for larger arrays. A typical L_9 Orthogonal array (3^4) is shown in Table 4.2.

Table 4.2 L9 Orthogonal array [52]

A	B	C	D
1	1	1	1
1	2	2	2
1	3	3	3
2	1	2	3
2	2	3	1
2	3	1	2
3	1	3	2
3	2	1	3
3	3	2	1

4.2.3 Signal-to-Noise (S/N) ratio

The signal-to-noise concept is closely related to the robustness of a product design. A Robust Design or product delivers strong 'signal'. It performs its expected function and can cope with variations ("noise"), both internal and external. In signal-to-Noise Ratio, signal represents the desirable value and noise represents the undesirable value. The uses of S/N ratio are:

- S/N ratios can be used to get closer to a given target value, or to reduce variation in the product's quality characteristic(s)
- Signal-To-Noise ratio is used to measure controllable factors that can have such a negative effect on the performance of design

- They lead to optimum by using a monotonic function
- They help improve additives of the effects
- To quantify the quality

The Taguchi method uses the signal-to-noise (S/N) ratio instead of the average value to convert the trial result data into a value for the evaluation characteristics in the optimum setting analysis. This is because the S/N ratio can reflect both the average and the variation of the quality characteristics. If the S/N ratio η is expressed in dB units, it can be defined by a logarithmic function based on the mean-square deviation around the target, $\eta = -10\log(\text{MSD})$, where MSD = Mean square deviation for the output characteristic. The three methods used to calculate S/N ratio are:

4.2.3.1 The smaller-the-better

Impurity in drinking water is critical to quality. The less impurities customers find in their drinking water, the better it is. Vibrations are critical to the quality of a car, the less vibration the customers feel while driving their cars the better, the more attractive the cars are. The Signal-To-Noise ratio for the Smaller-The-Better is

$$\eta = -10\,log\left(\frac{\sum y^2}{n}\right), where\ y\ is\ the\ output\ response\ , n\ is\ the\ number\ of\ responses \ldots\ldots\ldots\ldots\ldots\ldots 4\text{-}4$$

4.2.3.2 The larger-the-better

If the number of minutes per dollar customers get from their cellular phone service provider is critical to quality, the customers will want to get the maximum number of minutes they can for every dollar they spend on their phone bills. If the lifetime of a battery is critical to quality, the customers will want their batteries to last forever. The longer the battery lasts, the better it is. The Signal-To-Noise ratio for the bigger-the-better is

$$\eta = -10\,log\left(\frac{1}{n}\sum\frac{1}{y^2}\right), y\ is\ the\ output\ response\ , n\ is\ the\ number\ of\ responses \ldots\ldots\ldots\ldots\ldots\ldots 4\text{-}5$$

4.2.3.3 Nominal-the-best

When a manufacturer is building mating parts, he would want every part to match the predetermined target. For instance when he is creating pistons that need to be anchored on a given part of a machine, failure to have the length of the piston to match a predetermined size will result in it being either too small or too long resulting in lowering the quality of the machine. In that case, the manufacturer wants all the parts to match their target. When a customer buys ceramic tiles to decorate his bathroom, the size of the tiles is critical to quality,

having tiles that do not match the predetermined target will result in them not being correctly lined up against the bathroom walls. The S/N equation for the Nominal-The-Best is

$$\eta = -10\,log\left(\frac{\mu^2}{\sigma^2}\right), \mu\ is\ the\ mean\ of\ response\ , \sigma\ is\ the\ standard\ deviation \ldots\ldots\ldots\ldots\ldots\ldots\ldots\ldots 4\text{-}6$$

4.3 Analysis of Variance (ANOVA)

Analysis of variance (ANOVA) is a statistical method for determining the existence of differences among several population means. Analysis of variance is particularly effective tool for analyzing highly structured experimental data. Different factors affect the surface defect formation to a different degree. The relative effect of the different factors can be obtained by the decomposition of variance, which is commonly called analysis of variance (ANOVA). ANOVA is also needed for estimating the error variance for the factor effects and variance of the prediction error.

The original idea of analysis of variance was developed by the English Statistician Sir Ronald A. Fisher during the first part of this century. Much of the early work in this area dealt with agricultural experiments where crops were given different treatments, such as being grown using different kinds of fertilizers. The researchers wanted to determine whether all treatments under study were equally effective or some treatments were better than others.

The purpose of the analysis of variance (ANOVA) is to investigate which design parameters significantly affect the quality characteristic. This is accomplished by separating the total variability of the S/N ratios, which is measured by the sum of the squared deviations from the total mean S/N ratio, into contributions by each of the design parameters and the error. First, the total sum of squared deviations SS_T from the total mean S/N ratio can be calculated as:

$$SS_T = \sum_{i=1}^{n} (\eta_m - \eta_i)^2 \ldots\ldots\ldots\ldots\ldots\ldots\ldots\ldots\ldots\ldots\ldots\ldots\ldots\ldots 4\text{-}7$$

where n is the number of experiments in the orthogonal array, η_i is the mean S/N ratio for the i^{th} experiment and η_m total mean of S/N ratio.

The total sum of squared deviations SS_T is of two sources: the sum of squared deviations SS_d due to each design parameter and the sum of squared error SS_e. The percentage contribution by each of the design parameters in the total sum of squared deviations SS_T is a ratio of the sum of squared deviations SS_d due to each design parameter to the total sum of squared deviations SS_T.

In this discussion, the main focus is on developing full factorial experimental design and analyzing the data using ANOVA to find significant factors and interactions. For this purpose

Minitab has been used. Using this, the experimental design with randomized order has been developed using this. ANOVA analysis and the related plots were also developed. [52]

4.3.1 Terminology used in ANOVA

1. SS (Sum of squares: It is the sum of squares of deviations. It is calculated for each factor and the total SS is found by adding individual terms.
2. Seq SS: Sequential sum of squares are obtained by breaking down SS into main effects, interactions, blocks and each covariate. Seq SS depends on order of the terms entered into the model.
3. Adj SS: Adjusted sum of squares is the other part of SS which does not depend on the order in which values are entered.
4. DF: Degree of Freedom is the number of degrees of freedom associated with each sum of squares.
5. MS: Mean square is calculated as $\mathrm{MS} = \dfrac{\text{Adj SS}}{\text{DF}}$
6. F test: It is used to determine whether a given interaction or main effect is significant.

$$\mathrm{F} = \frac{\text{MS Term}}{\text{MS (Error)}} \quad \ldots\ldots\ldots\ldots\ldots\ldots\ldots\ldots 4\text{-}8$$

Note: Large value of *F* means the factor or interaction is significant.

7. p-value (P): It is also a test similar to F test but can be used to decide whether a parameter needs to be considered significant or not. The common criterion is if the value of P is less than 0.05, the factor is significant [53].

4.4 Gray relation analysis

In the year of 1980, gray systems theory was brought forward by Professor Deng Ju-long from China. Gray analysis uses a specific concept. It defines situations with no information as black, and those with perfect information as white. However, neither of these idealized situations ever occur in real world problems. In fact, situations between these extremes are described as being gray, hazy or fuzzy.

Therefore, a gray system means that a system in which part of information is known and part of information is unknown. With this definition, information quantity and quality form a continuum from a total lack of information to complete information from black through gray to

white. Since uncertainty always exists, one is always somewhere in the middle, somewhere between the extremes, somewhere in the gray area.

Gray analysis then comes to a clear set of statements about system solutions. At one extreme, no solution can be defined for a system with no information. At the other extreme, a system with perfect information has a unique solution. In the middle, gray systems will give a variety of available solutions. Gray analysis does not attempt to find the best solution, but does provide techniques for determining a good solution, an appropriate solution for real world problems.

The proposition of Gray theory occurring in the 1990 to 1999 time period resulted in the use of Gray theory to each field, and the development is still going on. The major advantage of Gray theory is that it can handle both incomplete information and unclear problems very precisely. It serves as an analysis tool especially in cases when there is no sufficient data. It was recognized that the Gray relational analysis in Gray theory had been largely applied to project selection, prediction analysis, performance evaluation, and factor effect evaluation due to the Gray relational analysis software development. Recently, this technique has also been applied to the field of sport and physical education.

Gray relational analysis was proposed by Deng in 1989 and is widely used for measuring the degree of relationship between sequences by gray relational grade. Gray relational analysis is applied by several researchers to optimize control parameters having multi-responses through gray relational grade.

Gray relational analysis is an impacting measurement method in gray system theory that analyzes uncertain relations between one main factor and all other factors in a given system. When the experiments are ambiguous or when the experimental method cannot be carried out exactly, gray analysis helps to face the shortcomings in statistical regression. Gray relational analysis is actually a measurement of the absolute value of data difference between sequences, and it could be used to measure the approximate correlation between the sequences [36].

The black box is used to indicate a system lacking interior information. Nowadays, the black is represented, as lack of information, and the white is full of information. Thus, the information that is either incomplete or undetermined is called Gray.

A system having incomplete information is called Gray system. The Gray number in Gray system represents a number with less complete information. The Gray element represents an element with incomplete information. The Gray relation is the relation with incomplete information. Those three terms are the typical symbols and features for Gray system and Gray

phenomenon. The Gray relational analysis uses information from the Gray system to dynamically compare each factor quantitatively.

4.4.1 Generation of gray relation

The use of Taguchi method with gray relational analysis to optimize the face milling operations with multiple performance characteristics includes the following steps:

1. Identify the performance characteristics and cutting parameters to be evaluated.
2. Determine the number of levels for the process parameters.
3. Select the appropriate orthogonal array and assign the cutting parameters to the orthogonal array.
4. Conduct the experiments based on the arrangement of the orthogonal array.
5. Normalize the experiment results of cutting force, tool life and surface roughness.
6. Perform the process of "gray relational generating" and calculate the gray relational coefficient.
7. Calculate the gray relational grade by averaging the gray relational coefficient.
8. Analyze the experimental results using the gray relational grade and statistical ANOVA.
9. Select the optimal levels of cutting parameters.
10. Verify the optimal cutting parameters through the confirmation experiment.

4.4.2 Data pre-processing

In gray relational analysis, the data pre-processing is the first step performed to normalize the random gray data with different measurement units to transform them to dimensionless parameters. Thus, data pre-processing converts the original sequences to a set of comparable sequences. Different methods are employed to pre-process gray data depending upon the quality characteristics of the original data. The original reference sequence and pre-processed data (comparability sequence) are represented by $x_0^{(0)}(k)$ and $x_i^{(0)}(k)$, i =1,2,….,m; k =1,2,.....,n respectively, where m is the number of experiments and n is the total number of observations of data. Depending upon the quality characteristics, the three main categories for normalizing the original sequence are identified as follows:

1. If the original sequence data has quality characteristic as 'larger-the-better' then the original data is pre-processed as 'larger-the-better':

$$x_i^*(k) = \frac{x_i^{(0)}(k) - min\, x_i^{(0)}(k)}{max\, x_i^{(0)}(k) - min\, x_i^{(0)}(k)} \dots\dots\dots\dots\dots\dots\dots\dots\dots\dots\dots 4\text{-}9$$

2. If the original data has the quality characteristic as ‘smaller-the better’, then original data is pre-processed as ‘smaller-the-better’:

$$x_i^*(k) = \frac{max\, x_i^{(0)}(k) - x_i^{(0)}(k)}{max\, x_i^{(0)}(k) - min\, x_i^{(0)}(k)} \quad \ldots\ldots\ldots\ldots\ldots\ldots\ldots\ldots\ldots\ldots\ldots 4\text{-}10$$

3. If the original data has a target optimum value (OV) then quality characteristic is ‘nominal-the-better’ and the original data is pre-processed as ‘nominal-the-best’:

$$x_i^*(k) = 1 - \frac{|x_i^{(0)}(k) - OV|}{max\{max\, x_i^{(0)}(k) - OV, OV - min x_i^{(0)}(k)\}} \quad \ldots\ldots\ldots\ldots 4\text{-}11$$

Also, the original sequence is normalized by a simple method in which all the values of the sequence are divided by the first value of the sequence.

$$x_i^*(k) = \frac{x_i^{(0)}(k)}{x_i^{(0)}(1)} \quad \ldots\ldots\ldots\ldots\ldots\ldots\ldots\ldots\ldots\ldots\ldots\ldots\ldots\ldots\ldots\ldots 4\text{-}12$$

where max $x_i^{(0)}(k)$ and min $x_i^{(0)}(k)$ are the maximum and minimum values respectively of the original sequence$x_i^{(0)}(k)$. Comparable sequence $x_i^*(k)$ is the normalized sequence of original data.

4.4.3 Gray relational grade

Next step is the calculation of deviation sequence, $\Delta_{oi}(k)$ from the reference sequence of pre-processes data $x_i^*(k)$ and the comparability sequence $x_i^*(k)$. The gray relational coefficient is calculated from the deviation sequence using the following relation:

$$\gamma\left(x_0^*(k), x_i^*(k)\right) = \frac{\Delta_{min} + \xi\ \Delta_{max}}{\Delta_{oi}(k) + \xi\Delta_{max}} \quad 0 < \gamma\left(x_0^*(k), x_i^*(k)\right) \leq 1 \quad \ldots\ldots\ldots\ldots\ldots\ldots\ldots\ldots\ldots 4\text{-}13$$

where $\Delta oi(k)$ is the deviation sequence of the reference sequence $x_0^*(k)$ and comparability sequence $x_i^*(k)$.

$$\Delta_{oi}(k) = |x_0^*(k) - x_i^*(k)| \quad \ldots\ldots\ldots\ldots\ldots\ldots\ldots\ldots\ldots 4\text{-}14$$

$$\Delta_{max} = \underset{\forall j \in i}{max}\ \underset{\forall k}{max} |x_0^*(k) - x_i^*(k)|\ ;\ \Delta_{min} = \underset{\forall j \in i}{min}\ \underset{\forall k}{min} |x_0^*(k) - x_i^*(k)| \quad \ldots\ldots\ldots\ldots\ldots\ldots\ldots\ldots 4\text{-}15$$

ξ is the distinguishing coefficient,$\xi \in [0,1]$. The distinguishing coefficient (ξ) value is chosen to be 0.5. A gray relational grade is the weighted average of the gray relational coefficient and is defined as follows:

$$\gamma(x_0^*, x_i^*) = \sum_{k=1}^{n} \beta_k \gamma(\left(x_0^*(k), x_i^*(k)\right), \sum_{k=1}^{n} \beta_k = 1 \quad \ldots\ldots\ldots\ldots\ldots\ldots\ldots\ldots 4\text{-}16$$

The gray relational grade $\gamma(x_0^*, x_i^*)$ represents the degree of correlation between the reference and comparability sequences. If two sequences are identical, then gray relational grade value equals unity. The gray relational grade implies the degree of influence related between the

comparability sequence and the reference sequence. In case a particular comparability sequence has more influence on the reference sequence than the other ones, the gray relational grade for comparability and reference sequence will exceed that for the other gray relational grades. Hence, gray relational grade is an accurate measurement of the absolute difference in data between sequences and can be applied to appropriate the correlation between sequences.[30]

4.5 Results and Discussion

In this section, the experimental results obtained for the cutting force, surface roughness and tool wear are summarized. The relationship between the cutting force (F_y), surface roughness (R_a) and tool wear (L) on the process parameters are discussed in this chapter. The experimental results are tabulated in Table 4.3.

Table 4.3 L9 experiment results and S/N ratio

Expt. No.	A	B	C	D	F_y(N)	Ra(µm)	L(µm)	S/N F_y (dB)	S/N Ra (dB)	S/N L (dB)
1	1	1	1	1	118.1	0.71	118.67	-41.445	2.974833	-41.4868
2	1	2	2	2	142.8	1.1	129.24	-43.0946	-0.82785	-42.2279
3	1	3	3	3	293.2	2.2	138.54	-49.3433	-6.84845	-42.8315
4	2	1	2	3	130.1	0.65	150.29	-42.2855	3.741733	-43.5386
5	2	2	3	1	139.5	1.2	153.41	-42.8915	-1.58362	-43.7171
6	2	3	1	2	102.5	1.54	145.57	-40.2145	-3.75041	-43.2614
7	3	1	3	2	156.4	0.66	155.93	-43.8847	3.609121	-43.8586
8	3	2	1	3	115.1	0.97	143.18	-41.2215	0.264565	-43.1176
9	3	3	2	1	180.6	1.63	168.36	-45.1344	-4.24375	-44.5248

4.5.1 Analysis and Optimization of process parameters using Taguchi Method

The experimental data in Table 4.3 L9 experiment results and S/N ratio will be used to understand the effects of parameters on Cutting Force (F_y), surface Roughness (R_a) and tool wear (L). It will be further used to find out optimal conditions for individually minimizing each of the output parameters i.e. F_y, R_a and L.

4.5.1.1 Analysis for Cutting Force (F_y)

Figure 4.1shows mean effects for Cutting Force. Cutting forces are higher at low speeds because of work hardening which is predominant at low speeds, whereas the cutting forces again increases at higher speeds as the tool wear mechanisms become predominant. Generally, increase in feed increases cutting force because of the increase in uncut chip thickness which increases area of the chip to be removed. But in this case, at lower feeds, built-up edge formation has been observed. As this makes the cutting point blunt, increase in cutting forces can be observed. Depth of cut increases the area of uncut chip thickness, increasing the amount ofForce

required to cut. Cutting was found to be lower at 45º. This is due to proper balancing of thrust and cutting forces that would reduce vibration and thus the mean value of cutting force.

Figure 4.2 shows the S/N response graph for cutting force. For lower-the-better characteristic of cutting force, the optimal parameter combination is A2-B2-C1-D2 as shown in Table 4.5.

Table 4.4 ANOVA for Cutting Force (F_y)

Parameters	DOF	SS	MSS	% Contr.
Speed	2	12.09804	6.04902	20.59451
Feed	2	11.80738	5.903688	20.09971
DOC	2	29.43831	14.71916	50.11286
AA	2	5.40029	2.700145	9.192918
Error	0			
Total	8	58.74402		

Table 4.5 S/N ratio Response Table for Cutting Force (F_y)

Level	Speed	Feed	DOC	AA
1	-44.6276	-42.5384	**-40.9603**	-43.1569
2	**-41.7972**	**-42.4025**	-43.5048	**-42.3979**
3	-43.4135	-44.8974	-45.3732	-44.2834
Delta	2.830445	2.494852	4.412839	1.885518
Rank	2	3	1	4

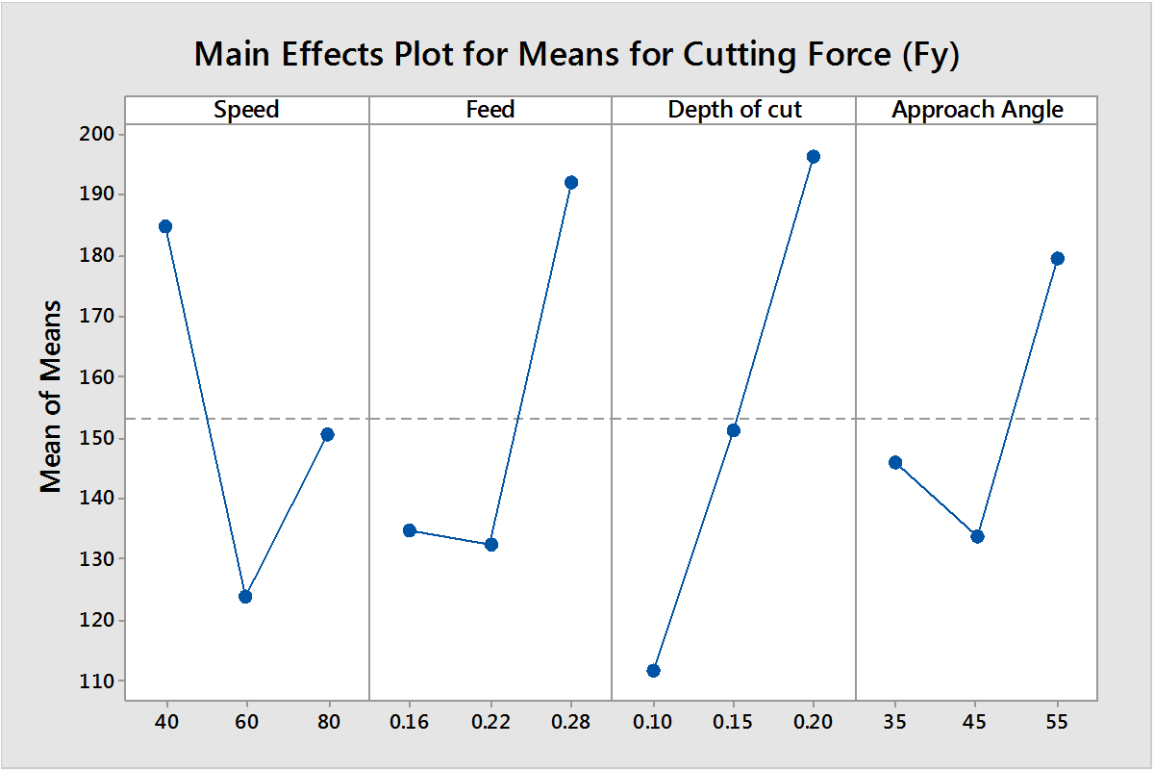

Figure 4.1 Main effects plot for means of Cutting Force (F_y)

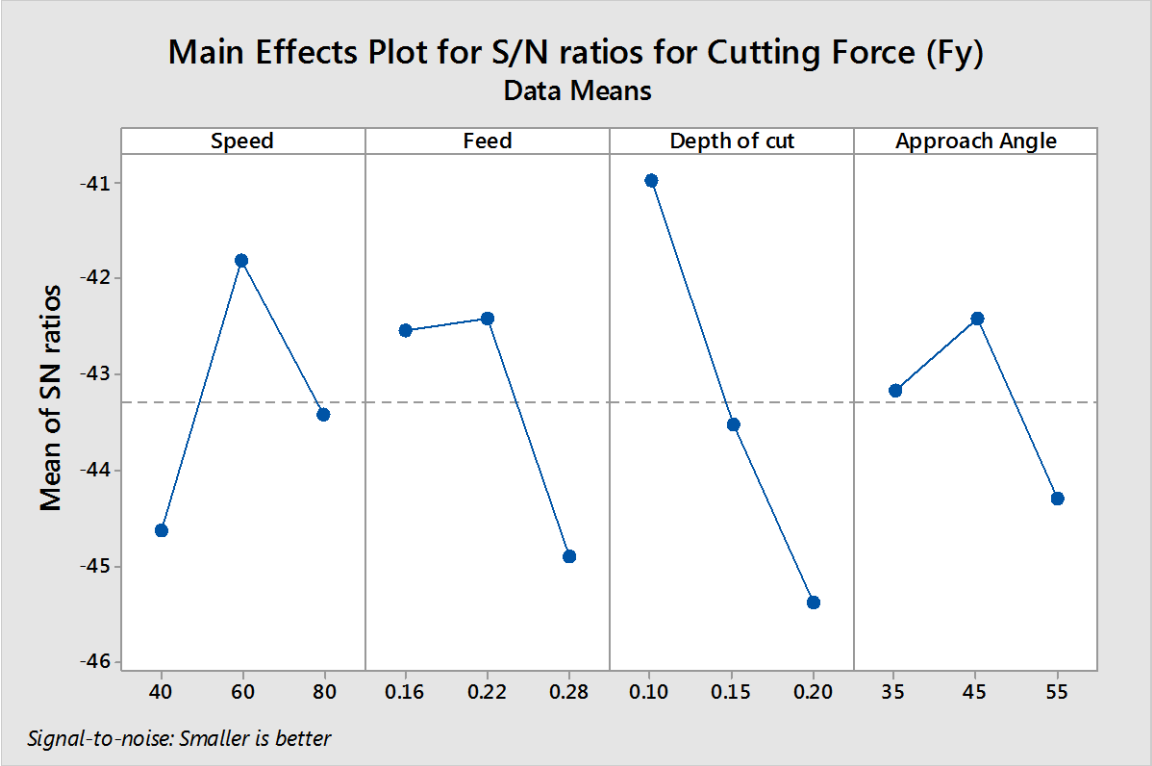

Figure 4.2 Main effects plot for S/N ratios of Cutting Force (F_y)

4.5.1.2 Analysis for Surface Roughness (R_a)

Figure 4.4 shows the S/N response graph for surface roughness. For lower-the-better characteristic of surface roughness, the optimal parameter combination is A3-B1-C1-D2. This can also be deduced from the response table presented in Table 4.7.

Figure 5.5 Main Effects plot for Surface Roughness (R_a). At low cutting speeds, the temperature generated in machining is low and duration of contact between the chip and the tool also is more. So there is sufficient time for the plastic deformation to occur and also Inconel 718 has greater weldability so it gets welded to the cutting edge which leads to poor surface finish. At high speeds, there are less chances of forming built up edge because of less time for establishing atomic bonds between chip and tool. Hence surface finish improves. In the present work, the optimum surface finish obtained at 80 m/min. According to the theory of metal cutting, the surface roughness is directly proportional to the square of feed. The same behavior of surface roughness with increase in feed has been observed in the present work. With increase in depth of cut, the change in surface roughness value is not significant. But as depth of cut increases, the surface roughness also increases. With decrease in approach angle from 55º to 35º, the surface finish increases from 55º to 45º and decreases from 45º to 35º. But the decrease is not significant as compared to increase from 55º to 45º. For lesser approach angle, the chip becomes thinner because the depth of cut is distributed over a longer surface of contact.

Table 4.6 shows the results of ANOVA for surface roughness. It can be found that feed is the most significant parameter affecting surface roughness. The effect of other parameters is negligible compared to feed.

Table 4.6 ANOVA analysis for Surface Roughness (R_a)

Parameters	DOF	SS	MSS	% Calc.
Speed	2	3.324656	1.662328	2.937457
Feed	2	105.5767	52.78836	93.28096
DOC	2	3.496111	1.748056	3.088945
AA	2	0.783939	0.39197	0.69264
Error	0			
Total	8	113.1814		

Table 4.7 S/N ratio response table for Surface Roughness (R_a)

Level	Speed	Feed	Doc	AA
1	-1.56716	**3.441896**	**-0.17034**	-0.95084799
2	-0.53077	-0.71564	-0.44329	**-0.32304894**
3	**-0.12336**	-4.94754	-1.60765	-0.94738514
Delta	1.443803	8.389436	1.437314	0.627799051
Rank	2	1	3	4

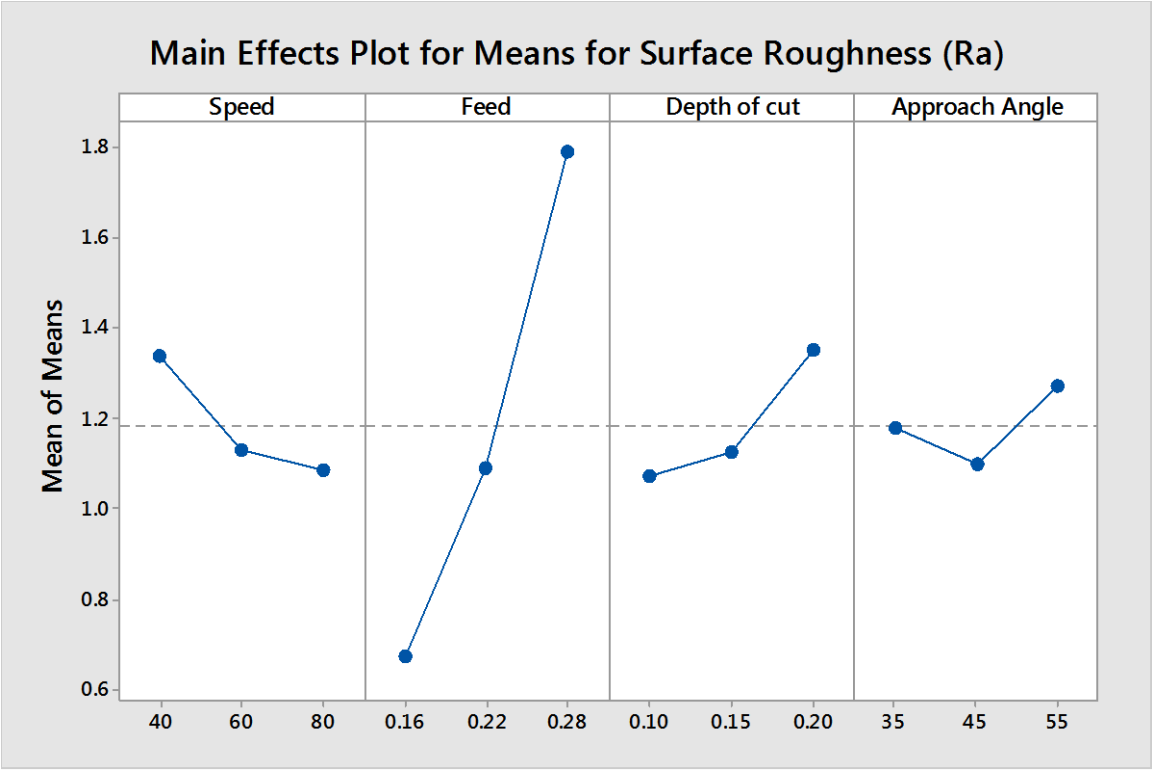

Figure 4.3Main effects plot for means of Surface Roughness (R_a)

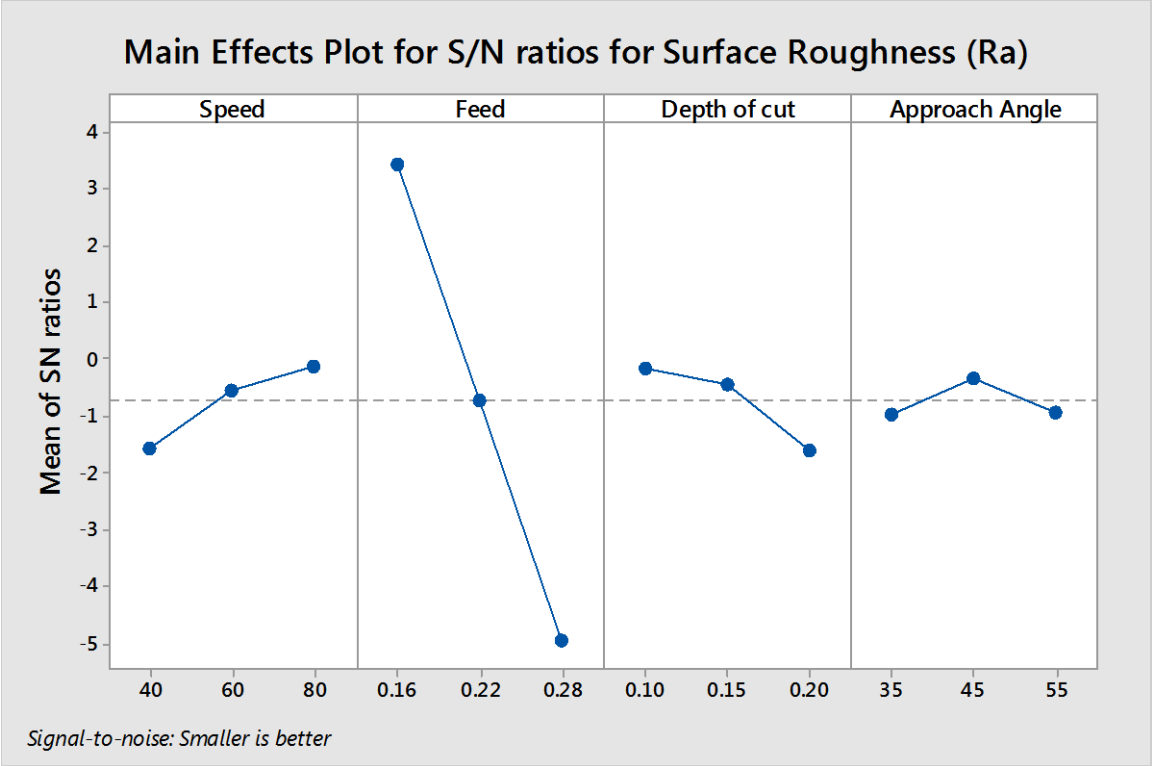

Figure 4.4 Main effects plot for S/N ratios for Surface Roughness (R_a)

4.5.1.3 Analysis for Tool wear (L)

Figure 4.6 shows the S/N response graph for tool wear. For lower-the-better characteristic of tool wear, the optimal parameter combination is A1-B1-C1-D2. Cutting speed has greatest influence on tool wear. At higher speeds, the hard particle of the workpiece tries to hit the tool with greater momentum which leads to abrasion. Further at high speeds temperature generated is also on the higher side, which softens the tool and leads to tool failure. From the Figure 4.5, it is clear that the tool wear increases with increase in cutting speed. When the feed is increased, the heat generated increases because of increase in the chip cross section. The time allowed for the heat thus generated to dissipate will also be decreasing. Hence the heat concentration per unit length of cutting edge increases which leads to tool failure. From the Figure 4.5, tool life is decreasing but not significantly as feed increases. When the depth of cut is increased, tool life decreases because of increase in chip cross-section but at the same time the length of cutting edge in contact with the workpiece is also increased. Hence, the heat concentration per unit length is increased. Next to cutting speed, depth of cut has significant effect on tool life. As approach angle decreases, the heat dissipating capacity increases which increases tool life. In the present work the optimum tool life is obtained at 45° approach angle because of minimum cutting forces.

Table 4.8 shows the results of ANOVA for tool life. It is found that cutting speed is the most significant parameter for affecting tool life. The next significant factors are depth of cut followed by feed. Approach angle has least significance.

Table 4.8 ANOVA analysis for Tool Wear (L)

Parameters	DOF	SS	MSS	% Calc.
Speed	2	4.587262	2.293631	69.60024
Feed	2	0.606207	0.303103	9.197675
DOC	2	1.372678	0.686339	20.82696
AA	2	0.024724	0.012362	0.375121
Error	0			
Total	8	6.59087		

Table 4.9 S/N ratios Response Table for Tool Wear (L)

Level	Speed	Feed	Doc	AA
1	**-42.1821**	**-42.9613**	**-42.622**	-43.2429
2	-43.5057	-43.0209	-43.4304	**-43.116**
3	-43.8337	-43.5392	-43.4691	-43.1626
Delta	1.651586	0.577902	0.847089	0.1269
Rank	1	3	2	4

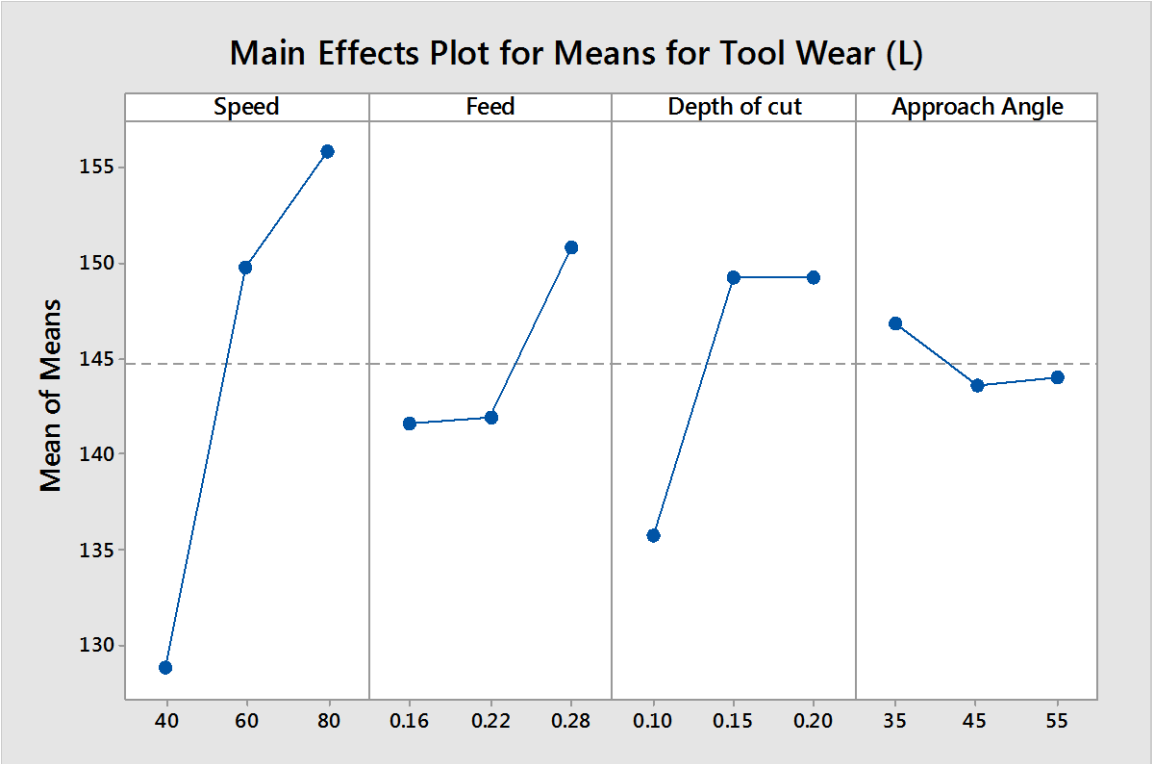

Figure 4.5 Main effects plot for means of Tool Wear (L)

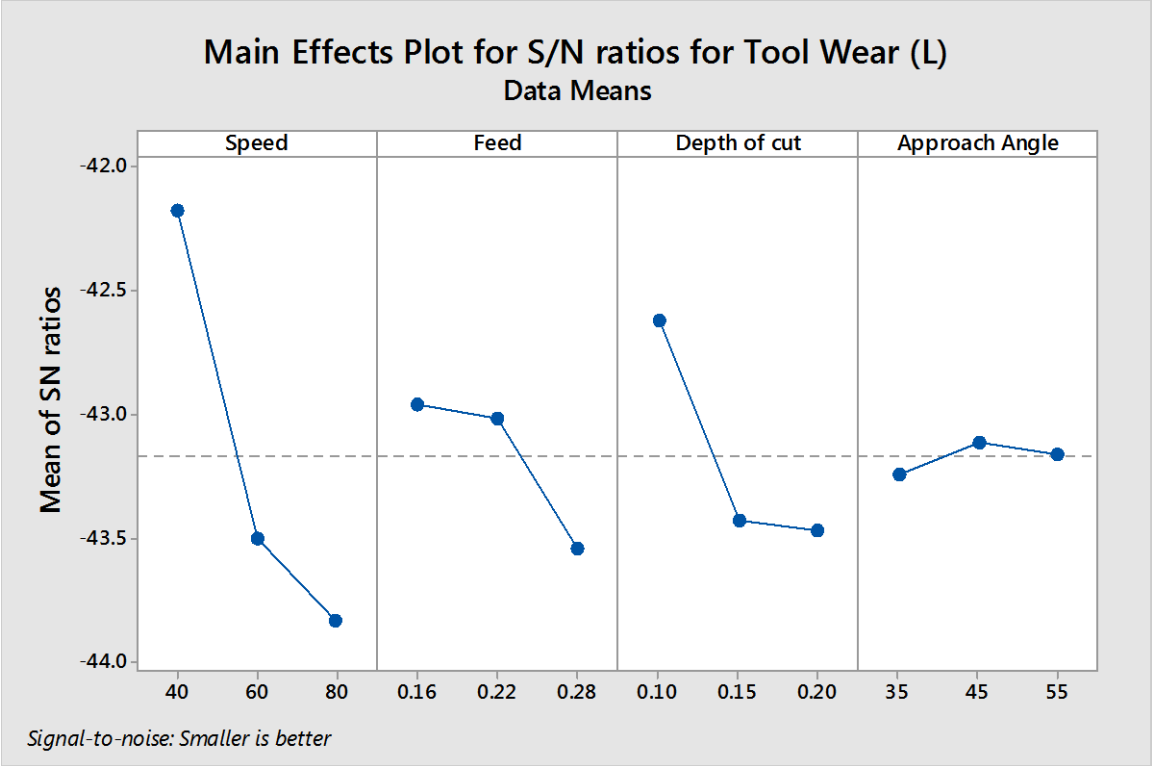

Figure 4.6 Main effects plot for S/N ratios of Tool wear (L)

4.5.1.4 Confirmation Tests

After identifying the optimal parameters, the final phase is to verify responses by conducting the confirmation experiments. Confirmation experiments were conducted for cutting force (F_y), surface roughness (R_a) and tool wear (L) based on the optimal parameter combinations obtained.

Table 4.10 Result of Confirmation Experiments

Response variable	**Optimal Parameter Combination**	**Predicted value**	**Experimental value**
Cutting Force, F_y (N)	A2-B2-C1-D2	76.91	98.7
Surface Roughness, R_a (µm)	A3-B1-C1-D2	0.56	0.62
Tool wear L (µm)	A1-B1-C1-D2	117.08	118.2

4.5.2 Multi-objective Optimization of Process parameters using Gray Relational analysis

In the previous section, process parameters were optimized on individual basis. In a practical situation we might need a combination of these properties like low cutting force along with low surface roughness and tool wear. When we consider all the parameters together, we make a compromise in some properties, while enhancing others so that the desired objective is attained. Here parametric optimization of process parameters for face milling of Inconel 718 using gray relational analysis is presented. The process parameters considered are speed, feed, depth of cut

and approach angle of the cutter . They are optimized with considerations of multiple process characteristics including cutting force, surface roughness and tool wear. Analysis of variance is performed to get the contribution of each parameter on the performance characteristics and it is observed that feed is the significant process parameter that affects the machining. The experimental results for the optimal setting show that there is considerable improvement in the process. The application of the technique converts the multi response variable to a single response gray relational grade and therefore simplifies the optimization procedure.

4.5.2.1 Gray relation generation

In the gray relational analysis, when the range of the sequence is large or the standard value is enormous, the function of factors is neglected. However, if the factor goals and directions are different, the gray relational analysis might also produce incorrect results. Therefore, one has to preprocess the data which are related to the group of sequences, which is called "gray theory relational generation". Table 4.11 shows the data pre-processing results and Table 4.12 shows deviation sequences. The calculations have been carried out based on Equations 4.4 -4.19.

Table 4.11 Data pre-processing results

Reference /Comparability sequence	F_y	R_a	L
Reference sequence	1	1	1
Comparability sequence			
Exp. No.1	0.918196	0.96129	1
Exp. No.2	0.788673	0.709677	0.787281
Exp. No.3	0	0	0.600121
Exp. No.4	0.85527	1	0.363655
Exp. No.5	0.805978	0.645161	0.300865
Exp. No.6	1	0.425806	0.458644
Exp. No.7	0.717357	0.993548	0.250151
Exp. No.8	0.933928	0.793548	0.506742
Exp. No.9	0.590456	0.367742	0

Table 4.12 Deviation sequences (After data pre-processing)

Comparability Sequence	Reference Sequence		
	F_y 1.0000	T 1.0000	R_a 1.0000
No. 1	0.081804	0.03871	0
No. 2	0.211327	0.290323	0.212719
No. 3	1	1	0.399879
No. 4	0.14473	0	0.636345
No. 5	0.194022	0.354839	0.699135
No. 6	0	0.574194	0.541356
No. 7	0.282643	0.006452	0.749849
No. 8	0.066072	0.206452	0.493258
No. 9	0.409544	0.632258	1

4.5.2.2 Best-experimental run

The experimental results for cutting force (F_y), Tool wear (L) and average surface roughness (R_a) are listed in the Table 4.13. Typically, smaller values of F_y, R_a and larger values of T are desirable. Thus the data sequences have the smaller-the-better characteristic, the "smaller-the-better" methodology was employed for data pre-processing.

The deviation sequences $\Delta_{01}(1)$ can be calculated as follows:

$\Delta_{o1}(1) = |x_0^*(1) - x_1^*(1)| = |1.00 - 0.918196| = 0.081804$

The values of the F_y, T and Ra are set to be the reference sequence $x_0^{(0)}$ (k), k =1–3.Moreover, the results of nine experiments are the comparability sequences $x_i^{(0)}$ (k), i=1, 2... 9, k =1–3 Table 4.11 listed all of the sequences after implementing the data preprocessing. The reference and the comparability sequences are denoted as x_0^* (k) and x_i^* (k), respectively. Also, the deviation sequences ∇oi, ∇oi max (k) and ∇oimin (k) for i =1–9, k =1–3 can be calculated. The distinguishing coefficient can be substituted for the Gray relational coefficient. If all the process parameters have equal weightage, is set to be 0.5. Table 4.13 lists the Gray relational coefficients and the grade for all nine comparability sequences.

This investigation employs the response table of the Taguchi method to calculate the average Gray relational grades for each factor level, as illustrated in Table 4.13. Since the Gray relational grades represented the level of correlation between the reference and the comparability sequences, the larger Gray relational grade means the comparability sequence exhibiting a stronger correlation with the reference sequence.

Table 4.13 The calculated Gray relational Co-efficient and gray relational grade

Experimental Run (Comparability Sequence)	Orthogonal Array $L_9(3^4)$				Gray Relational Coefficient			Gray Relational Grade	Gray Order
	A	B	C	D	F_y	T	R_a		
1	1	1	1	1	0.859396	0.928144	1	0.92918	1
2	1	2	2	2	0.702912	0.632653	0.701539	0.679035	4
3	1	3	3	3	0.333333	0.333333	0.55563	0.407432	9
4	2	1	2	3	0.775519	1	0.440007	0.738509	2
5	2	2	3	1	0.720438	0.584906	0.416967	0.574104	7
6	2	3	1	2	1	0.465465	0.480143	0.648536	6
7	3	1	3	2	0.638861	0.987261	0.400048	0.67539	5
8	3	2	1	3	0.883279	0.707763	0.503394	0.698145	3
9	3	3	2	1	0.549726	0.441595	0.333333	0.441552	8

Based on this study, one can select a combination of the levels that provide the largest average response. In Table 4.13, the combination of A1, B1, C1, and D2 shows the largest value of the

Gray relational grade for the factors A, B, C and D, respectively. Therefore, A1-B1-C1-D2 with a cutting speed of 40 m/min, a feed rate of 0.16 mm/rev, a depth of cut of 0.10 mm, and approach angle of 45º is the optimal parameter combination for the face milling operation.

4.5.2.3 Analysis for Multi-objective Response

Table 4.15 gives the results of the analysis of variance (ANOVA) for the F_y, R_a and L using the calculated values from the Gray relational grade of and the response of. The factor B i.e. feed with 60.52% of contribution is the most significant parameter followed by the depth of cut with 33.66%, with negligible effects from cutting speed and approach angle. Figure 4.7 shows the influence of process parameters on multiple performance characteristics i.e. cutting force, surface roughness and tool life, in face milling of Inconel 718.

Table 4.14 The response table for Gray relational grade

Levels	Factors			
	A	B	C	D
1	-3.933	-2.227	-2.507	-4.186
2	-3.738	-3.768	-4.365	-3.511
3	-4.543	-6.220	-5.343	-4.518
Delta	0.805	3.994	2.836	1.007
Rank	4	1	2	3

Table 4.15 ANOVA results for Gray relational grade

Factor	DOF	SS	MS	% Contribution
A	2	0.00717	0.003585	3.634834
B	2	0.119375	0.059687	60.51668
C	2	0.066405	0.033203	33.66454
D	2	0.004308	0.002154	2.183942
Error	0			
Total	8	0.197258		100

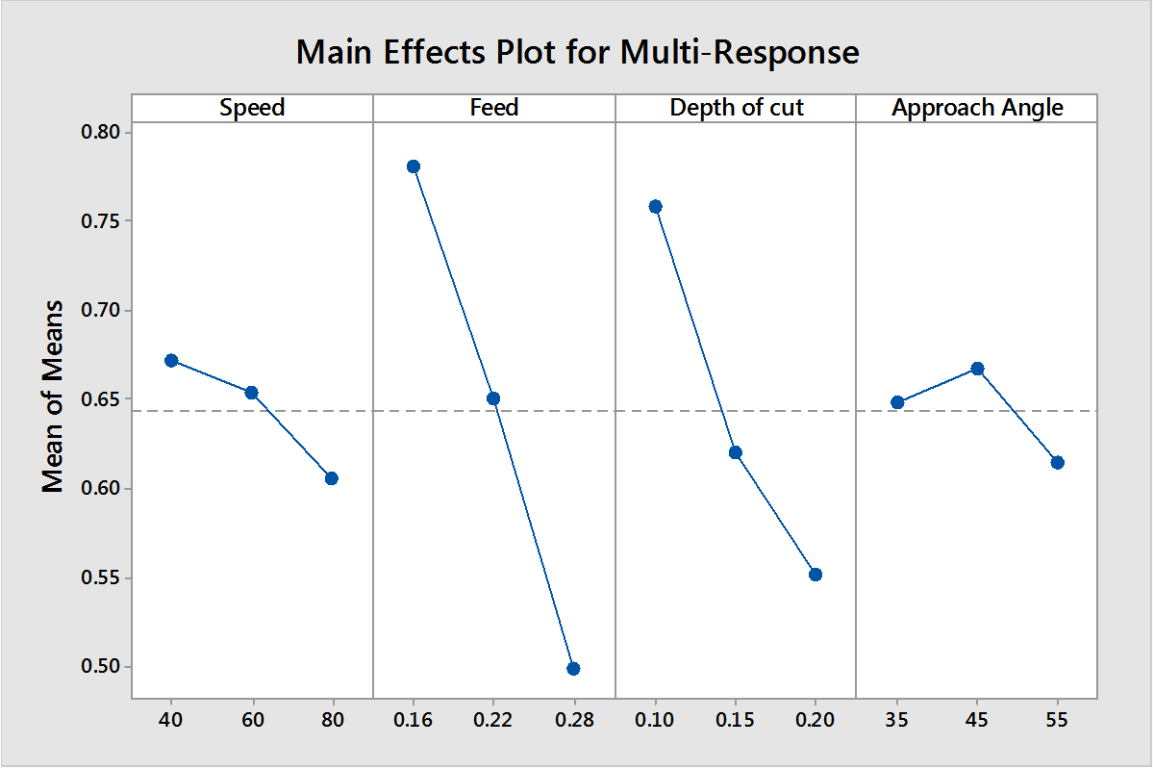

Figure 4.7Main effects plot for means of Gray relational grade

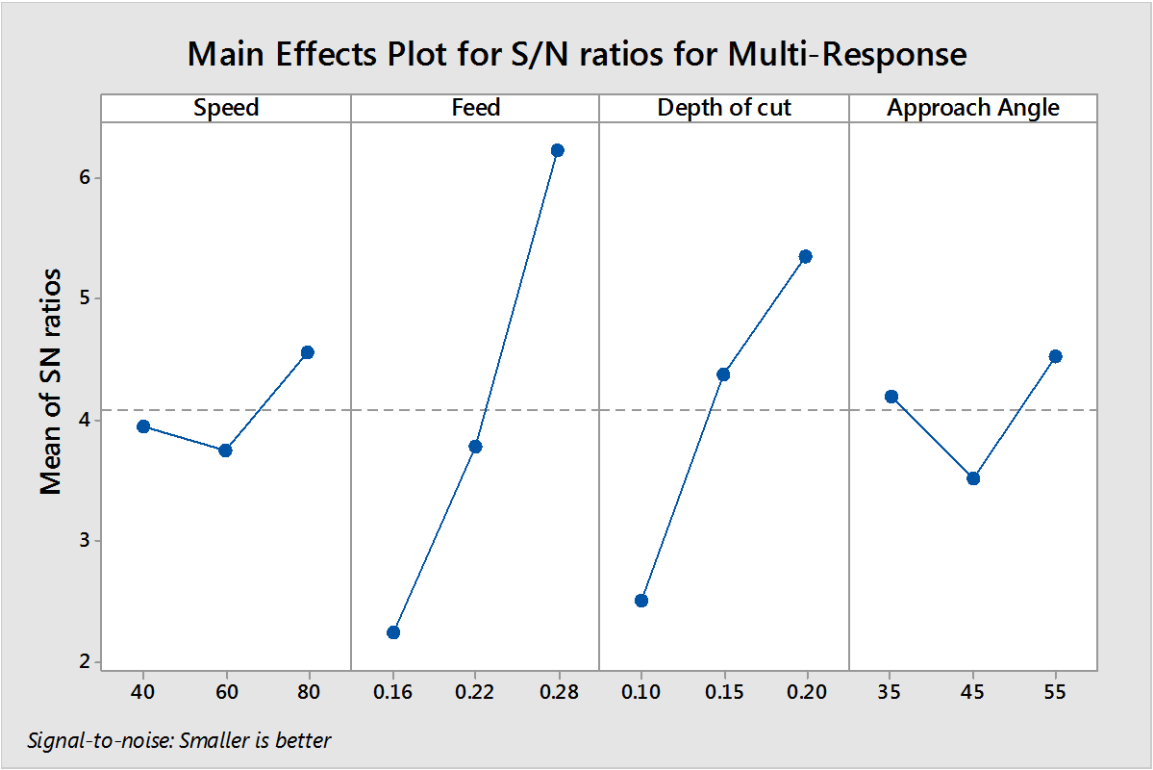

Figure 4.8 Main effects plot for S/N ratios of Gray relational grade

4.6 Conclusion

In this chapter, Taguchi methodology has been employed for analysing the effect of machining parameters and approach angle on face milling of Inconel 718. The method mainly focuses on

robust design methodology that makes it applicable for industrial applications where maintaining inputs accurately like in lab situations can be difficult. Data from the conducted experiments was used for multi-objective optimization using Gray relational analysis. The optimized set of parameters are cutting speed of 40 m/min, a feed rate of 0.16 mm/rev, a depth of cut of 0.10 mm, and approach angle of 45º . It has to be noted that the present study has been conducted with a limited number of experiments. For building a reliable model that can be applied for real life applications, we need to conduct detailed experiments. Moreover, understanding the tool wear mechanism for the tool work piece combination can be useful for further process improvements. These issues are dealt in subsequent chapters.

5 FULL FACTORIAL EXPERIMENTS AND ANN MODEL DEVELOPMENT

Previous chapter analyzed the process using very limited number of experiments. Although it is good for a preliminary analysis, it cannot provide us the details regarding possible interactions and the nature of variation of response variables with respect to input variables. Having a large dataset is also essential for developing a good model. The present chapter uses full factorial experiments as shown in Table 5.1 to develop a large data set. It allows a better analysis of the effects of parameters which can be used to develop an ANN model.

Table 5.1 Full factorial Experimental Design

Std Order	Run Order	Cutting speed	Feed rate	Doc	Approach angle
58	1	80	0.16	0.15	35
78	2	80	0.28	0.15	55
75	3	80	0.28	0.1	55
51	4	60	0.28	0.15	55
50	5	60	0.28	0.15	45
52	6	60	0.28	0.2	35
22	7	40	0.28	0.15	35
7	8	40	0.16	0.2	35
26	9	40	0.28	0.2	45
70	10	80	0.22	0.2	35
8	11	40	0.16	0.2	45
76	12	80	0.28	0.15	35
49	13	60	0.28	0.15	35
43	14	60	0.22	0.2	35
6	15	40	0.16	0.15	55
42	16	60	0.22	0.15	55
18	17	40	0.22	0.2	55
37	18	60	0.22	0.1	35
25	19	40	0.28	0.2	35
57	20	80	0.16	0.1	55
31	21	60	0.16	0.15	35
11	22	40	0.22	0.1	45
67	23	80	0.22	0.15	35
61	24	80	0.16	0.2	35
65	25	80	0.22	0.1	45
79	26	80	0.28	0.2	35
74	27	80	0.28	0.1	45
54	28	60	0.28	0.2	55
2	29	40	0.16	0.1	45
10	30	40	0.22	0.1	35
35	31	60	0.16	0.2	45

47	32	60	0.28	0.1	45
3	33	40	0.16	0.1	55
4	34	40	0.16	0.15	35
38	35	60	0.22	0.1	45
30	36	60	0.16	0.1	55
69	37	80	0.22	0.15	55
20	38	40	0.28	0.1	45
28	39	60	0.16	0.1	35
14	40	40	0.22	0.15	45
45	41	60	0.22	0.2	55
21	42	40	0.28	0.1	55
73	43	80	0.28	0.1	35
32	44	60	0.16	0.15	45
19	45	40	0.28	0.1	35
62	46	80	0.16	0.2	45
29	47	60	0.16	0.1	45
46	48	60	0.28	0.1	35
71	49	80	0.22	0.2	45
23	50	40	0.28	0.15	45
55	51	80	0.16	0.1	35
41	52	60	0.22	0.15	45
60	53	80	0.16	0.15	55
44	54	60	0.22	0.2	45
63	55	80	0.16	0.2	55
24	56	40	0.28	0.15	55
72	57	80	0.22	0.2	55
9	58	40	0.16	0.2	55
39	59	60	0.22	0.1	55
68	60	80	0.22	0.15	45
53	61	60	0.28	0.2	45
12	62	40	0.22	0.1	55
40	63	60	0.22	0.15	35
34	64	60	0.16	0.2	35
80	65	80	0.28	0.2	45
36	66	60	0.16	0.2	55
15	67	40	0.22	0.15	55
5	68	40	0.16	0.15	45
77	69	80	0.28	0.15	45
33	70	60	0.16	0.15	55
13	71	40	0.22	0.15	35
81	72	80	0.28	0.2	55
48	73	60	0.28	0.1	55
27	74	40	0.28	0.2	55

17	75	40	0.22	0.2	45
1	76	40	0.16	0.1	35
66	77	80	0.22	0.1	55
56	78	80	0.16	0.1	45
16	79	40	0.22	0.2	35
64	80	80	0.22	0.1	35
59	81	80	0.16	0.15	45

5.1 Developing a model using ANN

Artificial neural network is a mathematical model inspired by biological neural networks. It consists of an interconnected group of artificial neurons and processes information by using a connectionist approach. It is generally an adaptive system that changes its structure during learning phase. It can be used as a model for complex relationships between inputs and outputs.

A biological brain consists of a large number of highly connected elements called neurons. Each neuron has dendrites, cell body and axon. Dendrites are a tree like receptive networks of nerve fibers that carry electrical signals to the cell body. The cell body acts as a summing up and threshold device for incoming signals. Axon is a long fibre that carries signal from cell body to other neurons. The point of contact between an axon of one cell and a dendrite of another is called synapse. The function of a neural network is mainly dependent on arrangement of neurons and strengths of synapses. Some part of the neural structure is defined at birth and the other part is developed through learning. During this time new connections are made and some are broken. This happens mainly in the early stages of life of an organism. Neural structures change through the life but changes are mainly in strength of synapses.

Artificial neural networks are a very simplified case of a biological neuron. It is similar to biological network on the following issues:

1. Building blocks are simple computational devices that are interconnected.
2. Connections determine the function of the network.

A simple artificial neuron model is as shown in Figure 5.1.

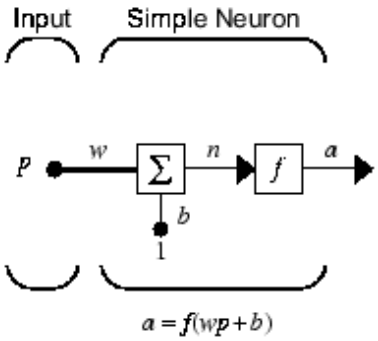

Figure 5.1 A simple model for Neuron [54]

The artificial neuron tries to emulate the biological neuron by using the above network. In the above network, input *p* is multiplied by weight *w*. This step is known as weight function. To this *wp* a bias *b* is added to get the net input *n*. This addition of bias is known as net input function. The net input is passed through a function *f* to produce an output *a*. The function *f* is called transfer function. The main idea of ANN is to modify these functions and parameters *a* and *b* so that it can act as a model to the experimentally observed data.

In the present discussion, neural network has been used as a fitting tool. Neural network fitting tool from MATLAB has been used directly to generate the model.[54]

5.1.1 Developing ANN model using MATLAB

The following steps are involved in developing model using MATLAB fitting tool [54]:

1. Collect data
2. Create the network
3. Configure the network
4. Initialize the weights and biases
5. Train the network
6. Validate the network
7. Use the network

The experimental data collected is first normalized so that better convergence and accuracy can be obtained. The data has been normalized to 0.1 and 0.9 individually for every factor and response. The following formula was used to normalize:

$$\text{Normalized value} = \left(\frac{\text{experimental value} - \text{minimum value}}{\text{maximum value} - \text{minimum value}} \right) \times 0.8 + 0.1$$

The data is now made into Input matrix consisting of all the input parameters. Force and surface roughness vectors have also been developed. These are stored as variables in MATLAB workspace. In the tool box, the Inputs and targets are selected from the variables defined. The data is then randomly divided into 3 sets for training, validation and development. The default division was used i.e. 70% for training, 15% for validation and another 15% for an independent test of network generalization. The validation step is used for generalizing and to stop training to avoid over-fitting.

The standard network is used in this discussion is shown in Figure 5.2. This consists of

1. Two-layer feed forward network, hidden layer and output layer.
2. Sigmoid transfer function in hidden layer
3. Linear transfer function in output layer
4. Neurons have been selected as 10 after trial and error with different values.

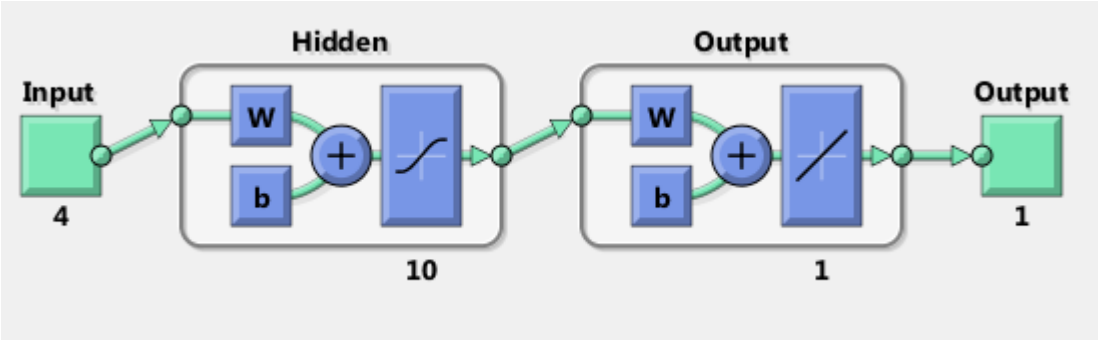

Figure 5.2 ANN Network with 10 neurons in the hidden Layer

This model is trained, validated and tested by the tool. Levenberg-Marquardt back propagation algorithm is used by the tool. The related plots regarding convergence, mean square error and regression can be directly obtained. For a good model, the value of R i.e. correlation between output and target values, must be close to 1. A reasonable fit can be obtained if R>0.93. Mean square error must be close to 0. Mean square error is the average of squared difference between outputs and targets. Network performance can be increased by the following methods:

1. If network performance is poor, increase the number of neurons
2. Retraining
3. Use a larger data set

If performance of training set is good but test set is worse, it means that the data is over-fit. In this case neurons are reduced. If training performance is poor, number of neurons has to be increased [54].

The following discussion analyses the experiments for obtaining maximum information. In both cases full factorial experiments have been conducted and analyzed. The first set of experiments analyses the major factors affecting Machinability and the goal is to develop a model that can be used for face milling of Inconel within the machining limits specified.

5.2 Effect of cutting parameters and approach angle on machinability

The full factorial experimental design is determined using Minitab software. It also takes care of randomization. The experiments were randomized to reduce the possible effects of changes with respect to time during the duration of experiments. The following sections present ANOVA analysis and effects plot.

5.2.1 Analysis of Experimental data

As described in previous section, Minitab has been used to find out significant factors and interactions from the experimental data. Three way interactions have been neglected. The analysis of variance for Force using adjusted SS values is shown in Table 5.2.

Table 5.2 ANOVA Table for Cutting Force (F_y)

Source	**DF**	**Adj SS**	**Adj MS**	**F**	**P**	**Source**
Cutting speed	2	6538	3269.1	27.03	<0.01	Cutting speed
Feed rate	2	44547	22273.7	184.15	<0.01	Feed rate
Doc	2	76158	38079.1	314.83	<0.01	Doc
Approach angle	2	22715	11357.7	93.9	<0.01	Approach angle
Cutting speed*Feed rate	4	475	118.7	0.98	0.427	Cutting speed*Feed rate
Cutting speed*doc	4	129	32.3	0.27	0.898	Cutting speed*doc
Cutting speed*Approach angle	4	364	91	0.75	0.561	Cutting speed*Approach angle
Feed rate*doc	4	5839	1459.7	12.07	<0.01	Feed rate*doc
Feed rate*Approach angle	4	19957	4989.2	41.25	<0.01	Feed rate*Approach angle
doc*Approach angle	4	309	77.3	0.64	0.637	doc*Approach angle
Error	48	5806	121			Error
Total	80					Total

As can be seen from the Table 5.2 , depth of cut is the most significant factor because of the direct relation it has in increasing the shearing area without changing specific cutting pressure. The next factor is feed rate which increases shearing area but also decreases specific cutting pressure which results in increase in force but not as significant as depth of cut. Approach angle is the next significant factor that affects the force because of the change in thickness of the chip

that affects chip area. Larger angles increase the chip thickness. It also affects the balance of axial and radial force. The effect of cutting speed is minimal because of the intermittent cutting process which allows for cooling of the tip during the cycle. As average values of force are taken, the effect of impact forces due to cutting speed has not been studied. An interaction effect of feed rate and approach angle has been observed. This can be mainly due to their effect on changing chip thickness and the length of tool contact. A small effect of Feed rate and depth of cut interaction effect has been observed as shown in Figure 5.3. This can possibly be due to the effect of slenderness ratio on the dynamics of the process. This can cause vibrations which might have increased the force values.

The analysis of variance for surface roughness using adjusted SS values is shown in Table 5.3:

Table 5.3 ANOVA Table for Surface Roughness (R_a)

Source	**DF**	**Adj SS**	**Adj MS**	**F**	**P**	**Source**
Cutting speed	2	0.3991	0.1996	41.93	<0.01	Cutting speed
Feed rate	2	17.4962	8.74811	1838.08	<0.01	Feed rate
Doc	2	0.7017	0.3509	73.72	<0.01	Doc
Approach angle	2	0.6277	0.3139	65.95	<0.01	Approach angle
Cutting speed*Feed rate	4	0.0235	0.0059	1.23	0.31	Cutting speed*Feed rate
Cutting speed*doc	4	0.0248	0.0062	1.3	0.283	Cutting speed*doc
Cutting speed*Approach angle	4		0.00215	0.45	0.771	Cutting speed*Approach angle
Feed rate*doc	4		0.00936	1.97	0.115	Feed rate*doc
Feed rate*Approach angle	4	0.0709	0.01772	3.72	0.01	Feed rate*Approach angle
doc*Approach angle	4	0.063	0.01575	3.31	0.018	doc*Approach angle
Error	48	0.2284	0.0476			Error
Total	80	19.6814				Total

Feed rate is the most significant factor. This is mainly due to the feed ridges which are the main source for surface roughness. Effect of depth of cut and approach angle can be in mainly vibrations developed in the system. Lower effect of cutting speed can be due to the lack of formation of BUE in the cutting range. Making the process stable without any rubbing or ploughing effect is associated with BUE.

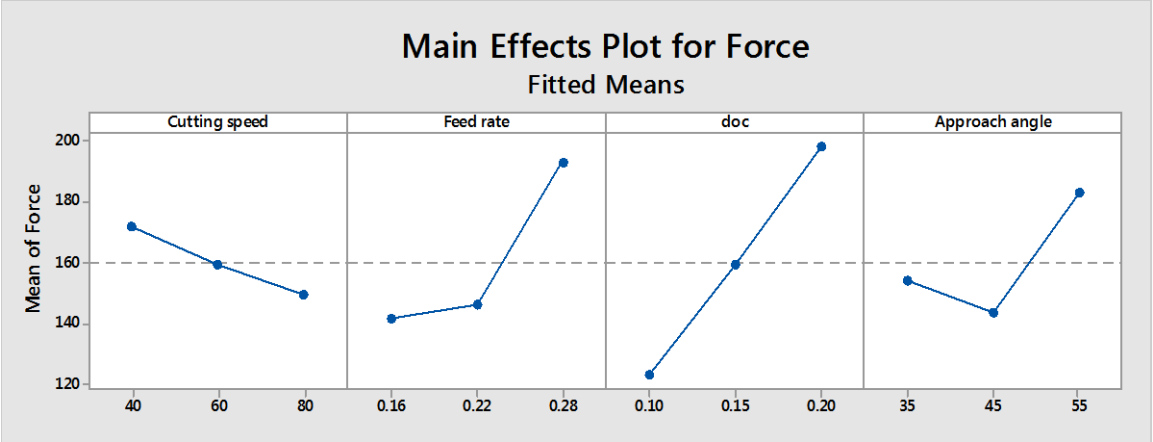

Figure 5.3 Main effects plot for Cutting Force (F_y)

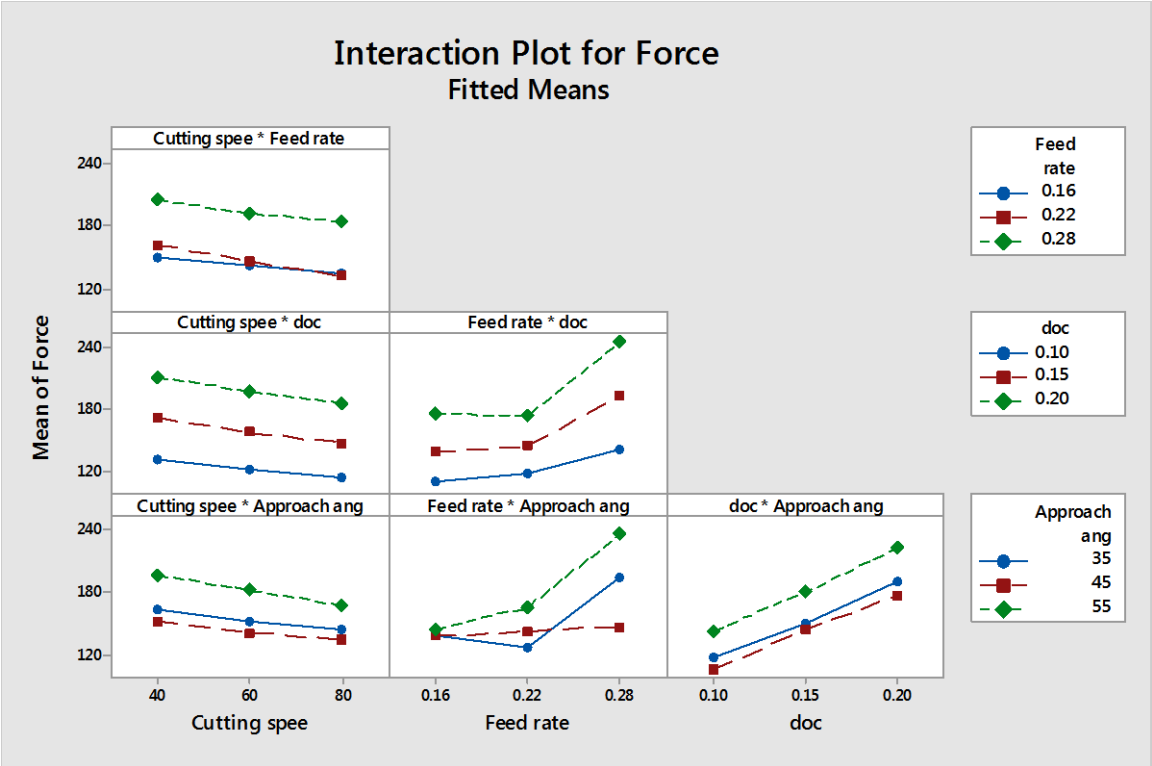

Figure 5.4 Interaction plot for Cutting Force (F_y)

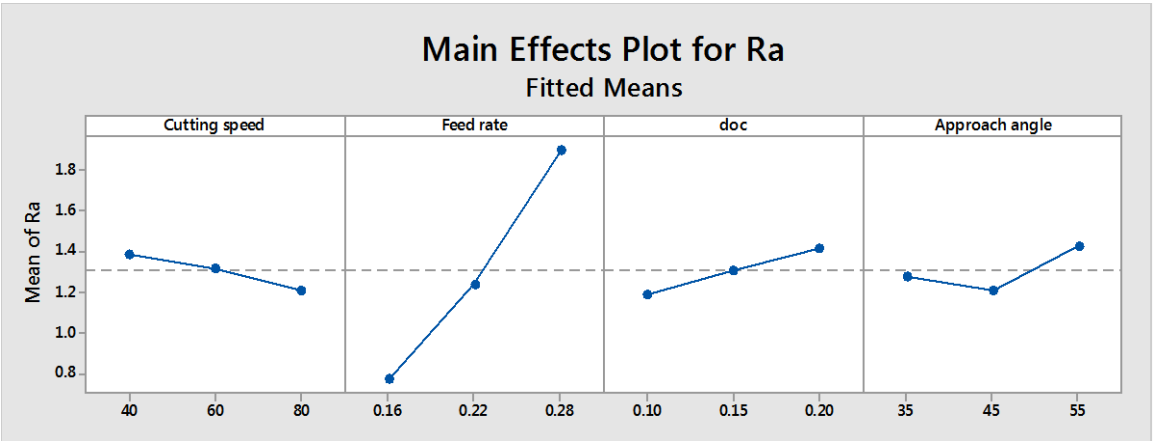

Figure 5.5 Main Effects plot for Surface Roughness (R_a)

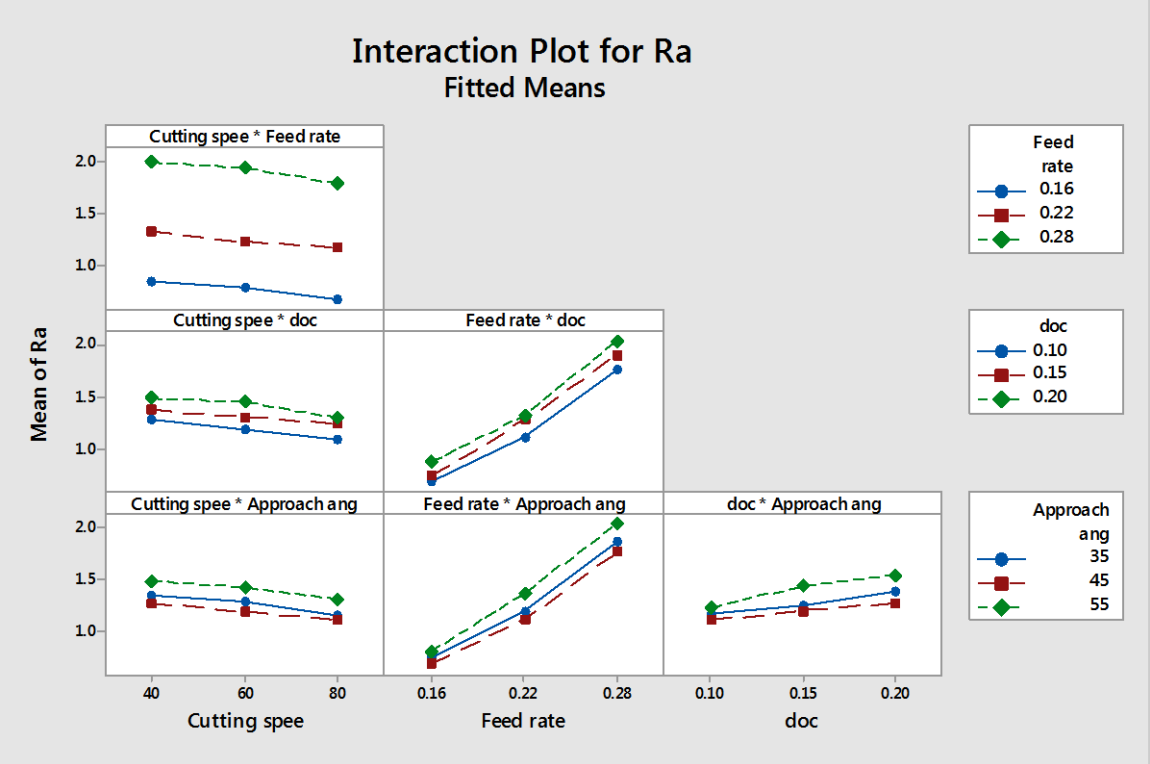

Figure 5.6 Interaction plot for Surface Roughness (R_a)

5.3 MODELING USING ANN

Artificial neural network fitting tool of MATLAB R2010a has been used to develop a model individually for Force and surface roughness. The data has been normalized to 0.1 and 0.9 individually for every factor and response. The following formula was used to normalize:

$$\text{Normalized value} = \left(\frac{\text{experimental value} - \text{minimum value}}{\text{maximum value} - \text{minimum value}} \right) \times 0.8 + 0.1$$

The normalized data was arranged as input matrix of all input parameters and a vector each for Force and surface roughness (R_a) was initialized in MATLAB. A 2 layer ANN model was developed by trying out with different values of neurons. After a series of trials, 10 neurons were found to be apt for the data. By further retraining the model, a satisfactory model with R value close to 1 was achieved.

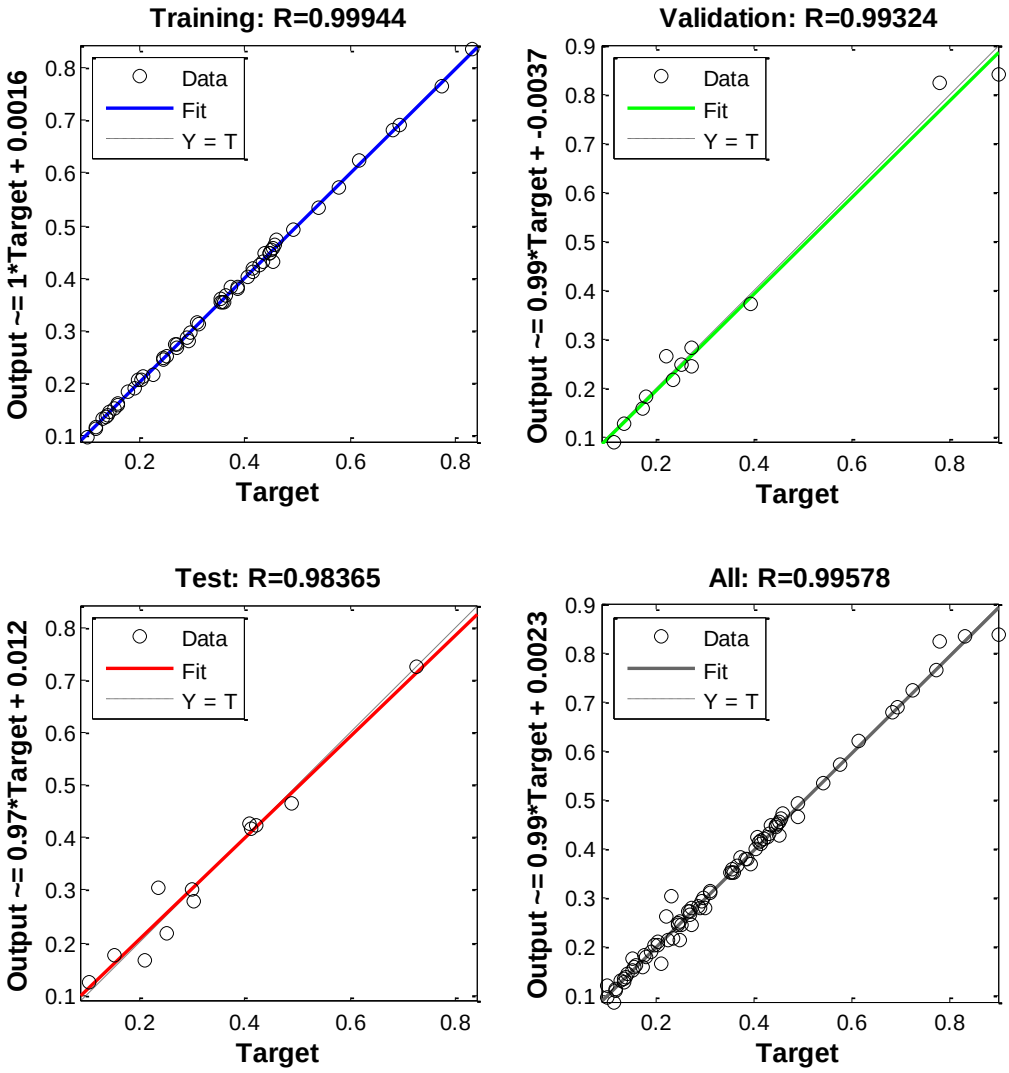

Figure 5.7 Residual Graphs for the ANN model of Cutting Force (F_y)

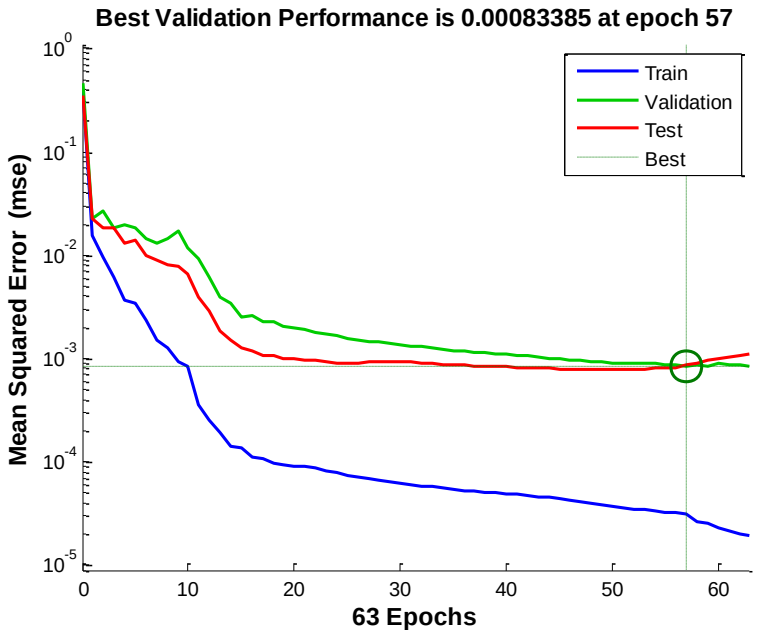

Figure 5.8 Mean Square Error vs Iterations for ANN model of Cutting Force (F_y)

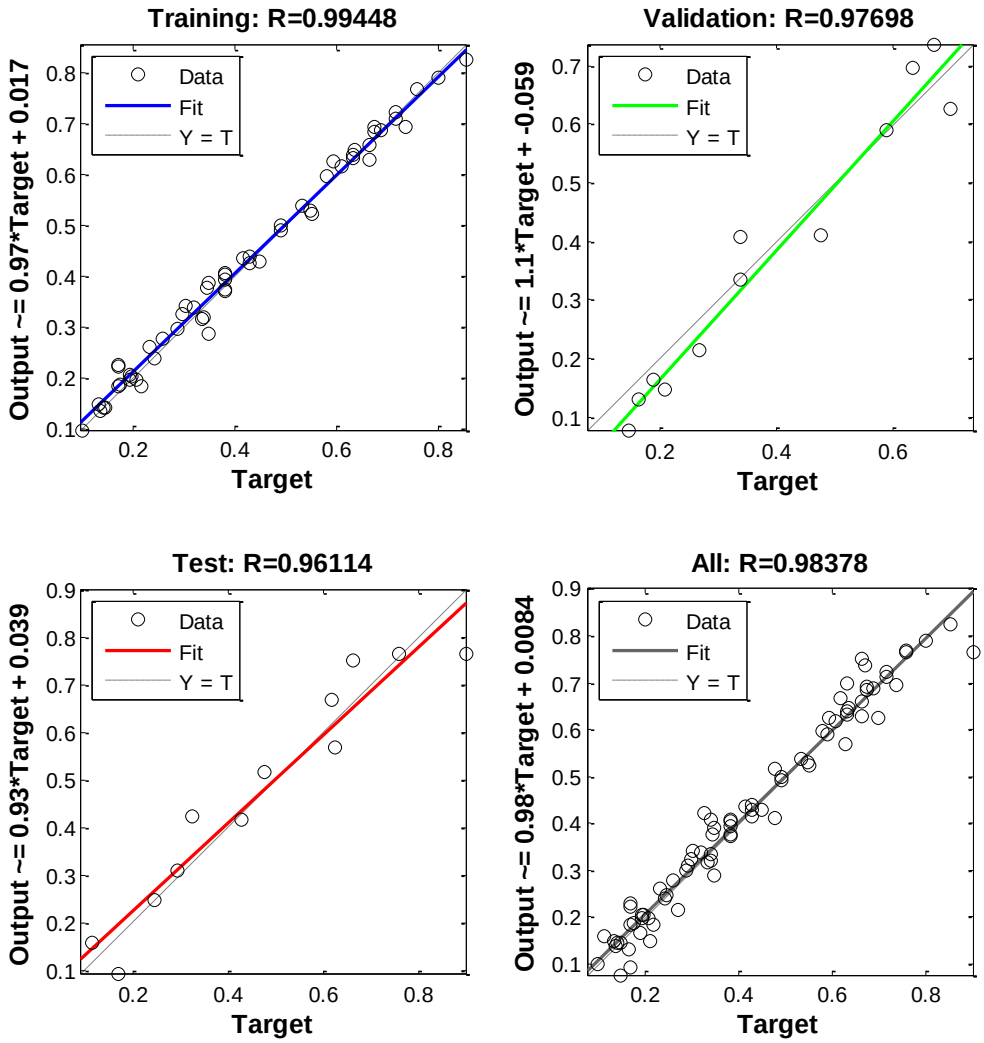

Figure 5.9Residual Graphs for the ANN model of Surface Roughness (R_a)

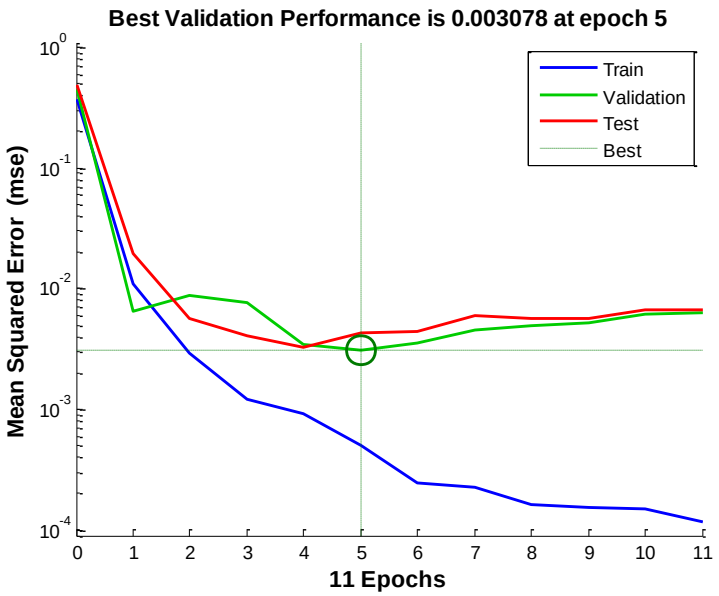

Figure 5.10 Mean square error vs iterations for ANN model of Surface Roughness (R_a)

5.4 Conclusions

From the analysis of effect of parameters and approach angle it can be concluded that:

1. Significant factors affecting the cutting Force are depth of cut, feed, approach angle, interaction of feed rate and approach angle, cutting speed and interaction feed rate and depth of cut in decreasing order of magnitude. The possible reasons for their effects have been discussed thoroughly.
2. Significant factor affecting surface roughness (R_a value) is feed. Depths of cut, approach angle and cutting speed have small influence on R_a value. No significant interactions were observed.
3. ANN model has been developed individually for Force and surface roughness using neural network fitting tool. It provides an efficient and easier method to develop a model that can be easily used and is accurate.

The present chapter dealt with the macroscopic effects of machining in terms of observable parameters like Cutting force and surface roughness. To better understand the process analysis of microscopic wear mechanism occurring at the tool interface is essential. The next chapter focuses on this.

6 SEM AND EDS STUDIES

As mentioned in the previous chapter, microscopic wear phenomenon helps us in explaining qualitatively reasons behind the macroscopic effects observed during face milling of Inconel 718. The first step in understanding wear at the interface is observing the worn tool surface. To get a better idea of the type of wear, a high resolution image of the surface is essential. This can be achieved by using Electron microscopy as it allows for higher resolution and greater magnification compared to optical methods. Once the surfaces are analyzed, the next step would be observing the chemical composition of worn out areas of the tool. Understanding the chemical composition is essential for checking formation of oxides at the interface or even presence of diffusion wear, a phenomenon occurring at high temperature where difference in concentration of elements between two mating surfaces results in flow of that element from one component to another. As Inconel 718 is a Heat resistant super alloy, interface temperature is generally high. Hence, analyzing diffusion wear for this case is important. Measuring elemental compositions can be performed by Electron discharge spectroscopy (EDS). This is generally available in most of the Scanning Electron Microscopy (SEM) machines, both measurements can be conducted quickly without changing any set-up.

6.1 Functional Principle of SEM

Microscopes generally consist of an illumination source, a condenser lens to converge the beam on to the sample, an objective lens to magnify the image, and a projector lens to project the image onto an image plane which can be photographed or stored. In electron microscopes, the wave nature of the electron is used to obtain an image. Scanning electron microscopy (SEM) utilizes electrons as the source for illuminating the sample. Electromagnetic lenses are used in electron microscopes [55].

The electron in a magnetic field undergoes rotation. As the radial component of the magnetic field reverses after the center of the lens, the rotation in the first half of the lens is reversed. The electron leaves the lens without any net change in the angular momentum, but it undergoes deflection towards the axis. In SEM, the scanned image is formed point by point and the scan is achieved by the scan coils. The electron beam is swept across the sample. The secondary electrons produced by the sample are detected. The intensity of the signal at the CRT is proportional to the secondary electrons. An intense signal can illuminate several dots on the screen, while a weak signal would mean that no dots will be illuminated by the electron gun. The detector therefore gives the intensity of the signal, while the raster pattern gives the location

of the signal. The image on the CRT is built up point by point to match what is happening on the surface of the sample.

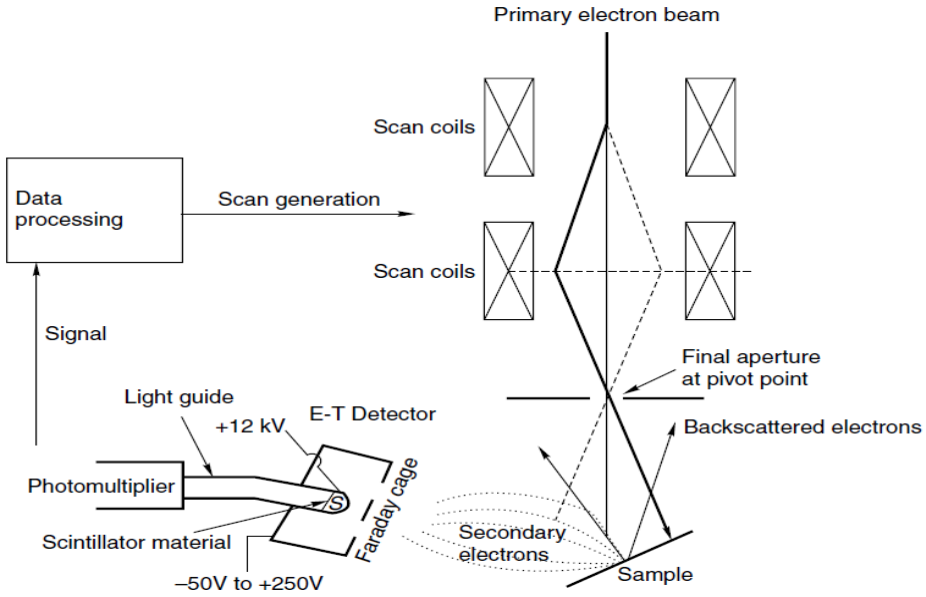

Figure 6.1 Schematic of SEM

6.2 Functional principle of EDS

Mostly EDS is integrated in same setup of instruments of SEM. Electrons from electron gun are bombarded on sample. When an electron approaches the atom, it gets decelerated due to the columbic field. This results in a loss of energy for the electron and that energy appears as photon, referred to as bremsstrahlung or 'breaking radiation'. This radiation contains photons of all energies. The electrons of higher energy lose energy to reach stable state and hence emit the energy in the form of radiation. In EDS, all photons emitted by the sample are collected and measured simultaneously by a solid state X-ray detector. In EDS, a signal from the detector is proportional to both the energy and intensity of the X-rays. The common EDS detector is lithium-drifted silicon, Si (Li).

6.3 SEM and EDS Analyzer

The VEGA3 SB - Easy Probe is a compact scanning electron microscope (SEM) fully integrated with a selected energy dispersive X-ray microanalyser (EDX). Superior imaging quality, high level of automation, easy usage and quick quantitative elemental results directly in the live image are among the characteristic features of the instrument. A variable pressure vacuum system allows investigation of non-conductive samples in their natural uncoated state.

Figure 6.2 SEM and EDS Instrumentation and analysis Panel

6.3.1 Technical specifications

Electron Optics:

Electron Gun: Tungsten heated cathode

Resolution:

High Vacuum Mode (SE):	3 nm at 30 kV 8 nm at 3 kV
Low Vacuum Mode (BSE):	3.5 nm at 30 kV
Magnification:	3x – 1,000,000x
Maximum Field of View:	7.7 mm at WD analytical 10 mm, 24 mm at WD 30 mm
Accelerating Voltage:	200 V to 30 kV
Probe Current:	1 pA to 2 µA

The VEGA 3 works like other common three lens microscopes. The aperture is nearly optimal for lower BI values (small spot size, low beam current), short working distances (4 - 5 mm) and for the accelerating voltage 30 kV. The pivot point of the scanning and the electric image shifts are close to the principal plane of the objective OBJ, so that the curvature of the field, distortion and field of view are as good as possible. The centering of the objective is performed by defined

beam tilt of the central electron beam, which does not cause image shift. This mode is intended for displaying with the highest resolution. The Figure 6.3 shows specimen holder used for analysis. The specimen is normally glued with conductive glue or stuck on with double-sided sealing tape.

Figure 6.3 Standard specimen holder

6.4 Tool wear Studies

Tool wear is generally a gradual process and wear rate depends on tool and workpiece materials, process parameters, tool shape, cutting fluid, and machine-tool characteristics. In milling of Nickel based alloy with coated tools, the boundary wear width decided the tool life, whereas in cemented carbide tools, the major flank wear width decided the tool life.

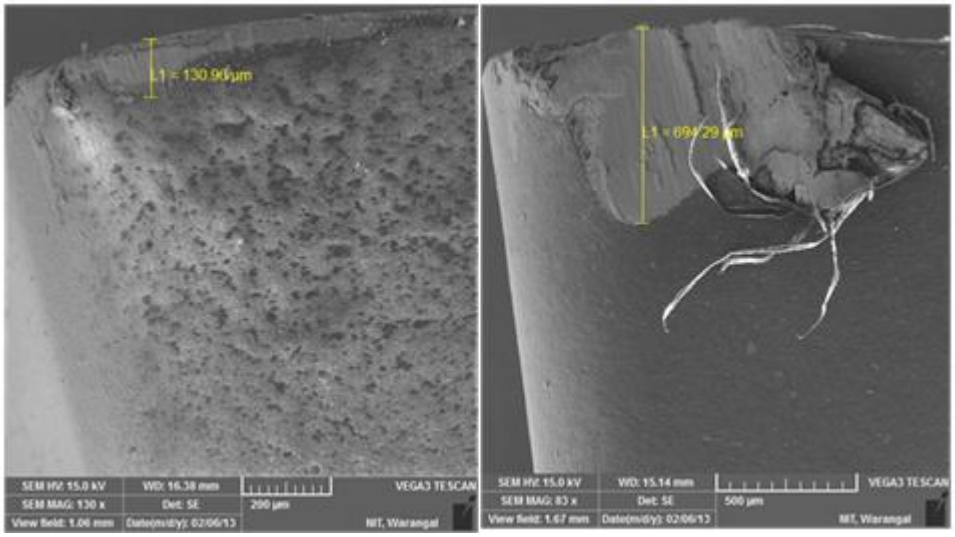

Figure 6.4 Left: Tool Wear measurement Right; Presence of Built-Up-Edge on a specimen

There are several types of wear mechanisms that can influence the tool wear and subsequently the tool life when machining Inconel 718. The temperature generated within the primary and secondary shear zones affects the wear rate of tool materials. Hence, high cutting temperature often results in severe tool wear, such as plastic deformation, chipping and fracture at the cutting edge.

The observed wear mechanisms were flank wear, chipping and plastic deformation as shown in Figure 6.4. Also in one case, built up edge BUE is observed as shown in Figure 6.4. Damage observed on the rake surface, such as crater wear, was quite limited. Fig. shows the typical flank face wear at the speeds of 40, 60 and 80 m/min when machining Inconel 718 with inserts SPMW 120408 TN7535. The flank wear rate was rapid at higher cutting speeds. Increased flank wear rate was observed with increase in the cutting speed. With increase in speed, cutting temperature rises. The increased temperature reduces the strength of insert, which in turn leads to higher wear rates as mentioned in Table 4.8. While at lower cutting speed, cutting forces are higher which probably caused higher wear. At medium cutting speed, flank wear is found to be minimum.

Chipping of tool edge is observed at higher cutting speeds, being reported as dominant wear mechanism while milling Inconel 718. Chipping is directly related to attrition wear and thermal cracking occurring at higher temperatures [56]. The intrinsic characteristics of Ni alloys cutting; such as the irregular flow of work material against cutting edge, chip segmentation inducing variable forces and in consequences, fatigue and also thermo mechanical fatigue leading to cracking, are the origins of attrition.

It is worth to note that wear mechanisms are not independent; they are interrelated [17]. Adhesion of work material causing built up edge (BUE) formation tends to promote tool chipping, since BUE is never completely stable but it periodically breaks off taking with it a small lump of tool edge. The observation of BUE and that of chipping can be interrelated wear mechanisms here.

6.5 EDS Analysis

EDS analysis was performed to study the elements present at the surfaces of the worn cutting tool inserts. During visualization of samples, significant worn out areas of tool inserts were analyzed. Acceleration voltages used for SEM and EDS analyses were changed between 12 and 15 kV for different samples in order to focus the different depths worn out areas of the various samples used for analysis. Recorded EDS spectra were analyzed for elements known or expected to be present at the surface of the wear.

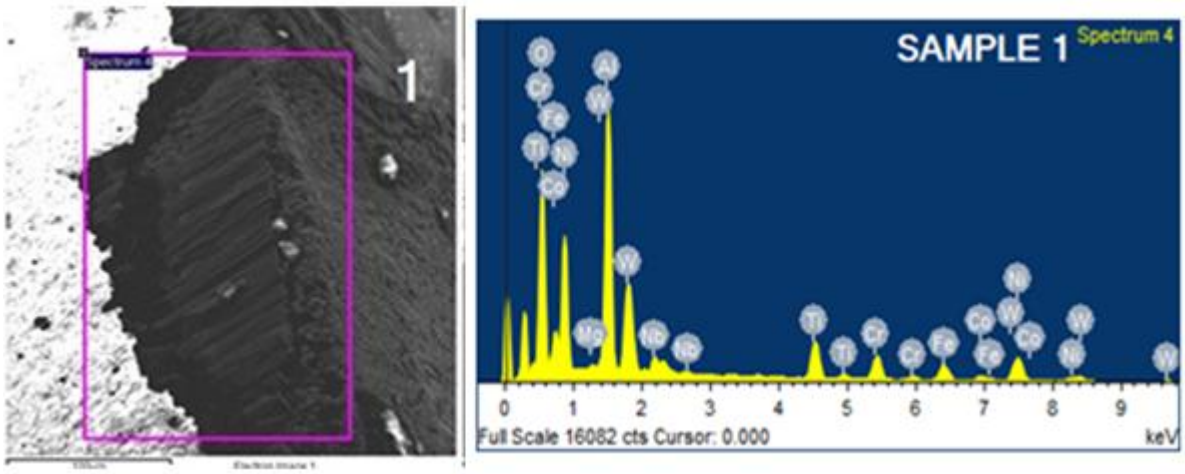

Figure 6.5 Left: EDS Capturing zone Right: EDS Spectrum for the Captured zone

The complete results from EDS spectra in terms of elemental composition in % for different samples are presented in Table 6.1.

Table 6.1 Percentage elemental compositions of samples

	V	F	D	AA	O	Al	Ti	Cr	Fe	Co	Ni	Nb	W
0	0	0	0	0	59.25	40.38	0.38	0	0	0	0	0	0
1	40	0.16	0.1	35	30.9	14.28	6.43	5.9	5.94	2.08	15.4	2.36	16.47
2	40	0.22	0.15	45	19.85	7.94	1.45	9.32	9.51	2.69	23.91	6.04	19.27
3	40	0.28	0.2	55	35.6	19.43	1.8	5.61	6.15	2.08	15.07	2.62	11.64
4	60	0.16	0.15	55	33.44	14.23	2.11	5.3	5.55	2.05	13.44	2.37	21.52
5	60	0.22	0.2	35	33.43	19.32	3.48	7.04	7.35	0.99	18.83	2.1	7.02
6	60	0.28	0.1	45	40.01	25.43	1.16	5.18	5.56	0.8	14.32	1.84	5.71
7	80	0.16	0.2	45	37.55	23.94	1.63	5.62	5.74	2.07	16.55	1.58	5.29
8	80	0.22	0.1	55	34.73	22.62	2.18	7.52	7.62	2.19	14.23	1.67	7.23
9	80	0.28	0.15	35	39.5	23.56	1.49	6.43	6.77	0.98	13.91	1.89	5.48

As can be seen from Table 6.1, the elemental compositions seem to consist of mainly O, Ni, W, Al, Cr and Fe while small quantities of Ti, Co and Nb are also found in all the spectra. Out of all, Ni, Cr, Fe and Nb can be supposed to be diffused from work material. Possibility of Diffusion of Al and Ti is also discussed as they both are constituent of workpiece and insert. Out of these Oxygen is found to have maximum percentage. Next comes Ni and Al. W is the main composition of the insert. Hence it is not needed to be discussed.

As Ni is the main composition of Inconel 718, it is important to discuss it. The detected amounts of Ni are found to be decreasing with increasing cutting speed as shown in Figure 6.6. The peak is found for intermediate feed since amounts of Ni first increases with increase in feed and then decrease as feed increases.

Cr and Fe are next main constituents of Inconel 718. The amounts of Cr and Fe seem to follow the same variation pattern as shown in Figure 6.7 and Figure 6.8. The elemental percentages of Cr and Fe are almost same in all samples' analyses. Both of them first reduce as speed increases to the intermediate value. Then they increase nearly up to the mean value as speed increases to maximum. This happens in the contrary with the feed. The amounts of Cr and Fe first increase as feed increase to intermediate value. Then they decrease as feed increases to maximum.

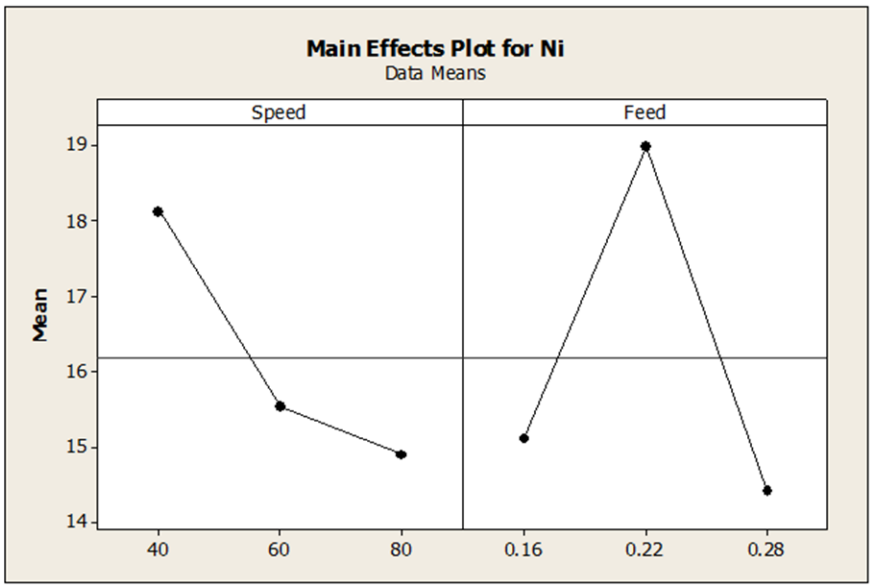

Figure 6.6 Ni% vs Cutting speed and Feed

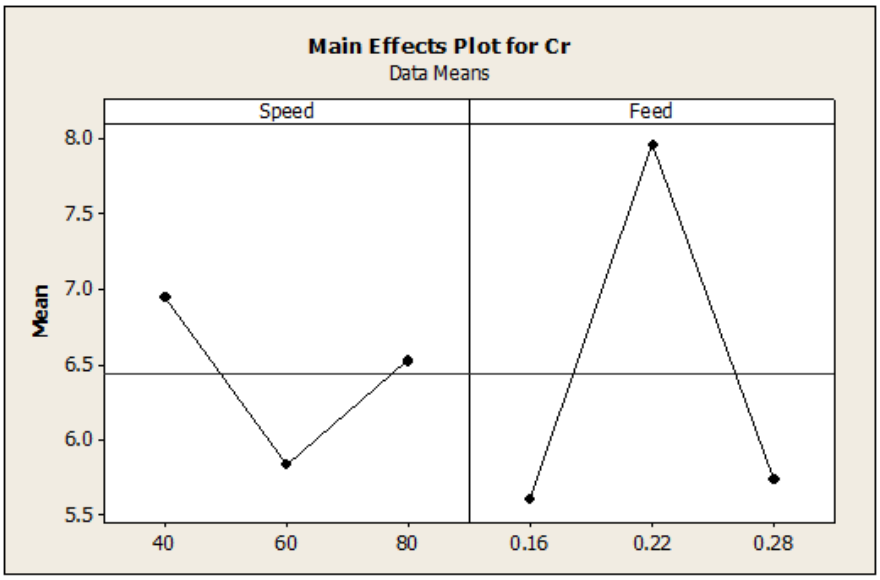

Figure 6.7 Cr% vs Cutting Speed and Feed

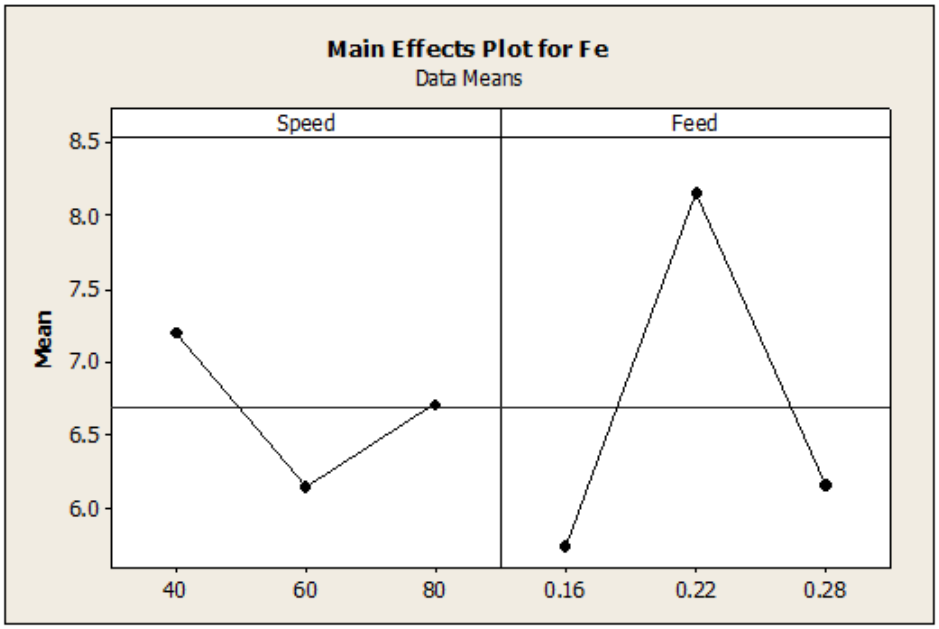

Figure 6.8 Fe% vs Cutting speed and feed

The amounts of Co are found to be constant around 2% except sample 5, 7 and 9 in which they are close to 1%. The Nb amounts decreases with as cutting speed increases. Amounts of Ti do not follow any specific pattern. Also behavior of its elemental percentage does not match with any other element. Amounts of Al and O are found to vary similarly. In samples 2 and 4, random variation of Al is found.

6.6 Conclusions

The following conclusions can be made from the analysis:

1. It can be concluded that Ni, Cr, Fe and Nb are diffused from work material. As they are found in all samples' analyses, it can be confirmed that diffusion has taken place in all conditions of process parameters.
2. During machining, the cutting edge will reach very high temperatures and the cooling time after the completion of the machining operation may be long enough for the cutting tool to react chemically with the surrounding atmosphere at elevated temperatures. In this situation, there possibility of forming oxides.
3. Presence of O shows the possibility of formation of oxides. As Ni, Cr and Fe have affinity towards oxygen, there is possibility of formation of their oxides. Those will also contribute to the amount of O along with Al_2O_3. Since the amounts of Cr and Fe are same, the percentages of their oxides can also be the same. Earlier researchers suggested the formation of titanium oxide in machining of Titanium based super alloys, which

could be possible here, but this has to be further investigated before any conclusions can be drawn.

4. The random behavior of Al in sample 2 and 4 with oxygen than that in other samples, also shows the possibility of the diffusion of Al from workpiece.
5. Ti is in composition of both the work material and the insert coating. Also the depth up to which wear has gone will have significant effect on the elemental percentage of Ti since TiC is one of the coatings of insert. Hence the diffusion of Ti cannot be properly concluded.

The present study provides a qualitative analysis of wear mechanism occurring at the interface based on the elemental compositions from EDS and the SEM images of the tool. Diffusion wear has been established as predominant wear mechanism. This can be controlled either by using an insert with different material than the element being diffused or by reducing the interface temperature by use of metal working fluid. The present study focuses on providing Coolant which has an additional benefit of reducing cutting forces and surface roughness.

7 MINIMUM QUANTITY LUBRICATION USING VEGETABLE OIL AND NANO-FLUIDS

The previous chapters were focused on dry machining and how to get the maximum possible efficiency from the tool. Inconel 718, being a heat resistant super alloy (HRSA) and having low thermal conductivity, generates high heat at the interface. This can cause increased tool wear and the heat can cause thermal distortion to the workpieces being machined. This led to extensive use of flood coolants for machining Inconel 718 and other HRSAs. With the increasing costs and potential health hazards of coolant fluids, this solution is not sustainable for future. The present study applies Minimum quantity Lubrication by use of environmental friendly vegetable oil. Nano-fluids from vegetable oils were prepared and analysed.

7.1 Cutting Fluids

The main function of cutting fluids is lubrication at low cutting speeds and cooling at relatively high speeds. At high cutting speeds there is no time for fluid to penetrate into the cutting zone or micro-cracks on the backside of the chip. The lubrication action at high speeds is attributed to the high pressure of the coolant that helps in chip curl and reducing the chip contact length. Apart from the cooling and lubrication effects, the other main advantages are chip breakage, chip disposal and transferring heat away from the metal cutting system, reducing the associated thermal affects. This makes cutting fluid an essential part of metal cutting. The costs associated with cutting fluids is around 8-10% while the tool costs are around 5-7% for simple operations to 12-15% in the case of advanced power train gear components. The costs further increase due to environmental issues involved. The cost of cutting fluids in USA alone is $48 billion. [6]

7.1.1 Environmental aspects and related issues of cutting fluids

The environmental issues are mainly due to exposure to cutting fluids. Though the exact effect on the individual depends on exact formulation and additives used, in general exposure to cutting fluids can be by skin contact, ingesting particles, mists or aerosols and inhaling. Skin exposure can result in skin diseases. Repeated inhalation affects functioning of lungs. Mists can cause respiratory diseases. Some cutting fluids are even carcinogenic. In view of these issues, the following methods are employed:

1. Balanced selection of cutting fluids keeping ecological and health aspects in view. Vegetable oils are being recommended by a major automotive manufacturer and even Canadian Auto workers Union. With highly fluctuating crude oil prices, vegetable oils have become suitable alternatives.

2. Proper application of cutting fluids by providing only the amount required rather than employing flood coolants can drastically reduce the costs and at the same time reduces the environmental effects. Studies in this area are mainly focused on nozzle design, placement, type of flow etc. The high pressure through the tool coolant system is one of the most effective technologies being used.
3. Management and maintenance of cutting fluids by extending the useful life of metal working fluids and disposing them off after their use at lowest costs.
4. Gradual reduction of Metal Working Fluids by using near-dry and dry machining

7.1.2 Near-dry machining (NDM)

Dry machining has the main advantage of clean parts, increased recycle value of swarf. This reduces the cost of machining and the need for cutting fluid maintenance equipment. The main problem with dry machining is the need for change of machines and tools as the present machines cannot be directly used for dry machining. Use of powerful machines, special tooling, altering cutting parameters and tool geometry to suit dry machining involve large capital expenditure and time. Processes like drilling will require cutting fluids for swarf removal. The quality of machined parts can reduce due to high forces and distortions due to temperature. Metallurgical properties and residual stresses will be significantly different from wet machining. Cooling solutions like use of cryogenic coolant and thermo-electric cooling of tools are costly for practical application. [57].

In Near-dry machining, coolant is atomized and an emulsion of pressurized air and atomized oil is sprayed in the cutting zone. It is an alternative to the traditional flood coolant. Near-dry machining is formerly known as Minimum quantity lubrication (MQL) that supplies very small amount of cutting fluids in the machining zone. NDM can solve some of the issues of dry machining and can be used along with existing flood coolant machine set-ups without many changes and is cost effective and easy to implement. In this method, the cutting fluid is supplied as a mixture of air and oil to form an aerosol (commonly known as mist). The oil droplets are taken to the cutting zone by pressurized air. Aerosol is made by atomization process forming small droplets of 1-5 μm. Studies show that temperature reduction in turning is approximately 5%, in case of end milling is 10-15% and it is 20-25% in case of drilling when compared to dry machining. By proper selection of NDM system, results comparable to flood coolant can be achieved [6].

7.1.3 Mechanism of Cutting Fluids

Aerosols do not act like boundary lubricants. With high pressures existing in the cutting zone, it is impossible for them to form a layer. Aerosols have lower cooling ability compared to cutting fluids. Cooling due to forced convection of air and droplet evaporation is also small. It cannot alter the chip flow direction as in the case of high pressure cutting fluids because of low momentum. The only possible explanation can be Rehbinder effect, also known as adsorption induced reduction of strength of solids (AIRS). [57], [58]

The shearing zone in metal cutting occurs mainly by formation of micro-cracks in the shear plane. These micro-cracks have a cycle of formation and healing. The healing of cracks is higher in case of ductile materials. These micro-cracks mainly act as stress concentrations enhancing material removal. In case of usage of NDM, the adsorption of cutting fluid results in reduced healing of micro-cracks as cutting fluid occupies the space. The atomized oil enhances this adsorption. This lowers the plasticity and results in lower cutting forces required to form a new surface. A similar effect of reducing surface energy can also be achieved by chemisorption, surface electrical polarization and surface chemical reactions [6].

7.1.4 Nano-fluids

Nano-fluids are engineered colloidal dispersion of Nano particles of metals, oxides, carbides, nitrides or Carbon Nano tubes (CNT) in base fluids. Nano-particles commonly used for preparing Nano-fluids are Carbon nanotube (CNT), TiO_2, Al_2O_3, MoS_2 and diamond. Nano-particles are generally in the size range of 1-100nm. They have high thermal conductivity due to high surface-volume ratio. [57]

The effectiveness of the Nano-fluids depends on homogeneity of Nano-particles in the colloid. Homogeneity depends on dynamic viscosity of the base fluid. Higher concentration increases thermal conductivity but can result in clogging. Thermal conductivity of Nano-fluids also increases with decreasing particle size. The shape of particles can also influence the thermal conductivity, temperature, Brownian motion of the particle and interfacial layer. Because of their small size and low concentrations, the fluids are generally stable without the issues of erosion, sedimentation etc.

Stable dispersion of particles can be obtained by magnetic stirring. Base fluids can be any of the previously used cutting fluids like emulsifiers. For the sustainability of manufacturing, bio-degradable vegetable oils (like coconut, sunflower, rapeseed and Canola) and water are being tried. Nano-particles are very reactive and can be toxic. CrO_3 is non-toxic. Fe_2O_3 is slightly

toxic. Al_2O_3 is moderately toxic. Most of the other Nano-materials are reactive and can be toxic. Al_2O_3 is widely used as Nano-fluid because of its lower reactivity and mechanical stability in high pressure environments [39].

7.2 Experimental set-Up

The set-up mentioned in the above discussion was used along with a spray gun and compressor for dispensing MQL coolant to the cutting zone. The outlet pressure of compressor was set at 50kg/cm^2. Flow rate for MQL oil was maintained in the range of 5-10ml/hour. Vegetable oil used in cooking applications was used initially. Al_2O_3 Nano-particles of 1% weight/weight solution with vegetable oil were prepared.

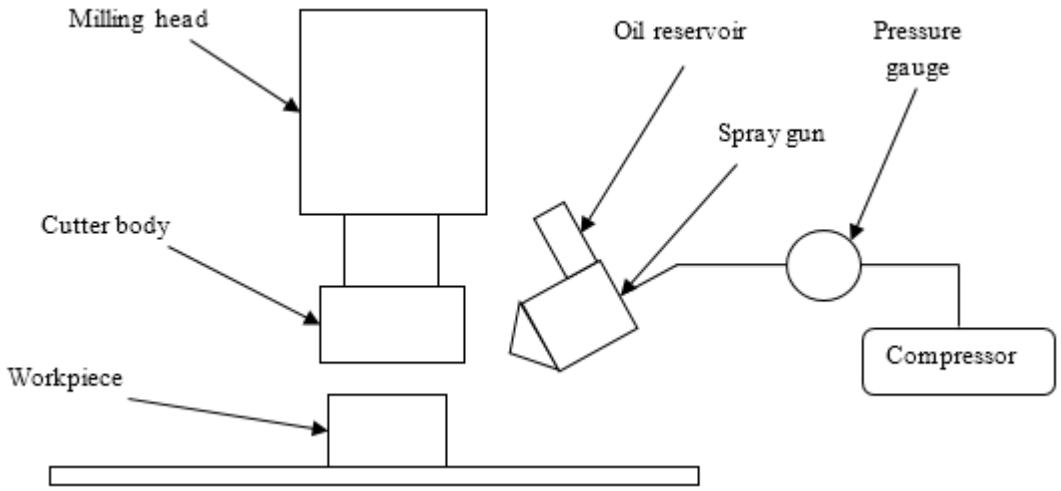

Figure 7.1 Schematic for MQL set-up

7.3 Process parameter Selection

Process parameter selection for effect of coolant was done based on the analysis of the experiments done in dry cutting mentioned in Chapter 5. Normal working range for cutting speeds is in the range of 30-120m/min. For equal spacing, availability of speeds and the considerations of tool wear, 40, 60 and 80m/min were considered as levels for cutting speed. Feed and doc were also selected based on the availability and equal spacing of levels. Approach angle was selected based on the optimized value from previous experiments which is 45^o. The present discussion does not consider the effect of depth of cut. The depth of cut is generally decided by the type of operation i.e. whether it is finishing or roughing operation. It also depends on the machining allowance provided. For the present discussion, it is considered to be a constant value of 0.1mm. Also, the effect of approach angle is not considered as the main goal is to understand the effect of coolant. Thus, three input parameters cutting speed, feed and coolant condition are considered. Coolant conditions considered are:

1. Dry
2. MQL using vegetable oil
3. MQL with vegetable oil and Al_2O_3(1%) based nano-fluid

The MQL coolant has been delivered in the cutting zone using a compressor and spray gun. The quantity delivered is around 5-10ml/hr. Flow rate has been kept constant by maintaining constant pressure. Nano-fluid has been prepared by mixing Al_2O_3 1% by weight. The solution is thoroughly mixed using a magnetic stirrer for 8 hours. This ensures uniform distribution and stability of the fluid. The parameters for experimentation are shown in Table 7.1.

Table 7.1 Process parameters for MQL Experiments

Symbol	Parameter	Level 1	Level 2	Level 3
A	Coolant condition	dry	MQL	Nano-MQL
B	Cutting speed(mm/min)	40	60	80
C	Feed rate (mm/rev)	0.16	0.22	0.28

Cutting speed and feed rate factors and their levels are similar to the previous experiment conducted. The full factorial experiments have been designed using Minitab as shown in Table 7.2. The experimental order has been randomized to minimize the error due to environmental effects.

Table 7.2 Full Factrial Experiments for MQL studies

Std Order	Run Order	Coolant condition	Cutting speed	Feed rate
7	1	Dry	80	0.16
15	2	MQL (oil)	60	0.28
20	3	MQL (nano)	40	0.22
5	4	Dry	60	0.22
22	5	MQL (nano)	60	0.16
6	6	Dry	60	0.28
26	7	MQL (nano)	80	0.22
25	8	MQL (nano)	80	0.16
12	9	MQL (oil)	40	0.28
16	10	MQL (oil)	80	0.16
2	11	Dry	40	0.22
17	12	MQL (oil)	80	0.22
1	13	Dry	40	0.16
9	14	Dry	80	0.28
4	15	Dry	60	0.16
13	16	MQL (oil)	60	0.16
21	17	MQL (nano)	40	0.28
10	18	MQL (oil)	40	0.16

23	19	MQL (nano)	60	0.22
18	20	MQL (oil)	80	0.28
24	21	MQL (nano)	60	0.28
27	22	MQL (nano)	80	0.28
8	23	Dry	80	0.22
19	24	MQL (nano)	40	0.16
11	25	MQL (oil)	40	0.22
14	26	MQL (oil)	60	0.22
3	27	Dry	40	0.28

7.4 Analysis of Experimental Data

As described in previous section, Minitab has been used to find out significant factors and interactions from the experimental data. Three way interactions have been neglected. The analysis of variance for Force using adjusted SS values is shown in Table 7.3.

Table 7.3 ANOVA Table for Cutting Force (F_y) in MQL Experiments

Source	**DF**	**Adj SS**	**Adj MS**	**F**	**P**
Coolant condition	2	10811.7	5405.84	233.02	<0.01
Cutting speed	2	745	372.48	16.06	0.002
Feed rate	2	644.4	322.19	13.89	0.003
Coolant condition*Cutting speed	4	238l.3	59.58	2.57	0.119
Coolant condition*Feed rate	4	46	11.5	0.5	0.74
Cutting speed*Feed rate	4	81.4	20.34	0.88	0.518
Error	8	185.6	23.2		
Total	26	12752.3			

As can be seen from Table 7.3, the coolant condition becomes most significant compared to all parameters. Cutting speed and feed changes affect the process in a very minimal way when compared to the coolant.

The analysis of variance for surface roughness using adjusted SS values is shown in Table 7.4.

Table 7.4 ANOVA Table for Surface Roughness (R_a) in MQL Experiments

Source	**DF**	**Adj SS**	**Adj MS**	**F**	**P**
Coolant condition	2	0.0886	0.0443	121.22	<0.01
Cutting speed	2	0.8708	0.04354	119.14	<0.01
Feed rate	2	4.28001	2.14001	5855.68	<0.01
Coolant condition*Cutting speed	4	0.00097	0.00024	0.66	0.634
Coolant condition*Feed rate	4	0.00519	0.0013	3.55	0.06
Cutting speed*Feed rate	4	0.00163	0.00041	1.12	0.412
Error	8	0.00292	0.00037		
Total	26	4.46641			

From Table 7.4, as expected, feed is the most significant factor on surface roughness due to the effect of feed ridges. A smaller effect of coolant and cutting condition has been observed in

reducing R_a values with high cutting speeds and application of coolant as shown in Figure 7.3. Figure 7.2 shows the effect of input parameters on Cutting Force F.

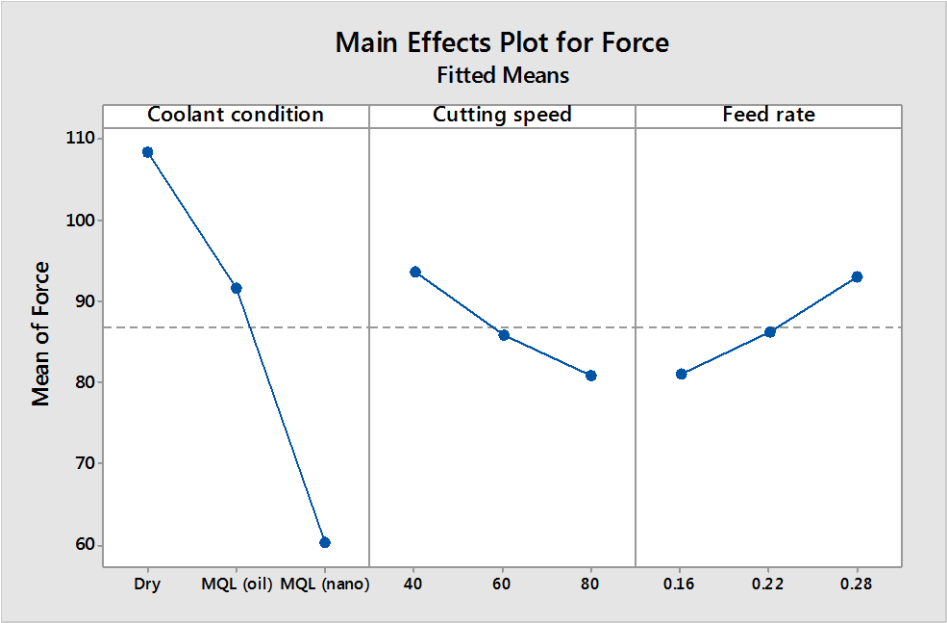

Figure 7.2 Main effects graph for Fitted Means for Cutting Force (F_y) in MQL

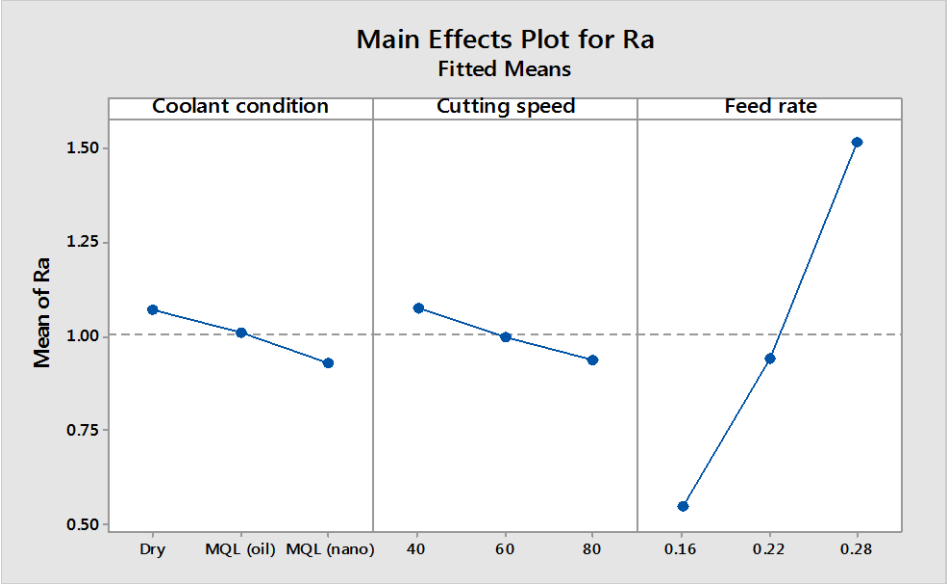

Figure 7.3Main Effects Plot for Fitted Means for Surface Roughness (R_a) in MQL

By considering average values of the output parameters, the effect of coolant can be quantified by percentage reduction. Figure 7.4 shows the average reduction found by using vegetable oil and nano-fluid in MQL. By application of MQL with vegetable oil, reduction in force observed is 14.29%. By using Nano-fluid the reduction in force is 43.66% and a reduction of 34.29% compared to MQL with vegetable oil. This can be attributed to the increased thermal conductivity of the fluid by the use of Nano-particles. In case of surface roughness value (R_a) the reduction due to MQL with vegetable oil is 5.78% and with Nano-fluid is 13.02%.

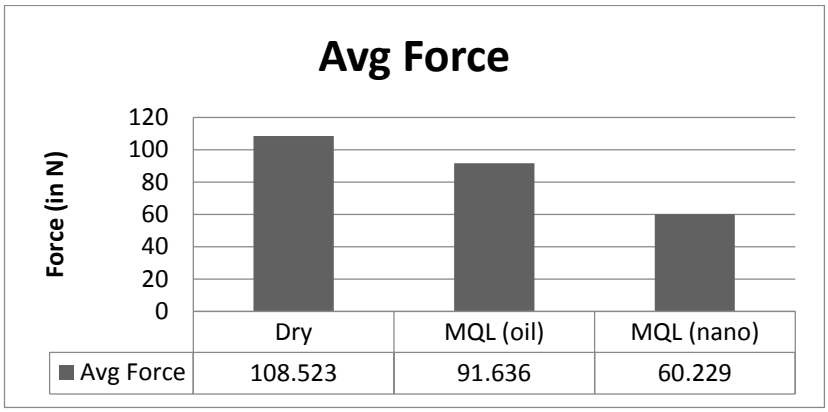

Figure 7.4 Effect of Coolant on Average Force

7.5 Conclusion

From the analysis of effect of coolant on Machinability of Inconel 718, it can be concluded that:

a. Simple method for MQL has been achieved without any new set-up by using an off-shelf spray gun and compressor.
b. Coolant condition was the most important parameter affecting Machinability.
c. Vegetable oil has been used as the MQL coolant, proving its usefulness in sustainable environment-friendly machining. It resulted in reduction of 14.29% in force and 5.78% in surface roughness (R_a) value.
d. Nano-fluid was successfully prepared and applied as an MQL coolant successfully. It resulted in reduction of 43.66% in force and 13.02% in surface roughness (R_a) value. Its usefulness in critical applications can be established from these results.

8 SUMMARY AND CONCLUSIONS

8.1 Summary

In the present work, a reliable procedure has been developed to investigate Machinability issues of Inconel 718 in face milling operation. To get a basic idea of the process, experimental studies were conducted based on Taguchi method using an L9 orthogonal array. The effect of speed, feed, depth of cut and approach angle on output parameters like Cutting Force (Fy), surface roughness (Ra), tool wear (L) and amplitude of acoustic emission(AE_{RMS}) has been analyzed. Initially, the effect was analyzed individually on each output parameter. Gray relational analysis (GRA) was used to conduct multi-objective optimization.

To get a better idea of the effect of parameters and interaction effects, full factorial (81) experiments were conducted. These experiments were conducted based on Design of experiment principles. ANOVA analysis was used to find out significant parameters. This data was further used to build a 2-layer ANN model each for surface roughness and cutting force. The ANN model was trained, validated and tested for multiple iterations to get a model with lower mean-square error. For getting a better idea of tool wear mechanism, the worn out tool was analyzed using Scanning electron microscope (SEM) and Electro-dispersive spectroscopy (EDS).

Dry machining of super-alloy like Inconel 718 can result in very low tool life. As costs of flood coolants are increasing and with strict environment regulations, applicability of MQL (minimum-quantity lubrications) for face milling was considered. A simple set-up for atomizing the cutting fluid was developed. The effect of use of nano-fluid (made of Al_2O_3 nano-particles and vegetable oil) in MQL was analyzed and compared along with only vegetable oil in MQL and dry cutting conditions.

8.2 Conclusions

The following conclusions can be made from the present work:

1. Optimum conditions for parameters according to the optimized parameters from L9 experiments are shown below :

Optimized parameter	Cutting speed (mm/min)	feed (mm/rev)	depth of cut (mm)	Approach angle (degrees)
Cutting Force (F_y)	60	0.22	0.1	45
Surface roughness (R_a)	80	0.16	0.1	45
Tool wear (L)	40	0.16	0.1	45

2. With Multi-objective optimization, the optimized parameters are:

Cutting speed (mm/min)	feed (mm/rev)	depth of cut (mm)	Approach angle (degrees)
40	0.16	0.1	45

3. The following conclusions are made from the full factorial experiments:
    a. Significant factors affecting the cutting Force are depth of cut, feed, approach angle, interaction of feed rate and approach angle, cutting speed and interaction feed rate and depth of cut in decreasing order of magnitude. The reason for such an affect can be attributed to the high strength of Inconel 718. With increase of depth of cut and feed, the uncut chip area increases leading to greater force required for shearing.
    b. Significant factor affecting surface roughness (R_a value) is feed. Depths of cut, approach angle and cutting speed have small influence on $_{Ra}$ value. No significant interactions were observed.
    c. The mean square errors of the ANN model for force and surface roughness are in the order of 10^{-4}.
4. The following are the conclusions made from the full factorial experiments conducted to analyze the effect of coolant on the cutting processes
    a. Coolant condition was the most important parameter affecting Machinability.
    b. Vegetable oil has been used as the MQL coolant, proving its usefulness in sustainable environment friendly machining. It resulted in reduction of 14.29% in force and 5.78% in surface roughness (R_a) value.
    c. Nano-fluid was successfully prepared and applied as an MQL coolant successfully. It resulted in reduction of 43.66% in force and 13.02% in surface roughness (R_a) value. Its use in critical applications can be established from these results.

8.3 Scope for future work

With the advent of advanced sensors and signal processing techniques, use of Acoustic emission and vibration sensors along with cutting force dynamometer would provide greater information from the process. Sensor fusion of these multiple signals can be used to build a Tool condition monitoring system. Tool wear mechanism was analyzed using EDS analysis. Understanding residual stresses due to machining can provide additional information to decide on process parameters based on surface integrity. In the MQL study, the parameters like air pressure and oil to air ratio were kept constant. The effect of these parameters can also be analyzed and optimum levels of the fluid can be established.

REFERENCES

[1] M. J. Donachie and S. J. Donachie, *Superalloys: A technical guide*, 2nd ed. ASM International, 2002.

[2] Special Metals Corporation, "INCONEL alloy 718," 2014. [Online]. Available: http://www.specialmetals.com/documents/Inconel alloy 718.pdf. [Accessed: 20-Oct-2014].

[3] M. Alauddin, M. a. Mazid, M. a. El Baradi, and M. S. J. Hashmi, "Cutting forces in the end milling of Inconel 718," *J. Mater. Process. Technol.*, vol. 77, no. 1–3, pp. 153–159, 1998.

[4] E. P. DeGarmo, J. T. Black, and R. a. Kohser, *DeGarmo's Materials and Processes in Manufacturing*. John Wiley & Sons, Inc, 2011.

[5] S. and S. R. S. Kalpakjian, *Manufacturing Engineering and Technology*, 6th ed. Pearson, 2009.

[6] J. P. Davim, *Machining: Fundamentals and Recent Advances*, 1st ed. Springer, 2008.

[7] E. O. Ezugwu, "Key improvements in the machining of difficult-to-cut aerospace superalloys," *Int. J. Mach. Tools Manuf.*, vol. 45, no. 12–13, pp. 1353–1367, 2005.

[8] Kenna Metal, "High-Temperature Machining Guide," 2013.

[9] A. Jawaid, S. Koksal, and S. Sharif, "Cutting performance and wear characteristics of PVD coated and uncoated carbide tools in face milling Inconel 718 aerospace alloy," *J. Mater. Process. Technol.*, vol. 116, no. 1, pp. 2–9, 2001.

[10] H. Z. Li, H. Zeng, and X. Q. Chen, "An experimental study of tool wear and cutting force variation in the end milling of Inconel 718 with coated carbide inserts," *J. Mater. Process. Technol.*, vol. 180, pp. 296–304, 2006.

[11] M. Nalbant, "The effect of coating material and geometry of cutting tool and cutting speed on machinability properties of Inconel 718 super alloys," *Mater. Des.*, vol. 28, pp. 1719–1724, 2007.

[12] M. Rahman, T. T. Teo, and K. Ridge, "The Machinability of Inconel 718," *Mater. Process. Technol.*, vol. 63, no. 1, pp. 199–204, 1997.

[13] R. M. Arunachalam, M. A. Mannan, and A. C. Spowage, "Surface integrity when machining age hardened Inconel 718 with coated carbide cutting tools," *Int. J. Mach. Tools Manuf.*, vol. 44, no. 14, pp. 1481–1491, 2004.

[14] L. Li, N. He, M. Wang, and Z. G. Wang, "High speed cutting of Inconel 718 with coated carbide and ceramic inserts," *J. Mater. Process. Technol.*, vol. 129, pp. 127–130, 2002.

[15] J. P. Costes, Y. Guillet, G. Poulachon, and M. Dessoly, “Tool-life and wear mechanisms of CBN tools in machining of Inconel 718,” *Int. J. Mach. Tools Manuf.*, vol. 47, no. 7–8, pp. 1081–1087, 2007.

[16] N. Fang and Q. Wu, “A comparative study of the cutting forces in high speed machining of Ti-6Al-4V and Inconel 718 with a round cutting edge tool,” *J. Mater. Process. Technol.*, vol. 209, no. 9, pp. 4385–4389, 2009.

[17] J. L. Cantero, J. Díaz-Álvarez, M. H. Miguélez, and N. C. Marín, “Analysis of tool wear patterns in finishing turning of Inconel 718,” *Wear*, vol. 297, no. 1–2, pp. 885–894, 2013.

[18] Y. S. Liao, H. M. Lin, and J. H. Wang, “Behaviors of end milling Inconel 718 superalloy by cemented carbide tools,” *J. Mater. Process. Technol.*, vol. 20, no. 1, pp. 460–465, 2007.

[19] D. Dudzinski, A. Devillez, A. Moufki, D. Larrouquère, V. Zerrouki, and J. Vigneau, “A review of developments towards dry and high speed machining of Inconel 718 alloy,” *International Journal of Machine Tools and Manufacture*, vol. 44, no. 4. pp. 439–456, 2004.

[20] C. Kuo, S. Su, and S. Chen, “Tool life and surface integrity when milling inconel 718 with coated cemented carbide tools,” *Journal of the Chinese Institute of Engineers*, vol. 33, no. 6. pp. 915–922, 2010.

[21] G. K. Dosbaeva, S. C. Veldhuis, a. Elfizy, G. Fox-Rabinovich, and T. Wagg, “Microscopic observations on the origin of defects during machining of direct aged (DA) inconel 718 superalloy,” *J. Mater. Eng. Perform.*, vol. 19, no. 8, pp. 1193–1198, 2010.

[22] G. S. Fox-Rabinovich, K. Yamamoto, M. H. Aguirre, D. G. Cahill, S. C. Veldhuis, a. Biksa, G. Dosbaeva, and L. S. Shuster, “Multi-functional nano-multilayered AlTiN/Cu PVD coating for machining of Inconel 718 superalloy,” *Surf. Coatings Technol.*, vol. 204, no. 15, pp. 2465–2471, 2010.

[23] H. a. Sonawane and S. S. Joshi, “Analytical modeling of chip geometry and cutting forces in helical ball end milling of superalloy Inconel 718,” *CIRP J. Manuf. Sci. Technol.*, vol. 3, no. 3, pp. 204–217, 2010.

[24] B. a Khidhir and B. Mohamed, “Machining of Nickel Based Alloys Using Different Cemented Carbide Tools,” vol. 5, no. 3, pp. 264–271, 2010.

[25] a. Devillez, F. Schneider, S. Dominiak, D. Dudzinski, and D. Larrouquere, “Cutting forces and wear in dry machining of Inconel 718 with coated carbide tools,” *Wear*, vol. 262, no. 7–8, pp. 931–942, 2007.

[26] D. G. Thakur, B. Ramamoorthy, and L. Vijayaraghavan, “Effect of High Speed Cutting Parameters on the Surface Characteristics of Superalloy Inconel 718,” in *Engineering*, 2010, vol. III.

[27] C. Andersson, M. Andersson, and J. E. Ståhl, “Experimental studies of cutting force variation in face milling,” *Int. J. Mach. Tools Manuf.*, vol. 51, no. 1, pp. 67–76, 2011.

[28] J. a. Ghani, I. a. Choudhury, and H. H. Hassan, “Application of Taguchi method in the optimization of end milling parameters,” *J. Mater. Process. Technol.*, vol. 145, no. 1, pp. 84–92, 2004.

[29] P. G. Benardos and G. C. Vosniakos, “Prediction of surface roughness in CNC face milling using neural networks and Taguchi ’ s design of experiments,” *Computer (Long. Beach. Calif).*, vol. 18, no. 5–6, pp. 343–354, 2002.

[30] C.-J. Tzeng, Y.-H. Lin, Y.-K. Yang, and M.-C. Jeng, “Optimization of turning operations with multiple performance characteristics using the Taguchi method and Grey relational analysis,” *J. Mater. Process. Technol.*, vol. 209, no. 6, pp. 2753–2759, 2009.

[31] D. G. Thakur, B. Ramamoorthy, and L. Vijayaraghavan, “Effect of cutting parameters on the degree of work hardening and tool life during high-speed machining of Inconel 718,” *Int. J. Adv. Manuf. Technol.*, vol. 59, no. 5–8, pp. 483–489, 2012.

[32] T. Rajmohan, K. Palanikumar, and M. Kathirvel, “Optimization of machining parameters in drilling hybrid aluminium metal matrix composites,” *Trans. Nonferrous Met. Soc. China (English Ed.*, vol. 22, no. 6, pp. 1286–1297, 2012.

[33] A. Kurt, “Modelling of the cutting tool stresses in machining of Inconel 718 using artificial neural networks,” *Expert Syst. Appl.*, vol. 36, no. 6, pp. 9645–9657, 2009.

[34] J. S. Senthilkumaar, P. Selvarani, and R. M. Arunachalam, “Intelligent optimization and selection of machining parameters in finish turning and facing of Inconel 718,” *Int. J. Adv. Manuf. Technol.*, vol. 58, no. 9–12, pp. 885–894, 2012.

[35] E. Uhlmann, M. G. Von Der Schulenburg, and R. Zettier, “Finite element modeling and cutting simulation of inconel 718,” *CIRP Ann. - Manuf. Technol.*, vol. 56, no. 1, pp. 61–64, 2007.

[36] R. S. Pawade and S. S. Joshi, “Multi-objective optimization of surface roughness and cutting forces in high-speed turning of Inconel 718 using Taguchi grey relational analysis (TGRA),” *Int. J. Adv. Manuf. Technol.*, vol. 56, no. 1–4, pp. 47–62, 2011.

[37] C. Nath, Z. Brooks, and T. R. Kurfess, “On Machinability Study and Process Optimization in Face Milling of Some Alloys with Indexable Copy Face Mill Inserts,” *Procedia Manuf.*, vol. XXX, pp. 1–14, 2015.

[38] Y. Kamata and T. Obikawa, “High speed MQL finish-turning of Inconel 718 with different coated tools,” *J. Mater. Process. Technol.*, vol. 192–193, pp. 281–286, 2007.

[39] V. Sridhara and L. N. Satapathy, “Al2O3-based nanofluids: a review.,” *Nanoscale Res. Lett.*, vol. 6, no. 1, p. 456, 2011.

[40] T. Obikawa and M. Yamaguchi, “Suppression of notch wear of a whisker reinforced ceramic tool in air-jet-assisted high-speed machining of Inconel 718,” *Precis. Eng.*, vol. 39, pp. 143–151, 2015.

[41] a. Devillez, G. Le Coz, S. Dominiak, and D. Dudzinski, “Dry machining of Inconel 718, workpiece surface integrity,” *J. Mater. Process. Technol.*, vol. 211, no. 10, pp. 1590–1598, 2011.

[42] S. Zhang, J. F. Li, and Y. W. Wang, “Tool life and cutting forces in end milling Inconel 718 under dry and minimum quantity cooling lubrication cutting conditions,” *J. Clean. Prod.*, vol. 32, pp. 81–87, 2012.

[43] a. Shokrani, V. Dhokia, S. T. Newman, and R. Imani-Asrai, “An initial study of the effect of using liquid nitrogen coolant on the surface roughness of inconel 718 nickel-based alloy in CNC milling,” *Procedia CIRP*, vol. 3, no. 1, pp. 121–125, 2012.

[44] Z. Vagnorius and K. Sørby, “Effect of high-pressure cooling on life of SiAlON tools in machining of Inconel 718,” *Int. J. Adv. Manuf. Technol.*, vol. 54, no. 1–4, pp. 83–92, 2011.

[45] V. Vasu and K. M. Kumar, “Analysis of Nanof luids as Cutting Fluid in Grinding EN-31 Steel,” *Nano-Micro Lett.*, vol. 3, no. November, pp. 209–214, 2011.

[46] S. Khandekar, M. R. Sankar, V. Agnihotri, and J. Ramkumar, “Nano-Cutting Fluid for Enhancement of Metal Cutting Performance,” *Mater. Manuf. Process.*, vol. 27, no. 9, pp. 963–967, 2012.

[47] Y. Kaynak, “Evaluation of machining performance in cryogenic machining of Inconel 718 and comparison with dry and MQL machining,” *Int. J. Adv. Manuf. Technol.*, vol. 72, pp. 919–933, 2014.

[48] G. Le Coz and D. Dudzinski, “Temperature variation in the workpiece and in the cutting tool when dry milling Inconel 718,” *Int. J. Adv. Manuf. Technol.*, vol. 74, no. 5–8, pp. 1133–1139, 2014.

[49] C. Wang, K. Li, M. Chen, and Z. Liu, “Evaluation of minimum quantity lubrication effects by cutting force signals in face milling of Inconel 182 overlays,” *J. Clean. Prod.*, vol. 108, pp. 145–157, 2015.

[50] T. . Sadasivan and D. Sarathy, *Cutting tools for productive machining*, 1st ed. Widia (India) Limited, 1999.

[51] Mitsubishi Carbide, “Function of tool features for face milling, Mitsubishi Carbide.” [Online]. Available: http://www.mitsubishicarbide.net/contents/mmus/enus/html/product/technical_information/information/f_shoumen.html. [Accessed: 16-Jun-2013].

[52] M. S. Phadke, *Quality engineering using robust design*. Prentice Hall, 1989.

[53] D. C. Montgomey, *Design and Analysis of Experiments*. Wiley, 2001.

[54] M. H. Beale, M. T. Hagan, and H. B. Demuth, *Neural Network Toolbox ™ User ' s Guide*. 2013.

[55] T. Pradeep, *Nano The Essentials*. 2007.

[56] K. Kadirgama, K. a. Abou-El-Hossein, M. M. Noor, K. V. Sharma, and B. Mohammad, "Tool life and wear mechanism when machining Hastelloy C-22HS," *Wear*, vol. 270, no. 3–4, pp. 258–268, 2011.

[57] U. S. Dixit, D. Sarma, and J. P. Davim, *Environmentally Friendly Machining*. Springer Science, 2012.

[58] M. C. Shaw, *Metal cutting principles*, 2nd ed. Oxford, 2005.

LIST OF PUBLICATIONS FROM RESEARCH WORK

International Journals

Sadasiva Rao T, et al, **"Studies on The Effect of Approach Angle and Process Parameters in Face Milling"** published in **International Journal of** Applied Mechanics and Materials (Volumes 110 – 116, PP 3147-3155). Online since October, 2011. DOI: 10.4028/ www.scientific.net/ AMM.110-116.3147.

List of International Conference Proceedings

1. Sadasiva Rao T, et al, **" Online tool condition monitoring in face milling operation using Acoustic Emission**". Paper published in the Proceedings of 3rd International & 24th AIMTDR (All India Manufacturing Technology, Design and Research) Conference held at A.U. College of Engineering (A), Andhra University, Visakhapatnam, during December 13-15, 2010.
2. Sadasiva Rao T, et al**, "Studies on The Effect of Approach Angle and Process Parameters in Face Milling"**. MMIT 2011, 2nd International Conference on Mechanical, Industrial, and Manufacturing Technologies (26-02-2011 to 28-02-2011) at Singapore. 2011 IEEE. ISBN: 978-1-4244-9264-0. VI (pp) 115-119.
3. Sadasiva Rao T., et al, **"Taguchi based GRAY Relational Analysis to Optimize Face Milling Process with Multiple Performance Characteristics""**. (Paper ID: 0312714). International Conference on Trends in Industrial and Mechanical Engineering (ICTIME'2012), (March 24-25 of 2012) held at Dubai. 2012. (pp) 166-170.